Volcanic geology of the early Pleistocene ignimbrite succession in the western Papamoa Region, Bay of Plenty

A thesis

submitted in fulfilment

of the requirements for the degree

of

Master of Science in Earth Science

at

The University of Waikato

by

Miriam Namaliu

THE UNIVERSITY OF
WAIKATO
Te Whare Wānanga o Waikato

2021

ABSTRACT

Volcanic activity in the Tauranga Volcanic Center (TgaVC) occurred between 2.95 to 1.9 Ma, some of the eruptions were explosive and led to the distribution of ignimbrites of varying volumes across the western Bay of Plenty Region (Tauranga Basin), North Island. The Papamoa Formation forms part of the landscape in this area. This study was aimed at determining the volcanic history and processes involved in the distribution of the Papamoa Formation within the eastern Tauranga Basin.

Stratigraphic, petrographic and geochemical investigations were undertaken in the field and from samples within the study area. Field observations of the ignimbrites involved stratigraphic logging and lateral relationships, component measurements and lithological descriptions. Ignimbrite petrography was undertaken by optical microscopy. To determine the geochemical characteristics of the source magmas for the ignimbrites, the following analyses were conducted: electron microprobe analysis (EMPA) on glass shards extracted from the ignimbrite matrices, glass from pumice, and on minerals in the pumice, x-ray fluorescence spectroscopy (XRF) on whole pumice clasts and laser ablation inductively coupled plasma mass spectrometry (LA-ICP-MS) on the same glass samples used for EMPA.

Five individual eruptions that led to the distribution of five ignimbrites have been identified within the ignimbrite succession of the Papamoa Formation: an early unnamed ignimbrite, followed by the Welcome Bay, Wharo, Arateka, and Otawera ignimbrites. The beige-brown, non-welded, pumice-rich, Welcome Bay Ignimbrite (2.4 Ma) is the most voluminous in the study area and also has an underlying pumice fall deposit. The dark brown to black, pumice-/fiamme-rich Wharo Ignimbrite (2.26 Ma, M. Prentice unpublished data, 2021) is the only moderate to densely welded ignimbrite. Both the Welcome Bay and Otawera ignimbrite contained black (andesitic-dacitic) and white (dacitic) pumice. The beige, non-welded Otawera Ignimbrite (2.21 Ma) is the least voluminous ignimbrite in the study area and comprises only white pumice. The beige-yellow brown Arateka ignimbrite is comprises of both the black and white pumice clasts. The unnamed Unit A ignimbrite, at the base of the succession has only one pumice population – grey pumice, but it is poorly exposed. All the ignimbrites are generally lithic poor. Petrographic analysis found that the main minerals occurring in the ignimbrites were: plagioclase, pyroxenes, hornblende and opaques. The main mineral in the black pumice was plagioclase and pyroxene. The white pumice, however, is mainly composed of plagioclase and hornblende. In terms of rock textures, the Welcome Bay Ignimbrite, Arateka Ignimbrite, Otawera Ignimbrite and Unit A-Unknown Ignimbrite had either a porphyritic or vitrophyric or a combination of both textures. The

Wharo Ignimbrite possessed a porphyritic and/or eutaxitic texture. Geochemical data showed that although the glass shards from each ignimbrite has a unique chemical composition, they were all rhyolitic. However, in terms of the two pumice types, the white pumice was dacitic while the black pumice was andesitic.

The presence of two pumice types (black and white) in the Welcome Bay, Wharo and Arateka Ignimbrites, supports the idea that the magma from which the ignimbrites were sourced, had a mixed andesitic to dacitic composition. The distribution and internal stratigraphy of the Papamoa Formation record a history of multiple ignimbrite-forming eruptions that were sourced locally, likely south of the study area; at least one ignimbrite (Welcome Bay Ignimbrite) was preceded by a sustained Plinian eruption column.

ACKNOWLEDGEMENTS

The completion of this Master of Science research project would not have been possible if it were not for the following people whom I wish to express my gratitude towards.

First and foremost, I would like to thank my Creator for blessing me with this opportunity to study in this beautiful country and for seeing me through my academic journey since 2018.

I am thankful, to the people of New Zealand for having granted me a New Zealand Development Scholarship through the Ministry of Foreign Affairs and Trade (MFAT). Thank you very much for this once in a lifetime opportunity to gain valuable knowledge and skills to equip me to further contribute to the development of my country, Papua New Guinea.

To my supervisor, Dr. Adrian Pittari, thank you for your continuous support and guidance throughout this research project. Thank you for your patience, understanding and for your tireless effort in ensuring that I complete my research project.

I would like to acknowledge the property owners: Addline Transport Ltd, Gina Winch, the McLeods, Gavin, Arnie, J. Holmberg, who were willing to have me work on their property for my research project. Without you, I wouldn't have a thesis to submit. Thank you very much.

I would like to thank the dedicated staff at the Victoria University of Wellington, School of Geography, Environment and Earth Sciences, Dr. Ian Schipper, Dr. Jenni Hopkins and Juergen Oesterle. Thank you very much for your guidance and assistance with the electron microprobe analysis of my samples.

Marlena Prentice, thank you for being an inspiration and for sharing with me your experiences, knowledge and enthusiasm in the work that you do. Being a mother myself, working with you has taught me that no matter what stage I am in my life journey, with hard work, dedication and determination, dreams can become reality.

To the hardworking technical staff of the School of Science and Engineering: Renat Radosinksy, Kirsty Vincent and Holly Harvey-Wishart, thank you for showing me how to use the analysing machines used for this project and in some instances, for accompanying me out in the field. Your time and efforts are greatly appreciated.

A special thank you to my family and friends for your continued support throughout my studies. To my dear husband, Augustine and son, Zephaniah, thank you very much for always being there, especially when I was at my lowest. Appreciate you both always.

Finally, a special thankyou goes out to my dear widowed mother, Ashwyn Namaliu and my late father Eric Namaliu. Thank you for your prayers and words of encouragement. To dad, thank you for having believed in me and for the love and support that you provided every day you were with us.

I would like to dedicate this thesis to my late father, Mr. Eric Namaliu. Thank you for all the sacrifices you made to provide for my siblings and I and for supporting us in pursuing whatever dream we had/have. I hope I make you proud with the completion of my thesis. Till that golden morning dad, may you rest in love and peace.

TABLE OF CONTENTS

LIST OF FIGURES

LIST OF TABLES

CHAPTER 1
INTRODUCTION

1.1 Introduction

Volcanic eruptions are broadly classified as being either explosive or effusive (Francis & Oppenheimer, 2004, Self, 2006), the latter potentially being a disastrous natural phenomenon when it occurs within proximity of infrastructure, agricultural land and settlements of people. Explosive volcanic eruptions sometimes result in the formation of calderas due to the collapse of the roof rock above an emptying magma chamber (Wilson et al., 1980). The products of explosive eruptions include air-fall deposits and pyroclastic density current deposit, which are further classified into surges and flows. Ignimbrites are pumice- (or scoria)-rich deposits of pyroclastic flows (Giordano and Cas, 2021) and can be destructive to infrastructure and human populations within its path

According to documented global explosive rhyolitic volcanic eruptions, it is observed that they tend to occur along subduction zones or where there is or has been rifting of continental interiors (Self, 2006). New Zealand is located along a subduction boundary of the Pacific Plate (subducting plate) and Australian Plate (overriding plate). Volcanism along the central part of the North Island is subduction-related while intraplate volcanism is evident on the western side (Krear, 2010; Pittari et al., 2021). From the mid-Miocene to Pliocene (since ~ 18 Ma) (Booden et al., 2012) rhyolitic volcanism in the North Island migrated south, through the Coromandel Volcanic Zone (CVZ) and then on to the present day it continued along the currently active Taupo Volcanic Zone (TVZ). Situated between the CVZ and TVZ is the Tauranga Volcanic Centre or TgaVC. Mapping through a series of University of Waikato Earth science masters studies during the early 1990s (Hughes, 1993; Hollis, 1995; Hall, 1994; and Whitbread-Edwards, 1994) led to the 1:50,000 geological map of Tauranga (Briggs et al 1996), which was later incorporated into the 1:250,000 QMap sheet (Leonard et al., 2010). This early research on the volcanic deposits within the Tauranga Basin developed the stratigraphy of the TgaVC, and the petrography and geochemistry of the deposits. One of the volcanic units that occurs within the eastern Tauranga Basin is the Papamoa Ignimbrite Formation. Although possible sources of the Papamoa Formation were suggested by Hughes (1993), the source remains unknown. This research project builds on from past research work, with a focus on the Papamoa Formation ignimbrites found in the eastern Tauranga Basin.

1.2 Study Aim and Objectives

The aim of this study was to determine the volcanic eruption history and processes of the Papamoa Formation in the context of modern volcanological thinking and using a range of modern volcanological techniques.

To achieve the aim of this research project, the following objectives were set:

1) to determine stratigraphy and deposit characteristics of the Papamoa Formation,

2) to determine the ignimbrite petrography and

3) to determine whole rock, mineral and glass chemistry of the ignimbrite.

1.3 Research method

The objectives were achieved by using field studies (stratigraphic logging; field photography and observations; sampling); optical microscope observations; scanning electron microscope (SEM) observation of pumice and ignimbrite matrix; whole rock geochemistry (pumice) - major and trace elements concentrations determined by X-ray fluorescence (XRF) spectroscopy , and trace element concentrations, including rare Earth elements (REE)s by laser ablation inductively coupled plasma mass spectrometry (LA-ICP-MS); and glass and mineral chemistry determined by electron microprobe analysis .

Most of the techniques above were conducted at the University of Waikato. Electron microprobe analysis was carried out at Victorian University, Wellington.

1.4 Study area

As described by Hughes (1993), the Tauranga Basin is located in the northern Bay of Plenty and is “bounded by the topographic highs of the Kaimai Ranges in the northwest and the Papamoa Hills in the south.” (p. 2). The study area (Figure 1.1) for this research project is situated in the eastern Tauranga region, approximately 3.3 km east of the town of Welcome Bay. It is bounded to the north by Welcome Bay Road, to the east by Reid Road, to the west by Waitao Road and to the south by the Kaiate Falls Road and Te Puke Quarry Road. Running through the study area is Rocky Cutting Road. Also situated within the field area is the dacite Kopukairua Dome.

Most of the study area is privately owned farmland, used for livestock grazing, although outcrops were also studied on the public roadside. The only location that is not privately owned is the Kaiate Falls which is protected by the Department of Conservation and is used for recreational purposes such as swimming.

The Papamoa Formation ignimbrites outcrop along the ridges of the study area as bluffs or are exposed by road cuttings. Some of the outcrops are covered with and/or surrounded by pastures, bush and trees while other outcrops have little to no vegetation growing on them. For the outcrops that were easily accessible, samples were collected.

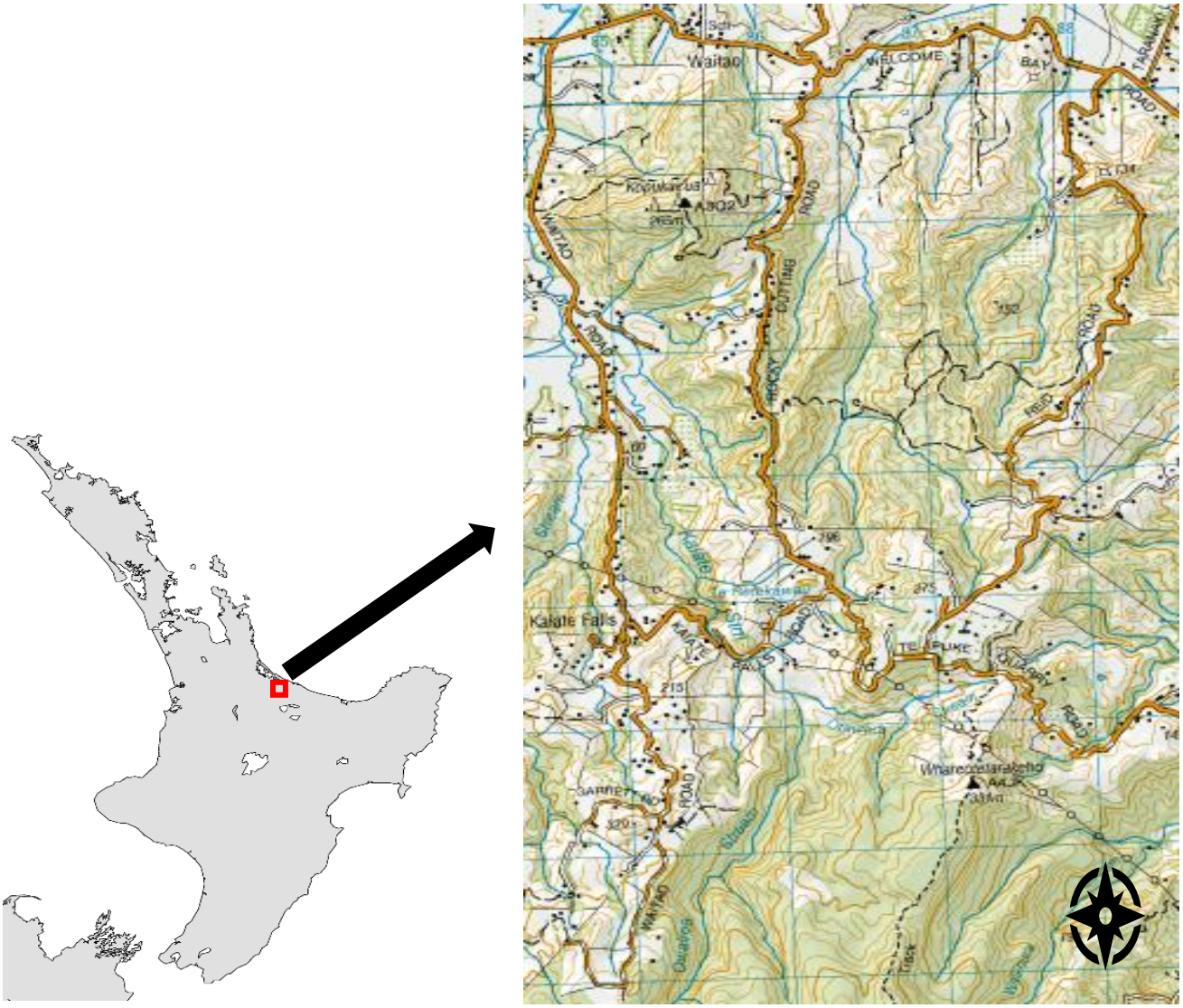

Figure 1.1. A map of the study area (right) and where it is located in the North Island (left, in the red square). Base map sourced from LINZ (2020). Map outline of the North Island on the left was sourced from Wikimedia and authored by Kahuroa (2010).

1.5 Thesis structure and chapter outline

Chapter Two is a review of literature in relation to the past and present volcanism in the North Island, New Zealand. The chapter comprises background on the tectonic setting and geological evolution of New Zealand and furthermore looks at the migration of volcanism from the Coromandel Volcanic Zone in the north-west part of the North Island, to the Tauranga Volcanic Centre and finally to the present-day active Taupo Volcanic Zone in central North Island.

Chapter Three is a description of the stratigraphy of the study area which is located in the eastern Tauranga basin. This chapter presents the four different ignimbrites in the study area: the Welcome Bay Ignimbrite, Wharo Ignimbrite, Arateka Ignimbrite and the Otawera Ignimbrite and their descriptions. Other geological units within the study area are also described.

Chapter Four is a description of the petrology of the Papamoa Ignimbrites and the other geological units in the studied localities. The methods used to assist in describing the petrology of the samples collected in the field include petrography, electron microprobe analysis, X-ray fluorescence (XRF) spectroscopy analysis and laser ablation inductively coupled plasma mass spectrometry (LA-ICPMS).

Chapter Five presents a discussion that brings meaning to the results obtained from this research. This chapter explains the eruption history and the processes involved in the distribution of the Papamoa Ignimbrite, using the finding of this study. Chapter Five also provides concluding remarks and recommendations for future research work.

CHAPTER 2

LITERATURE REVIEW

2.1 Tectonic setting and geological evolution of New Zealand

2.1.1 General Tectonic Setting

New Zealand is an island country situated in the southwest of the Pacific Ocean. The position of present-day New Zealand is a result of the evolution and deformation of the Zealandia continent (most of which is submerged), along the Australian and Pacific Plate boundary (Ballance, 2009; Booden, 2012; Mortimer, 2004; Stem, 2006). New Zealand straddles the Pacific and Australian plate boundary, the North Island and northern South Island, sitting on the Australian Plate while the rest of the South Island rests on the Pacific Plate (Figure 2.1). The Hikurangi Trough lies east of the North Island and extends further south to the north of the South Island. It marks the collision boundary whereby the Pacific Plate descends westward beneath the North Island; the subduction process assists in the production of magma from deep within the mantle which fuels and dictates the location of most of the active volcanoes in New Zealand (Stem et al, 2006). In the south of the South Island, the opposite occurs whereby the Australian Plate descends eastward under the Pacific Plate, along the Puysegur Trench (Ballance, 2009; Shane, 2017). The Alpine Fault, located on western South Island, is an oblique transpression fault whereby both strike-slip and compressive components of motion between the Australian and Pacific plates have aided the uplift of the Southern Alps at a maximum rate of 11 mm/year for the past 5 million years (Ballance, 2009; Shane, 2017).

2.1.2 Geological evolution of New Zealand

Approximately 505-110 million years ago, the basement geology of modern New Zealand, was accreted along the coastline of the Gondwana super-continent. The basement geology of New Zealand is comprised of terranes and igneous suites (Ballance, 2009; Leonard et al., 2010; Mortimer, 2004; Sutherland, 1999). The terranes are broadly grouped into the Western Province and Eastern Province and are separated by the Median Tectonic Zone or MTZ (Mortimer, 2004; Sutherland, 1999). These terranes mainly comprise

deformed sedimentary and metamorphosed sedimentary rocks (Ballance, 2009; Mortimer, 2004; Sutherland, 1999).

Around 110-83 million years ago, rifting occurred and the Zealandia continent broke off the southeastern margin of Gondwana. The Tasman Sea spread between c. 83-50 million years ago, however the ridge failed and resulted in the sealing of the Australian Plate with the Zealandia continental fragment (Ballance, 2009; Mortimer, 2004). The development of the Tasman Sea c. 100-80 million years ago had caused the Zealandia continent to heat up, stretch and thin out, gradually

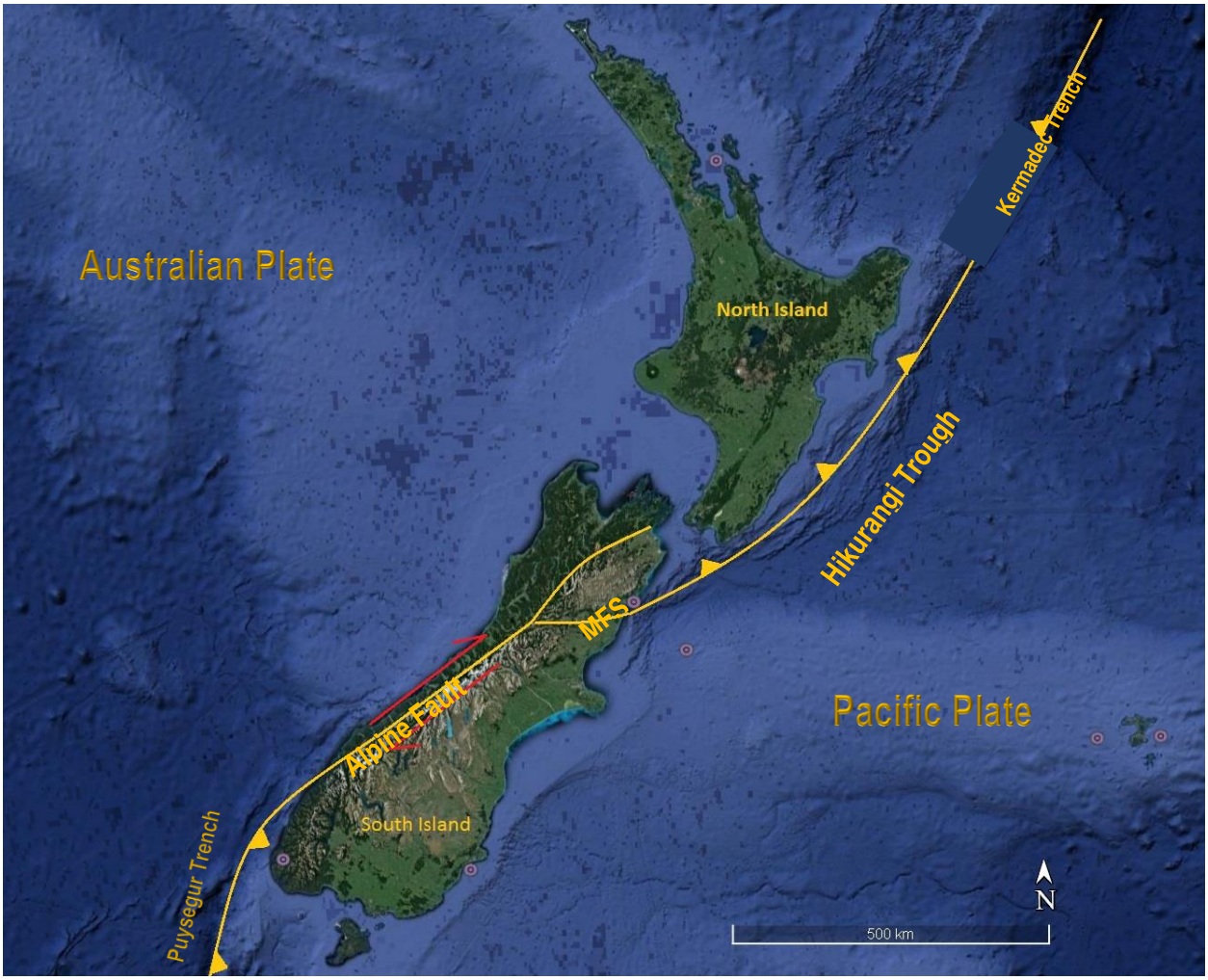

Figure 2.1 Tectonic setting of New Zealand. Base map sourced from Google Earth Pro (2020).
MFS= Marlborough Fault System

cool and subside. While the ridge failure had occurred, the ridge between Australia and Antarctica was re-activated c. 53 million years ago and continued to spread, contributing to the development of the mid-Pacific spreading ridge which was further linked to the spreading ridges in the Indian Ocean. Zealandia was mostly submerged with small, low-lying land areas c. 30-25 million years ago (Ballance, 2009; Mortimer, 2004). With the continuation of the spreading of the mid-Pacific, a new Australian/Pacific plate boundary was created c. 45 million years ago and continues to spread to date (Ballance, 2009). Arc volcanism in the North Island began c. 25-15 Ma along the Northland Arc (Adams et al., 1994; Balance, 2009; Kear, 1994). During this time, the spreading of the Norfolk Basin, located northwest of the North Island, caused the Three Kings Ridge (east of the Norfolk Basin and north of Northland) to converge with the Pacific Plate, resulting in the formation of a trench, which eventually began to generate a volcanic arc (Ballance, 2009; Hayward et al.,2001). The Northland Volcanic Arc was grouped into a subaerial and submarine volcanic belts that run through the sides of the Northland Peninsula and comprise early Miocene volcanic complexes and centres. Between 25-15 million years ago, after extending south to the Great Barrier Island north of Coromandel, volcanism along the Northland Volcanic Arc ceased and was followed by the overprint of a younger, northeast-trending Coville-Taranaki Arc (15-5 Ma) (Adams et al., 1994; Ballance, 2009). Since c. 4 Ma, the extension of arc volcanism continued to migrate southward, from the Coromandel Volcanic Zone (CVZ) to the Tauranga Volcanic Centre (TgaVC) and eventually to the currently active Taupo Volcanic Zone (TVZ) which has been active since c. 2 Ma (Ballance, 2009; Gibe 2010).

2.1.3 Volcanism in the North Island

Volcanism in the North Island is either subduction-related or intraplate-related. Subduction-related volcanism in the North Island occurs in relation to the westward subduction of the Pacific Plate beneath the Australian Plate. Volcanic activity within the eastern parts of the North Island are related to subduction processes; from the andesitic CVZ, in the northeast, towards the predominantly rhyolitic TVZ in the south (Shane, 2017). Volcanism within the eastern parts of the North Island predominantly produces andesitic/rhyolitic compositions (Kear, 2010). Intraplate volcanism in the North Island is confined to two extensional domains located behind the active volcanic arc (Sprung et al., 2007). These two domains are: 1) Northland Volcanic Province (active between 9.7 Ma- 13 ka) and 2) Auckland Volcanic Field (active between 2.69 Ma – 500 a.). Volcanism along the western parts of the North Island are mainly andesitic/basaltic in composition (Kear, 2010).

2.1.4 Coromandel Volcanic Zone

The Coromandel Volcanic Zone or CVZ is in the northeast of the North Island. The CVZ covers Great Barrier Island, Coromandel Peninsula and the Kaimai Range with evidence of basalts, andesites and rhyolites (Ballance, 2009; Booden et al., 2012). The CVZ extends for approximately 250 km in a NE-SW direction, from Great Barrier Island to beyond the Tauranga area (Booden et al., 2012; Briggs et al., 2005; Moore, 2013) as can be seen in Figure 2. Arc volcanism began between mid-Miocene to the earliest Pliocene in the CVZ, located northwest of present-day Taupo Volcanic Zone (TVZ) (Booden et al., 2012). The CVZ is complex in that it contains the overlapping portions of two separate volcanic arc systems: the purely andesitic Northland Volcanic Arc and Colville-Taranaki Arc (Ballance, 2009). Volcanic activity along the Northland Arc was purely andesitic. The two volcanic arc systems and their respective deposits, overlap each other at a 90° (Ballance, 2009; Booden *et al*., 2012).

Volcanic successions in the CVZ overlie Mesozoic metasedimentary basement rocks with complete coverage toward the southern parts of the volcanic zone compared to the northern parts (Booden *et al*., 2012). These volcanic successions are divided into three groups: Coromandel Group (18-3.8 Ma), Whitianga Group (9.1-2 Ma) and Mercury basalts (6.0-4.2 Ma) (Booden *et al*., 2012). The widespread Coromandel Group is comprised of andesite and dacite that "formed massive lava flows, breccias, lahars, tuff, dykes and tonalite plutons," (Hamilton et al., 2019, p. 210) sourced from eruptions at vents in the Coromandel Peninsula (Booden et al., 2012; Leonard et al., 2010). The Whitianga Group is formed by rhyolites sourced from volcanic centres and mainly occur as lavas and ignimbrite sheets on the Great Barrier Island and the eastern parts of the Coromandel Peninsula (Booden et al., 2012; Leonard et al., 2010). The Whitianga Group is further divided into three subgroups: the ignimbritic Coroglen and Ohinemuri subgroups and rhyolitic lavas of the Minden subgroup (Booden et al., 2012). The Mercury Bay or Mercury Basalts are basaltic and basaltic andesitic remnants of mainly strombolian volcanoes and dykes, erupted in the northern and eastern parts of the Coromandel Peninsula and Great Barrier Island (Booden et al., 2012; Hamilton et al., 2019).

2.1.5 Taupo Volcanic Zone

The TVZ is New Zealand's current active volcanic arc and is the world's most productive zone of silicic volcanism (Ballance, 2009; Wilson et al, 1995). The volcanic rocks of the TVZ are primarily "calc-alkaline andesites and dacites, high-Mg andesites, rhyolites and high-Al basalts" (Booden et al. 2012, p. 30). TVZ has been active since c. 2 million years ago and lies within a tectonic rift that is extending at a rate of approximately 7 mm/year (Ballance, 2009; Wilson et al, 1995). The TVZ is approximately 250-300 km in

length and up to 60 km wide (Houghton et al., 1995; Shane, 2017) and extends from White Island (an active andesite-dacite stratovolcano), off the coast of the Bay of Plenty, to the SSW Tongariro Volcanic Centre, terminating at Mt. Ruapehu (Figure 2.2) (Ballance, 2009; Spinks et al, 2005; Wilson *et al*., 1995). TVZ is divided into three segments; the andesitic to dacitic northern and southern segments, while the central segment is dominated by rhyolitic caldera volcanoes (Ballance, 2009; Houghton et al., 1995; Spinks et al., 2005 Wilson et al., 1995) as can be seen in Figure 2.2.

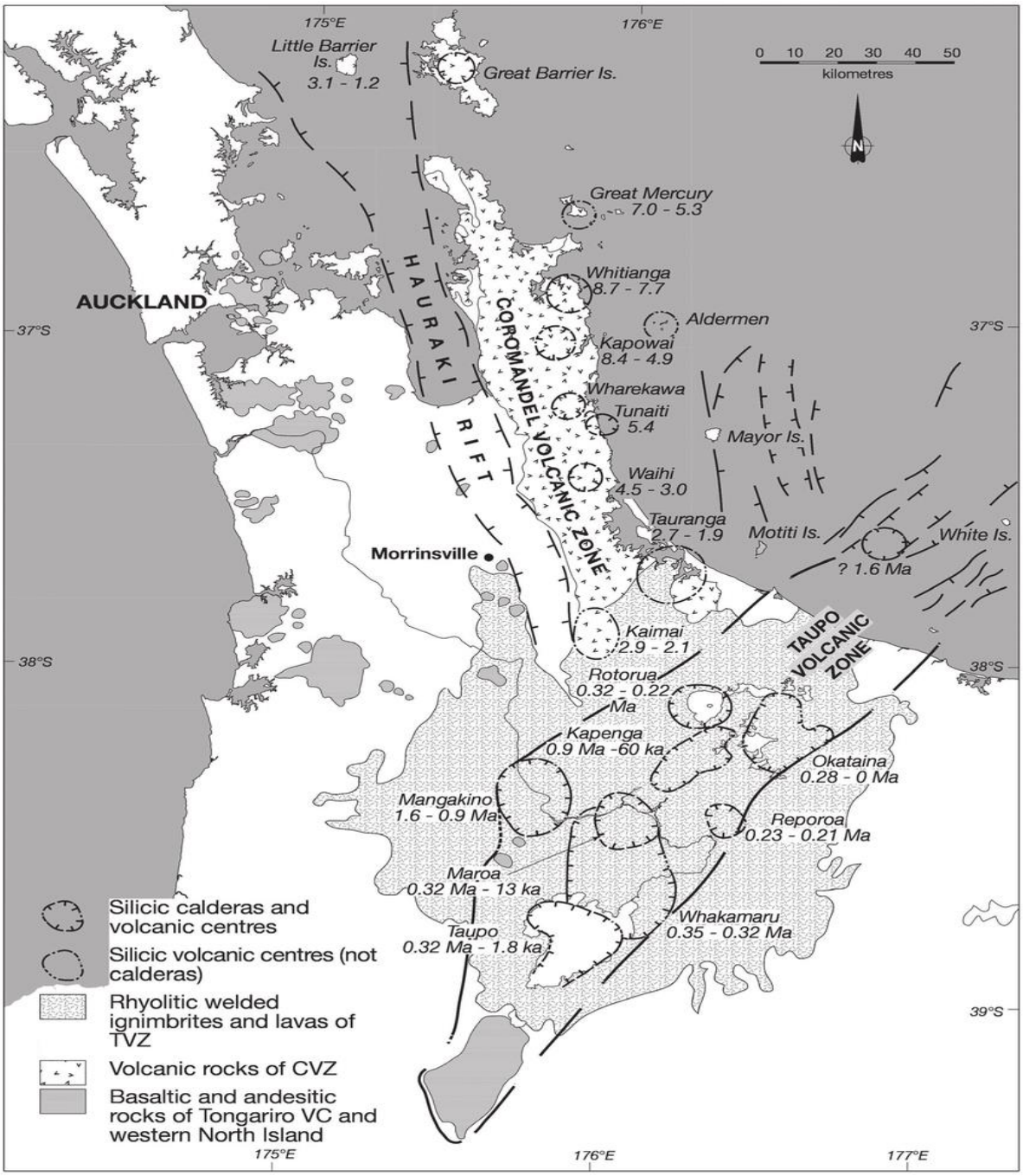

Figure 2.2 Map of northern and central North Island showing the Taupo and Coromandel Volcanic Zones, the Hauraki Rift, and the location of silicic calderas and volcanic centers since 10 Ma. Adapted from Briggs et al. (2005).

2.2 Tauranga Volcanic Centre

The Tauranga Volcanic Centre or TgaVC is located between the CVZ and TVZ (Figure 2.2). Volcanism in the Tauranga area occurred during late Pliocene to Pleistocene (Briggs et al., 1996). The TgaVC includes the Minden Rhyolite domes and lava flows in the southeastern parts of the Tauranga basin (Briggs et al. 1996; Briggs et al., 2005; Hollis, 1995). The boundary and size of the TgaVC are not known due to the lack of distinct geomorphological evidence for a caldera(s), the superposition and obscuring of TgaVC-deposits by younger ignimbrites sourced from the TVZ, and the infilling of boundaries and/or structures by large amounts of volcanoclastic material (Briggs et al., 2005). Volcanic units in the TgaVC and their respective ages are presented in Figure 2.3. The Minden Rhyolite domes are mainly of late Miocene-Pliocene in age and include all the rhyolites in Tauranga and Bay of Plenty regions (Briggs et al., 2005). Briggs et al. (2005) further divided the Minden Rhyolite domes and lava flows into four groups (Minden Peak, Mount Maunganui, Mangatawa, Mount Misery) according to their spatial association, minerology and geochemical properties. The geochemical properties of silicic rocks in the TgaVC demonstrate close similarities to those from the TVZ, i.e. they are calc-alkaline and contain similar major and trace element and isotopic compositions (Briggs et al., 2005).

A detailed study by Hollis (1995) investigated the stratigraphy and geochemistry of the volcanic geology of the Central Tauranga Basin and compared the results obtained to that of the volcanic geology of CVZ and TVZ. The study discovered that the geochemistry of the ignimbrites (Waiteariki Ignimbrite, Te Puna Ignimbrite, Te Ranga Ignimbrite, Waimakariri Ignimbrite) are characteristic of subduction-related arc magmatism as exemplified by the geochemistry of the volcanic rocks found in the TVZ. The study also found that the Matakana Basalts possess a similar geochemistry to that of basalts from the TVZ, i.e., the Matakana Basalts are calc-allkaline and of a high alumina content. Based on these findings, the study proposed that the Matakana Basalts were probably sourced from the mantle wedge subduction boundary in a similar fashion as that of the TVZ basalts. Overall, the study concluded that, although the Tauranga Basin comprises members of both the CVZ and TVZ, the volcanic rocks in the Central Tauranga area are of a closer resemblance to the TVZ than CVZ.

The southern migration of silicic volcanism from the CVZ to the present-day TVZ was determined to have occurred between 1.90-1.55 Ma (Briggs et al. (2005). The similar geochemistry and age (c. 2 Ma) of the youngest silicic units (Upper Papamoa Ignimbrite; Otanewainuku and Puwhenua domes) in the TgaVC and

the oldest in the TVZ, suggest that the silicic volcanism from both volcanic zones had originated from the fractionation and partial melting of the crust. The transition period of silicic volcanism from CVZ to TVZ was a significant period in the volcano-tectonic history of New Zealand as it marked initiation of volcanism of the Kermadec arc, the development of the Hauraki Rift, "extensional block faulting in western North Island" (Briggs et al., 2005, p. 465) and a significant rise in the silicic volcanic activity in the TVZ.

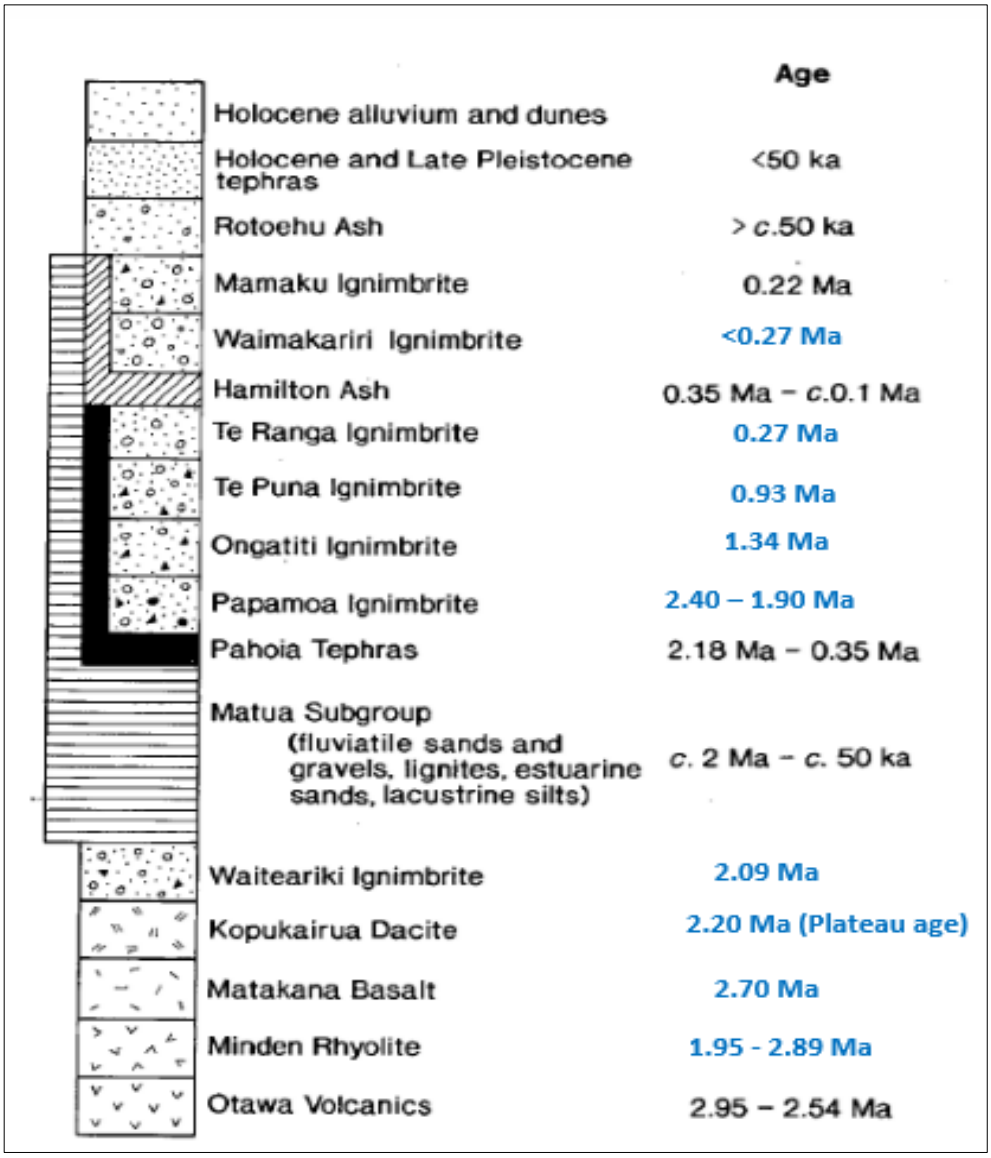

Figure 2.3 General Stratigraphy of the Tauranga Area from Briggs et al. (1996) and modified by 40Ar/39Ar ages (in blue) from Briggs et al. (2005).

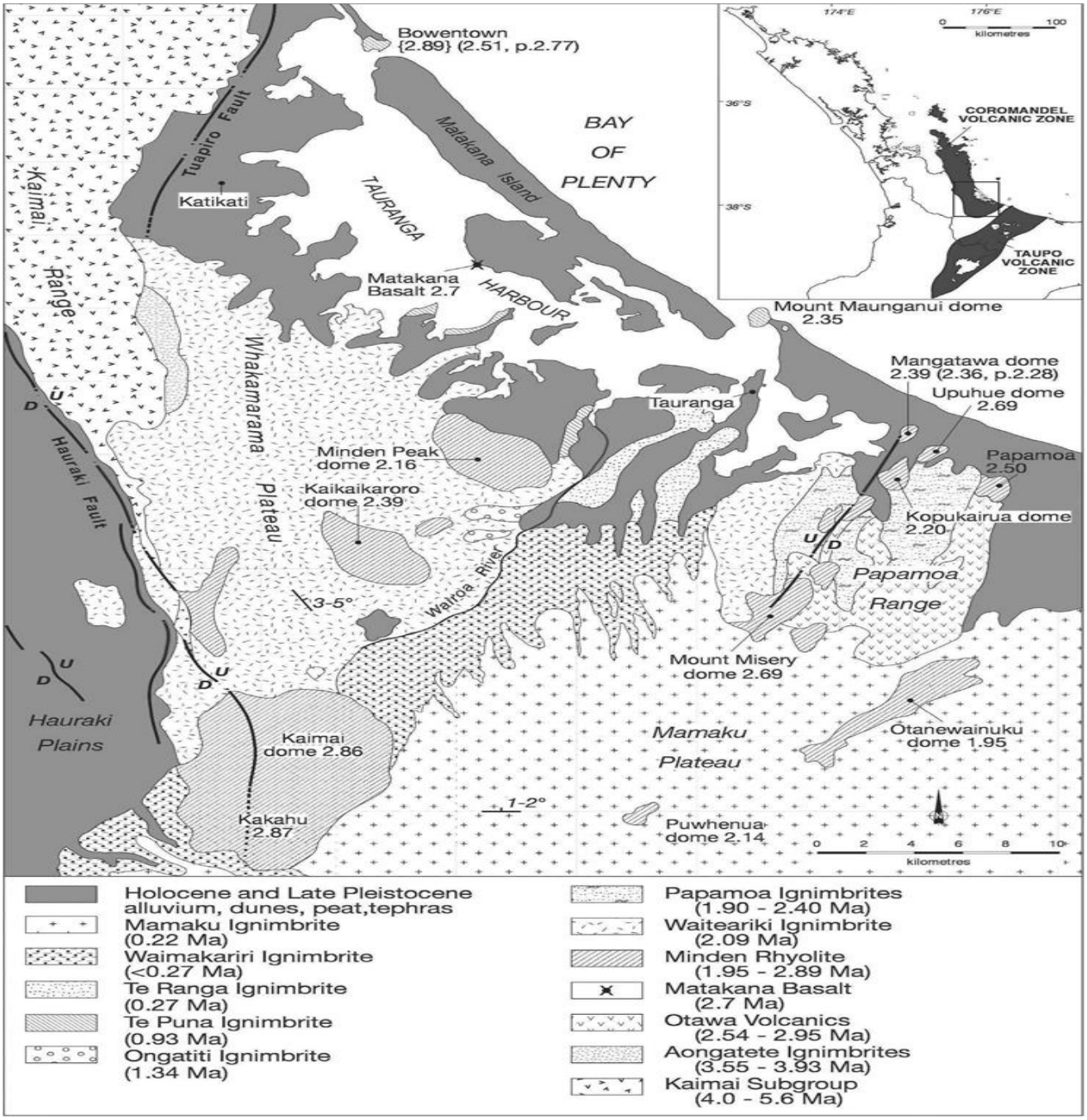

Figure 2.4 Geological map of Tauranga and southern Kaimai Range showing the distribution of rhyolite and dacite domes and their 40Ar/39Ar ages (adapted from Briggs et al., 2005).

2.2.1 Kaimai Volcanic Centre

The Kaimai Volcanic Centre or KaiVC is defined by the southwesterly spatial separation of the Kaimai and Kakahu domes from the other domes in the Tauranga area (Figure 2.2) and was active between 2.87-2.09 Ma (Briggs et al., 2005). The boundaries of the KaiVC are poorly defined due to the lack of exposure, being overlain by younger ignimbrites, the voluminous Waiteariki Ignimbrite and the displacement caused by the Hauraki Fault (Briggs et al., 2005). The Kaimai dome is the largest lava dome, located south of the Kaimai Range, through which the Hauraki Fault runs and is overlain by the Waiteariki, Waimakariri and Mamaku ignimbrites to the north, south and east, respectively (Briggs et al., 2005). Although the typical geomorphological characteristics of calderas are not evident, the surface exposure of voluminous rhyolitic lava suggests that the KaiVC was once a major rhyolitic volcanic centre in the southern Kaimai Range (Briggs et al., 2005).

2.2.2 Papamoa Ignimbrite

The Papamoa Ignimbrite occurs in the eastern parts of the Tauranga area (Figure 2.4). It possesses a confined fan distribution along the foothills and valleys of the Papamoa Range, dipping gently to the north (Briggs et al., 2005). The Papamoa ignimbrite is predominantly dacitic and contains juvenile scoria and pumice clasts with a range in composition from basaltic-rhyolitic (Briggs et al., 2005; Hughes, 1993). In a study on the volcanic geology of the Eastern Tauranga Basin and the Papamoa Range, Hughes (1993) discovered that the Papamoa Formation consisted of an upper (Upper Papamoa Ignimbrite) and a lower (Lower Papamoa Ignimbrite) unit. Briggs et al (2005) determined the age of the Papamoa Formation using $^{40}Ar/^{39}Ar$ dating and concluded that the ages of the upper and lower Papamoa Ignimbrites were c. 2.4 Ma and c. 1.9 Ma, respectively. Although the upper and lower Papamoa Ignimbrites outcrop as bluffs and cliffs and are petrographically similar, the lithology of the two units are different (Hughes, 1993). Hughes (1993) discovered that the lower Papamoa outcrop comprised of five different types of pumice and one scoria and described the unit to be weakly welded. In contrast, the studied upper Papamoa outcrops showed a uniform lithology, texture and an overall, welded structure (Hughes, 1993). By studying the petrology and geochemistry of the five different pumice types, Hughes (1993) proposed that the Lower Papamoa Ignimbrite was sourced from a fissure-type eruption with multiple vents. However, there is no physical evidence of a

fissure in the study area, it is thought to be possibly buried by sediments (Hughes, 1993). Study of the spatial association, mineralogy and geochemistry of the Papamoa Ignimbrite, suggest that the Papamoa Ignimbrite was sourced locally from the eastern TgaVC. (Briggs et al. 2005). To date, the source of the Papamoa Ignimbrite remains to be determined.

CHAPTER 3

STRATIGRAPHY

This chapter presents the internal stratigraphy of the Papamoa Formation as observed in the study area. The new stratigraphic framework proposed for this study area provides a better understanding of the landscape evolution and the source of the ignimbrites within the Papamoa Formation. A total of 14 localities (shown in Figure 3.1) are included in this study, a table of which is presented in Appendix 1. There is a group of localities which display the best exposure of the Papamoa Formation and other geological units, a detailed stratigraphic description will focus on these localities. Descriptions of other localities will also be presented.

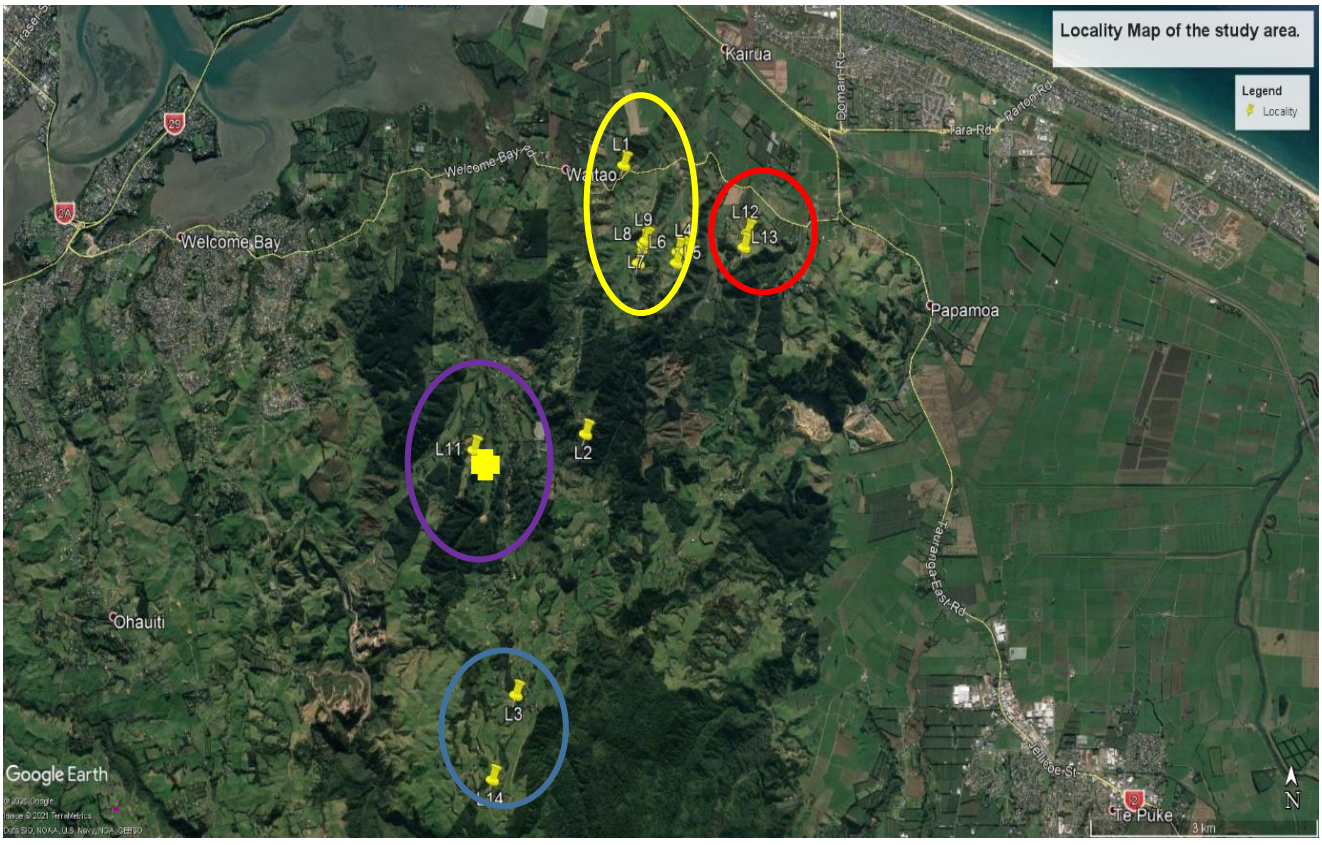

Figure 3.1 Locality map of the study area. (Base map sourced from Google Earth Pro, 2021). The circles indicate the groups of localities which were worked on. Red circle: Northern Reid Road (L12, L13), Yellow circle is the localities east of the Rocky Cutting Road (L1 and L4 – L9), Purple: Northern Waitao Road: (L11 and L10) and the Blue circle are the localities south of the Waitao Road.

3.1 Field methods

The stratigraphy of the study area was achieved by making field study of the outcrops at each of the 14 localities. Field study comprised of making observations (measuring the thickness of the outcrop, describing the lithology of each of the outcrop units and sampling), stratigraphic logging, field photography and from relevant previous and present literature of works carried out in the study area. The localities (Localities 1 - 14) in the study area are numbered in the order in which they were visited, i.e., in chronological order from first visited area to the last visited site. The localities are grouped according to where they occur in the study area. The groups of localities are: 1) East of Rocky Cutting Road (comprising of the "Addline Sequence"), 2) Southern Waitao Road, 3) Northern Reid Road and 4) Northern Waitao Road. A composite stratigraphic log is presented for each group of localities.

The stratigraphic logs presented in this chapter have been drawn according to the ages of the deposits. Where the age is not available, where the deposits are positioned in the study area in relation to the other geological units. An unpublished date of 2.26 Ma for the Wharo Ignimbrite was provided by Prentice (2021). The age for the Otawera Ignimbrite is sourced from Pittari et al. (2021) and is 2.21 Ma. With regards to the Welcome Bay Ignimbrite, the Ar^{39}/Ar^{40} age provided by Briggs (2005) of 2.9 Ma is used. The Arateka Ignimbrite is yet to be aged and is therefore positioned in the stratigraphic log (Figure 3.17) as observed in the study area.

3.2 Overall Stratigraphy and Geomorphology

The Papamoa Formation in the study area comprises of the newly-defined Wharo Ignimbrite, Welcome Bay Ignimbrite, Otawera Ignimbrite and Arateka Ignimbrite, with intercalated unnamed pyroclastics. The geomorphology of the study area consists of ridges that are topped with either bluff-forming ignimbrites or rolling hills (Figure 3.2). These ridges naturally dip into narrow or wide valleys, through which, in some localities, there are streams. Throughout the field area, some of the ignimbrites at the studied localities occur along the same ridge (e.g., L 8 and L 9), exposed as continuous, non- to partially welded bluffs or cliffs. Some of the ignimbrites of the Papamoa Formation fan out at the foothills of the Papamoa Range (Hughes, 1993)

or along valley walls. Most of the ignimbrites are completely covered by commercial pine forest, pastures, and/or bush.

Figure 3.2 Examples of the typical Papamoa Ignimbrite landscapes from some of the localities within the study area. (A) A bluff outcrop of the Wharo Ignimbrite studied at Locality 14. (B) Bluffs of the Wharo Ignimbrite at Locality 13. (C) The Welcome Bay Ignimbrite at Locality 4.(D) Bluff forming Welcome Bay Ignimbrite that was studied at Locality 4 at the forefront. The same ignimbrite (recorded as Locality 6) can be seen in the background, forming the ridge.

Within the field area, the property with the best exposure of the Wharo and Welcome Bay Ignimbrites of the Papamoa Formation as well as other geological units is 940 Welcome Bay Road and comprises Localities L4, L5, L6, L7, L8 and L9. In this thesis, the outcrops studied in these localities are referred to as the "Addline Sequence." In the southwestern parts of 940 Welcome Bay Road, L6 and L4 occur as bluffs along ridges and are composed of the pumice-rich Welcome Bay Ignimbrite, which Hughes (1993) had identified as the Lower Papamoa Ignimbrite. Between the ridges on which L4 and L6 occur, the Wharo Ignimbrite at L5 outcrops as bluffs along a valley wall. At Locality 7, there are four units: from the bottom of the valley upwards, Unit A is overlain by Unit B, which is then overlain by a fall deposit (Unit C), then by an ignimbrite (Unit D, the Welcome Bay Ignimbrite). The top boundary of Unit D at L7 is not exposed, until the outcrop emerges again further up the valley slope at L8.

3.3 East of Rocky Cutting Road

Introduction

This section of the field area occurs on the property behind the Addline Transport company (off Welcome Bay Rd) and includes roadside outcrops surrounding the property on Welcome Bay and Rocky Cutting roads. Most of the Papamoa Formation in this section of the study area form ridges or infill palaeovalleys and are exposed along road cuttings or as bluffs on private farmland.

Localities 1 and 2 are road cuttings along Welcome Bay Road and Rocky Cutting Road, respectively.

Localities 4 to 9 are all located on the farm property south of Welcome Bay Road. This location is a good geological representative of the study area as it contains deposits of both the Welcome Bay and Wharo ignimbrites, as well as other deposits which will assist in a better understanding of the eruption history of the Papamoa Formation. Localities 4, 6, 8 and 9 occur as bluffs on ridges and alongside farm track cuttings while L5 and L7 are located within valleys. Locality 7 is referred to in this research as the "Addline Sequence" and is comprised of four different units. The Addline Sequence is bounded to the north by pastures, trees and bush to the south and a farm track runs through the locality from east to west and vice versa. The other localities on this farm are surrounded by pastures.

Lithology

Locality 1: Wharo Ignimbrite, Welcome Bay Road

The outcrop along Welcome Bay Road comprises a massive deposit with a greyish-brown colour. The deposit is ~7 m thick and ranges from weakly welded in the lower ~5 m to a densely welded in the upper ~2 m of the deposit (Figure 3.3). Above the mid-way mark of the unit, there are vertical joints of ~1.5 m in height and a horizontal spacing of 0.5 – 0.7 m. Pumice abundance is 15 % while lithics have an abundance of 7 %. Flattened and/or lenticular pumice and fiamme are present in the outcrop. The flattened pumice and fiamme are purple-coloured in the lower 1-2 m of the outcrop, have a woody texture and are phenocryst-poor. The ignimbrite matrix, on the other hand, is crystal-rich. Lithics were observed to be brown- to black-coloured andesites

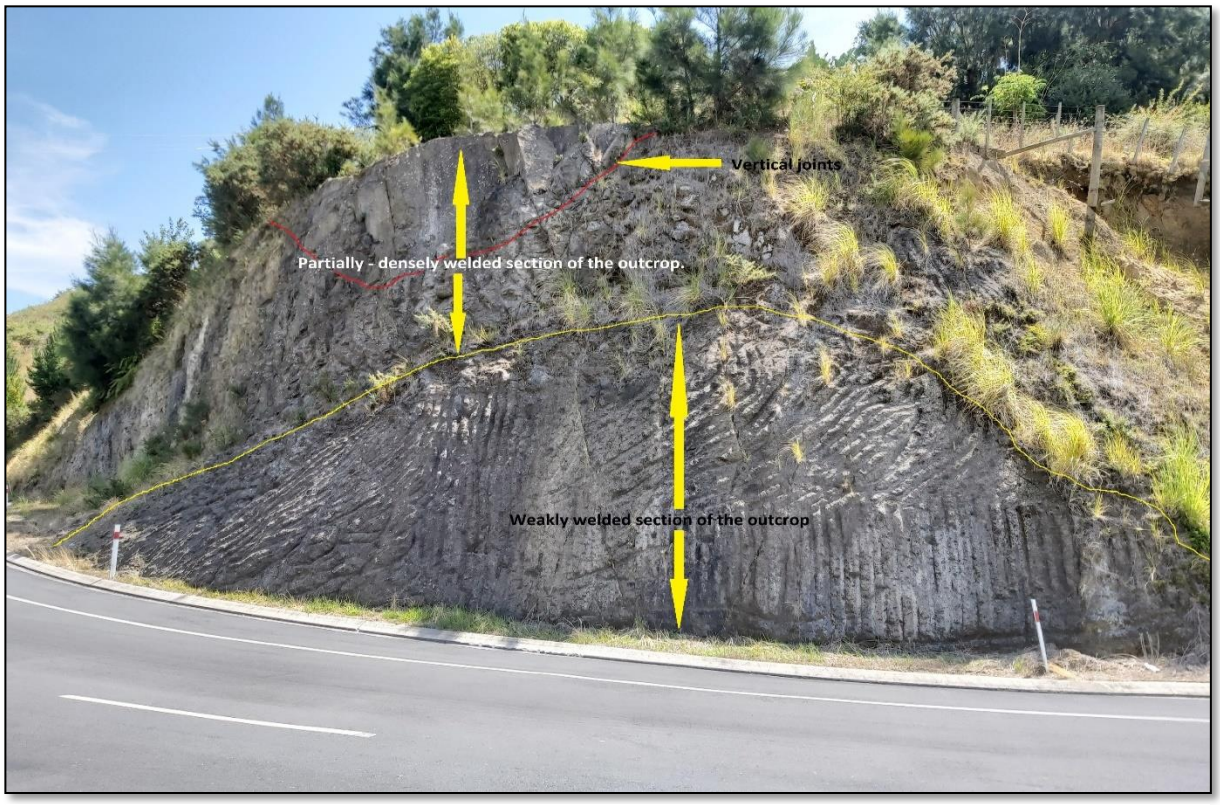

Figure 3.3 The studied outcrop at Locality 1 shows an increasing degree of welding with height. Vertical joints can be seen in the mid-section of the top of the outcrop.

Locality 2: Welcome Bay Ignimbrite, Rocky Cutting Road

The outcrop at Locality 2 (Fig. 3.4a) comprises massive and light brown to beige coloured ignimbrite that is ~ 15 m thick and shows irregular jointing of 3 m spacing. Pumice and lithic abundance at the bottom 2 m of the deposit is 30% and 15 – 20% respectively. The average clast size at the bottom 2 m of the whole outcrop is fine to medium lapilli. Figure 3.4B shows the poorly sorted ignimbrite, with the pumice clasts protruding out of the outcrop. In Figure 3.4C, a closeup of the same ignimbrite is shown with the two pumice types and grey andesitic lithic clasts.

Figure 3.4 ***A*** *Welcome Bay Ignimbrite at Locality 2.* ***B****: A close-up of the Welcome Bay Ignimbrite showing pumice clasts embedded in a fine-grained matrix. Pumice and lithic/scoria clasts can be easily plucked out of the massive outcrop.* ***C:*** *The close-up shows the different pumice types (black and white coloured) and lithics, set in a fine-grained matrix. BP=black pumice, WP=white pumice, L=lithics (Photo courtesy for images B and C: M. Prentice, 2020).*

Locality 4: Welcome Bay Ignimbrite

The deposit at Locality 4 (Figure 3.5) is massive, beige in colour, moderately welded, poorly sorted and pumice-rich. The exposed outcrop is ~6.5 m thick. At a height of 1 m above ground level, there are black to dark brown and white pumice clasts. These different pumice clasts can be seen in both Figure 3.6 A and B. Some of the pumice found at this height are flattened or lenticular (Figure 3.6 A). Lithics are grouped together

with scoria as some clasts could not be easily differentiated. Pumice and lithic clast abundances are 25-30 % and 10-15 %, respectively. The average maximum size for pumice is 82.4 mm while for lithics, it is 18 mm. From 2 to 2.3 m above ground level, the pumice abundance decreases to 20%. Similarly, the lithics abundance decreases to 5 %. Average maximum sizes for pumice and lithics are 54 mm and 20.8 mm, respectively. At 2.3 m to the top of the unit, reverse grading of pumice clasts is evident. At this height, the abundance of pumice is 25-30% while for lithics it is 15%. Average maximum sizes for pumice and lithics are 43.6 mm and 15.4 mm, respectively.

Figure 3.5 The Welcome Bay Ignimbrite at Locality 4.

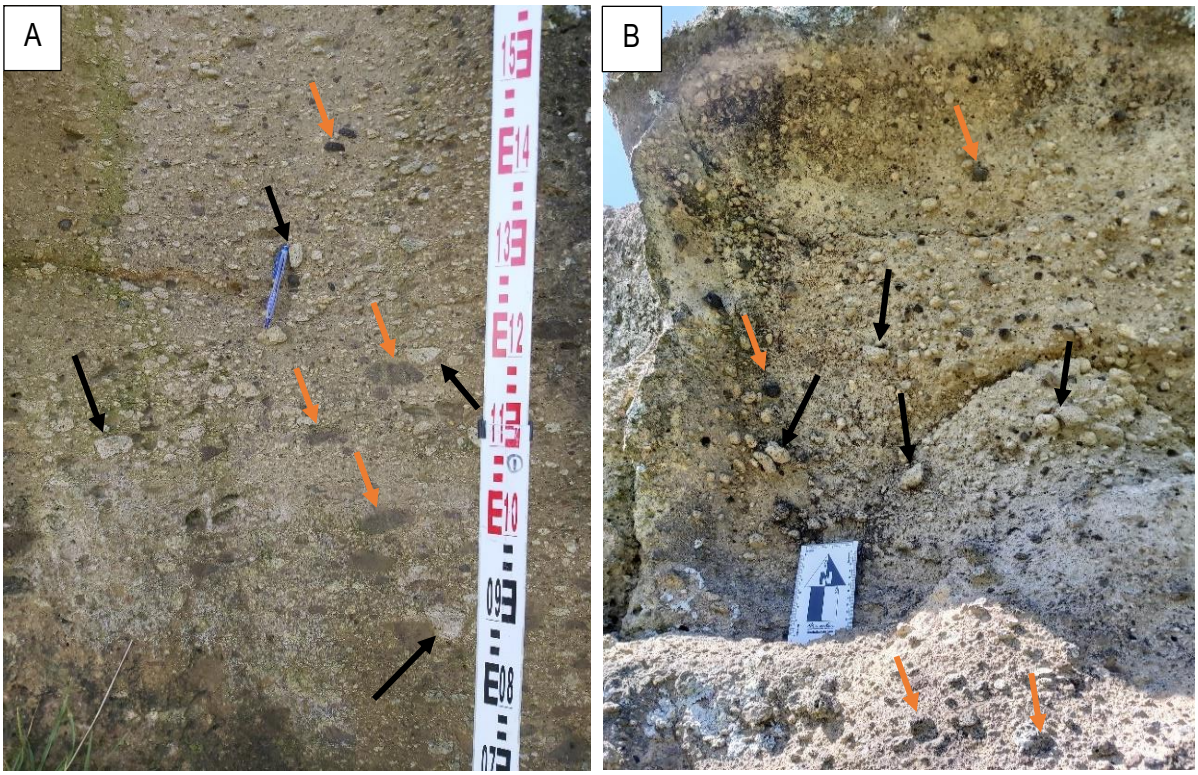

Figure 3.6 The Welcome Bay Ignimbrite at Locality 4 from 1 to 1.5 m. Some of the black and white pumice clasts are shown with orange and black arrows, respectively. Between 0.90 m and 1.2 m, some of the black pumice are flattened. The mechanical pencil is 14 cm. ***B****: A close-up of the Welcome Bay Ignimbrite at Locality 4, at 2.3 m. At this section of the outcrop, lithics/scoria are shown with orange arrows while the white pumice are shown with black arrows.*

Locality 5: Wharo Ignimbrite

The deposit at L5 is dark brown- to black-coloured, massive and moderately welded . The ~ 10 m thick section outcrops as bluffs on the side of a valley (Figure 3.7 A). The exposed base of the outcrop is softer (non-welded) than the moderately welded upper sections (Figure 3.7 B). The lithics are andesites and have an abundance that decreases with height, from 7-10% at 2 -3.3 m above the exposed base of the outcrop, to 3-5% at 3.3 m, to 2-3% above 3.3 m. In this outcrop of the Wharo Ignimbrite, it is mainly comprised of black pumice clasts (Figure 3.7 C). Although there was one or two pink pumice clasts, there was little to no white pumice clasts present. Pumice abundance was measured at the same heights and produced the following results: 20%, 15-20% and 25–30%, respectively. The average maximum pumice sizes, in order from the bottom of the outcrop to the top were: 25 mm (at 1 m above ground level), 50.6 mm (at 2-3.3 m), 43.2 mm (at 3.3 m) and 49.0 mm (above 3.3 m). Lithics, on the other hand had average maximum sizes of 23.4 mm

(at 1 m), 15.8 mm (at 2-3.3 m), 15.2 mm (at 3.3 m) and 15.5 mm (above 3.3 m). Hence the basal 1 m is characterized by having relatively smaller pumice and larger lithics compared to the upper part.

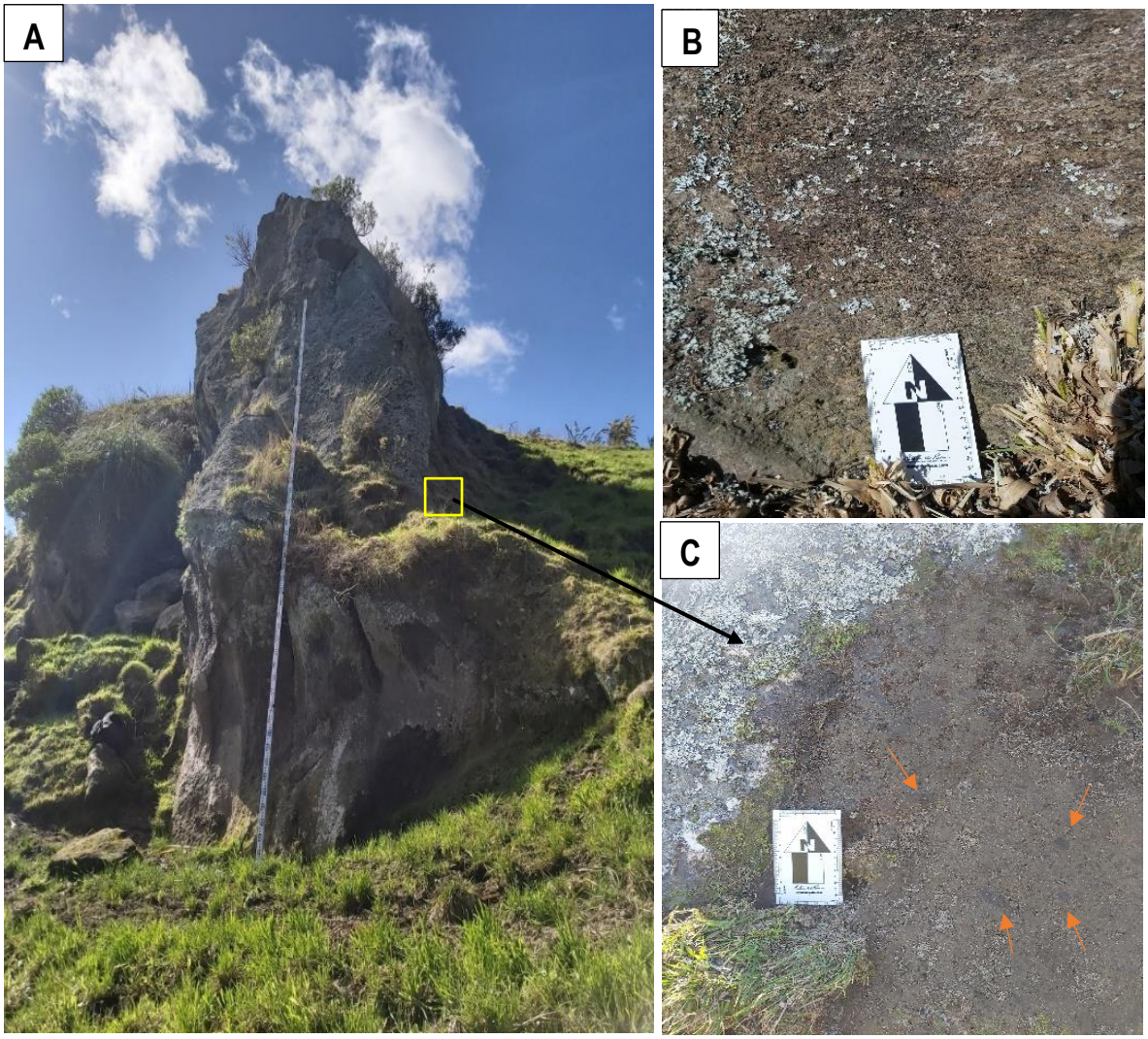

Fgure 3.7 ***A:*** *Bluff-forming Wharo Ignimbrite at Locality 5.* ***B:*** *Densely welded, top section of the Wharo Ignimbrite, parts of which are covered in lichen. Flattened pumice clasts can also be seen.* ***C:*** *Non- to weakly welded bottom section of the Wharo Ignimbrite. The orange arrows point to black pumice clasts.*

Locality 7: Addline Sequence

The Addline Sequence comprises of four discrete pyroclastic subunits of the Papamoa Formation (units A – D) at Locality 7. Unit D is the Welcome Bay Ignimbrite which also outcrops further up the valley at localities 8 and 9. A composite stratigraphic log of the Addline Sequence is provided in Figure 3.10 and shows the

stratigraphic relationship of the pyroclastic deposits with each other, the abundance (in percentages) and maximum sizes (in millimeters) of the pumice and lithic clasts in the four discrete ignimbrites, three (WBI, Wharo and L7/3-Unit B) of which were well exposed for measurements to be made. The unknown Ignimbrite or Unit A was poorly exposed therefore measurements could not be taken.

Unit A

Unit A (Figure 3.8 A) is a relatively non-weathered, greyish-white, deposit with iron mottles or iron staining. Only the upper ~0.20 m is visible above ground level. Unit A is possibly an ignimbrite with a glassy or pumiceous matrix and large angular lithic lapilli. The lithics are dark grey andesite, and the average maximum lithic size is 23 mm. Overall, Unit A is lithic-poor.

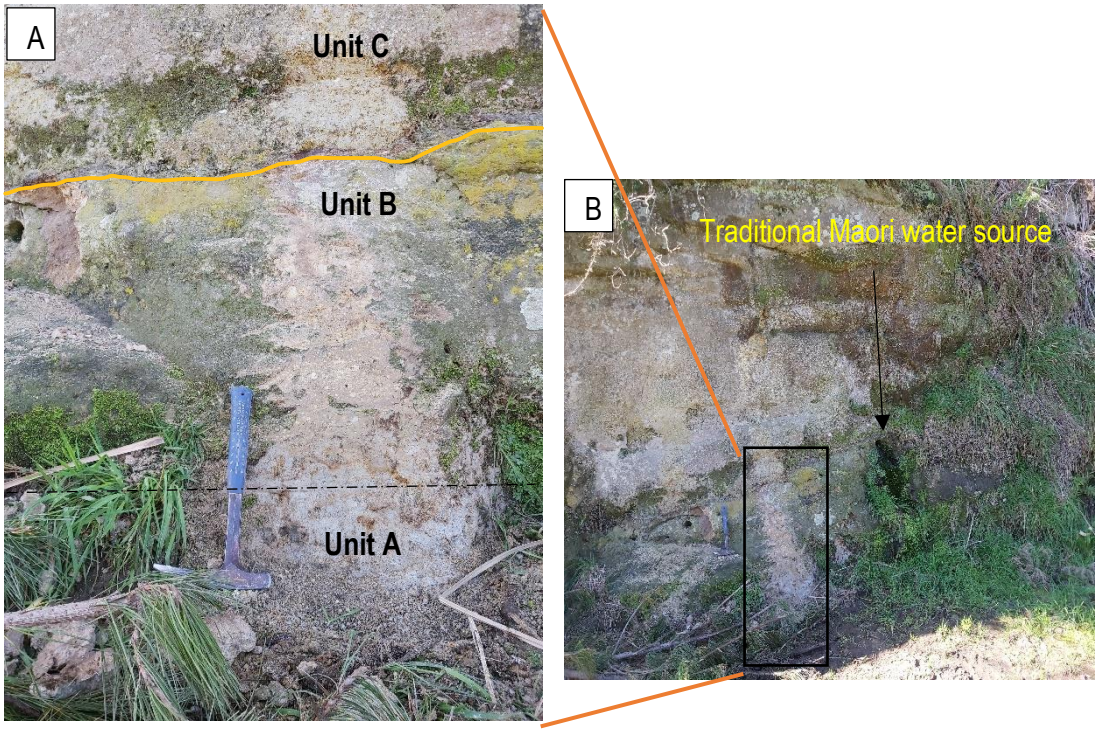

Figure 3.8 ***A*** *Photograph of Unit A at the base of Addline Sequence, and overlying units B and C. Red iron-rich stains or mottles can be seen in Unit A.* ***B:*** *Traditional Maori groundwater spring is shown with a black arrow.*

Unit B

Unit B is a silicified, non-welded but very hard deposit. The unit is ~0.60 m thick and it shares a gradational contact with Unit A (Figure 3.9 A). At approximately 0.05 m above the contact of Units A and B, is fine ash with coarse sub-angular pumice, lithics and fine matrix from the mid to upper sections of the Unit B. The colour of the deposit darkens with height, i.e., from brown at the base to dark brown towards the top of the unit. There is a lensoidal concentration of pumice and lithics further up the unit. The abundance of pumice and lithics vary laterally throughout the unit. Units B and C share a case-hardened, sharp contact with a thickness of approximately 2 cm. This sharp contact is shown with an orange line in Figure 3.8 A. In Figure 3.8 B, to the right of the studied section is a traditional Maori groundwater spring which was piped from within the rock units.

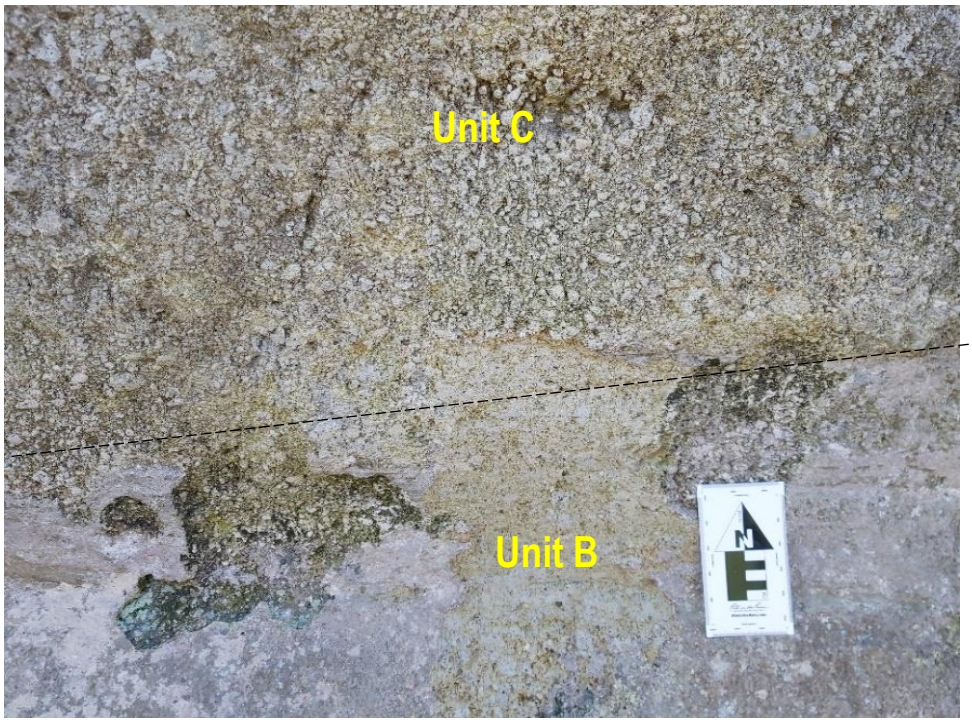

Figure 3.9 The airfall deposit, Unit C, of the Addline Sequence, overlying Unit B.

Unit C

Unit C is a mottled yellow white, well-sorted and massive fall deposit (Figure 3.9). The unit is ~1.2 m thick. This deposit is almost entirely made up of pumice lapilli but with a lithic abundance of 1 – 2 %. The pumice

clasts are of medium lapilli size and have a maximum average size range of 20.8-28.0 mm. At 0.12 m before the contact of Unit C and D, pumice size fines off to very fine lapilli. Lithics have an average maximum size range from 5.2 -10.6 mm.

Unit D

Unit D is a massive, poorly sorted ignimbrite with an orange-brown colour and is identified as the Welcome Bay Ignimbrite. The unit is ~8 m thick and is non-welded. At 1 m above the base of the deposit, the pumice abundance is 25-30% while the lithic abundance is 10%. There are two pumice clast types present: orange pumice and beige or white-coloured pumice. The two pumice types can be seen in Figure 3.10. The average maximum size for pumice clasts increases up the unit, ranging from 23 to 28.4 mm. Similarly, lithic size increases with height, the average maximum sizes range from 10.8 to 16.8 mm. Lithics are mostly dark grey andesite.

Figure 3.10 Unit D, showing orange (black arrow) and white/beige (yellow arrow) pumice clasts within in a fine-grained matrix.

Localities 8 and 9: Welcome Bay Ignimbrite

Localities 8 and 9 are approximately 20 m apart and outcrops occur along a road cutting and as bluffs, approximately 60 m in elevation above the top of the sequence at Locality 7. The deposit at L8 is a massive, brown and pumice-rich ignimbrite (Figure 3.11 A), identified as the Welcome Bay Ignimbrite. The unit is ~7 m thick, is poorly sorted and non-welded. There are three types of pumice clasts: white, orange and white with orange bands. This unit has fewer orange pumice (Figure 3.11 B) than that observed in Unit D at Locality 7. The pumice clasts are medium to very coarse lapilli. Throughout the whole unit, the abundance of pumice is 25 % while that of lithics is 1 %. At 1 m above the ground level of the outcrop, the average maximum pumice and lithic sizes are 36.1 mm and 13.4 mm, respectively.

Similar to the ignimbrite in L8, the deposit at L9 is a massive (Figure 3.11 C), greyish brown pumice-rich ignimbrite. The unit is ~ 10 m thick and is also non-welded and poorly sorted. In contrast to L8, the sizes of the pumice clasts in L9 range from very coarse lapilli to bombs. Throughout the whole outcrop, the pumice and lithics abundances were uniform at 30% and 7%, respectively. As at L8, there are also two main types of pumice clasts at L9, classified according to their colours: dark grey and white, with the odd grey-banded pumice clasts (Figure 3.11 D). The average maximum sizes for pumice and lithics are 70.5 mm and 12.4 mm, respectively. In contrast to L8, cavities with diameters of up to 70 mm (Figure 3.11 C) can be seen, covering an area of ~ 6 x ~1 m^2 on the outcrop at L9. The cavities are thought to be the result of plucked or fallen pumice clasts due to some form of weathering.

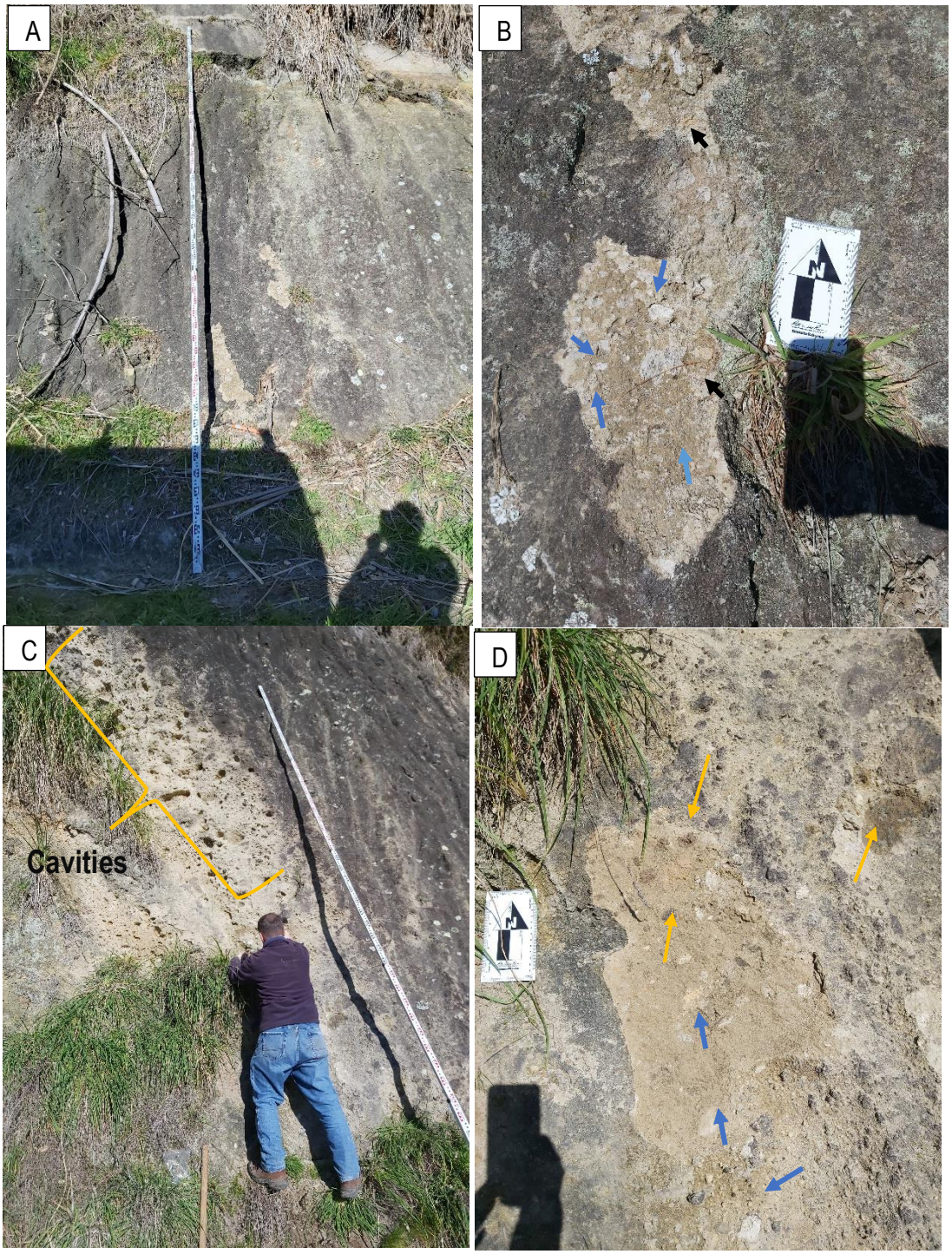

Figure 3.11 **A and B:** Outcrop at Locality 8, forming bluffs along a ridge, through which a farm track runs through. **B:** Both white (shown by blue arrows) and pink (shown by black arrows) pumice clasts can be seen, embedded in a fine-grained matrix. **C and D:** Outcrop at Locality 9 which occurs as bluffs on the same ridge as that of Locality 8. **C:** Big cavities on a section of the outcrop at L9. **D:** Grey (orange arrows) and white (blue arrows) set in a fine-grained matrix at L9.

ADDLINE SEQUENCE STRATIGRAPHIC LOG

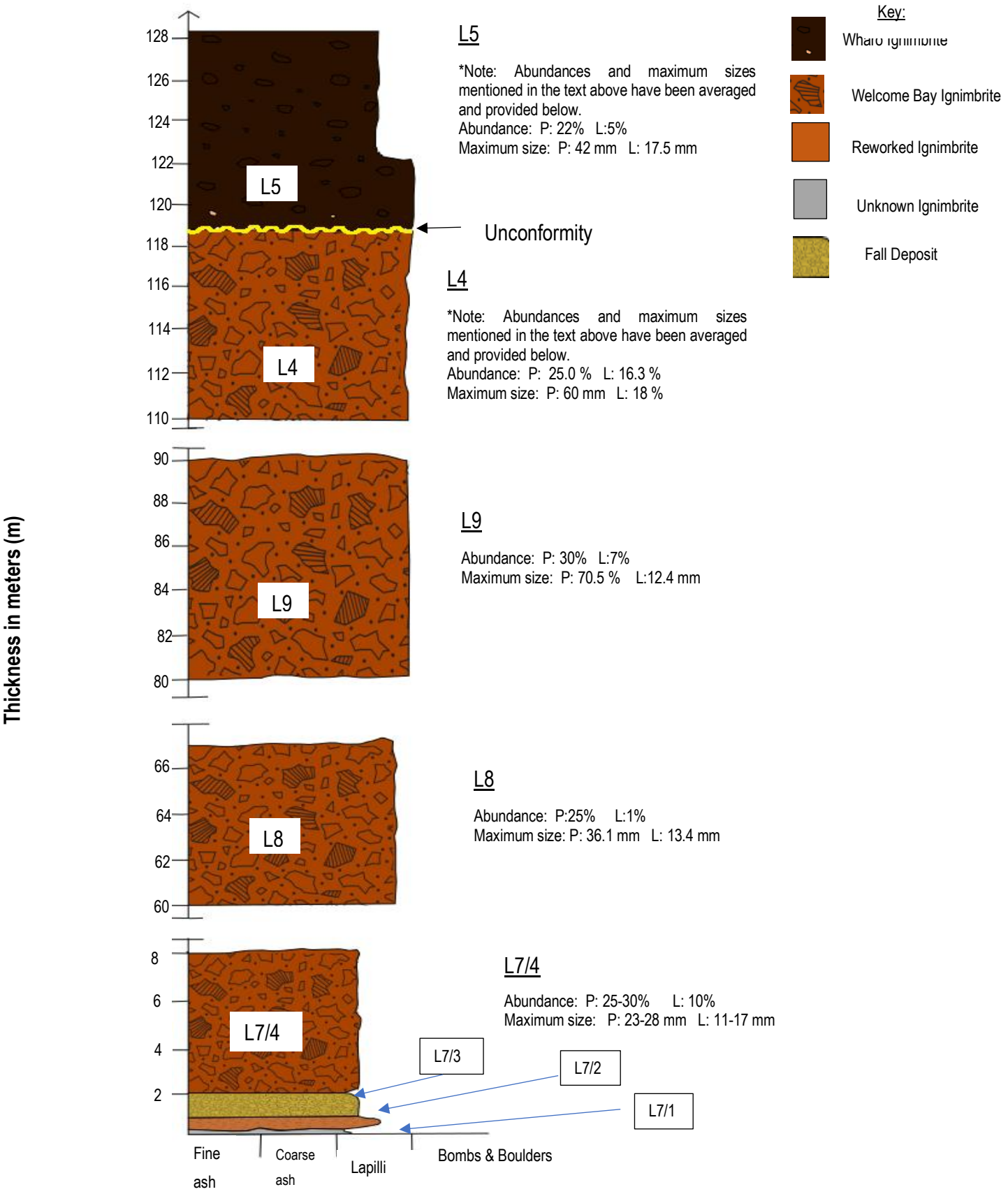

Figure 3.12 Stratigraphic log of the Addline Sequence. P=pumice, L=lithics

3.3 Southern Waitao Road: Wharo Ignimbrite

Introduction

Locality 3 is situated along the southern parts of the Waitao Road. The deposit (Figure 3.13 A) outcrops on a hillside, at ~325 m above sea level, on a private farm property. Located southwest of L3 and being the southern-most part of the study area is Locality 14 (Figure 3.13 A). The studied outcrop at L14 occurs as bluffs and monoliths along a ridge which dips slightly to the north into a valley. The monoliths form the highest point in the study area, standing at ~450 m above sea level. Surrounding the monoliths and bluffs along the ridge are pastures for livestock grazing and bush. The bluffs have vegetation growing on sections throughout the outcrop. especially on the top of the outcrop (Figure 13 A and B).

Figure 3.13 ***A:*** *Bluff-forming Wharo Ignimbrite at L14, topping a ridge along the southern Waitao Road.* ***B:*** *The location where L14/1 (yellow star), L14/2 (blue) and L14/3 (black) were sampled and described.*

Lithology

At Locality 3, the deposit is a massive, beige to brown coloured ignimbrite (Figure 3.14 A). The base of the deposit is not visible but the thickness from the exposed base to the top is ~3 m. The ignimbrite is densely welded and shows cast weathering flutes. The pumice abundance is 30%, with an average maximum size of 20 – 30 mm. There is a mixture of fiamme and non-compressed pumice clasts; the fiamme having an average aspect ratio of 10 (Figure 3.14 B). Lithics throughout the deposit are angular and have an overall average abundance of 10%. Crystals that could be identified using a hand lens are hornblende, quartz, plagioclase and pyroxene. The identified mafic minerals showed iron staining around them. Since there was insufficient exposure, a stratigraphic log was not produced, however a sample was collected for petrographic analysis.

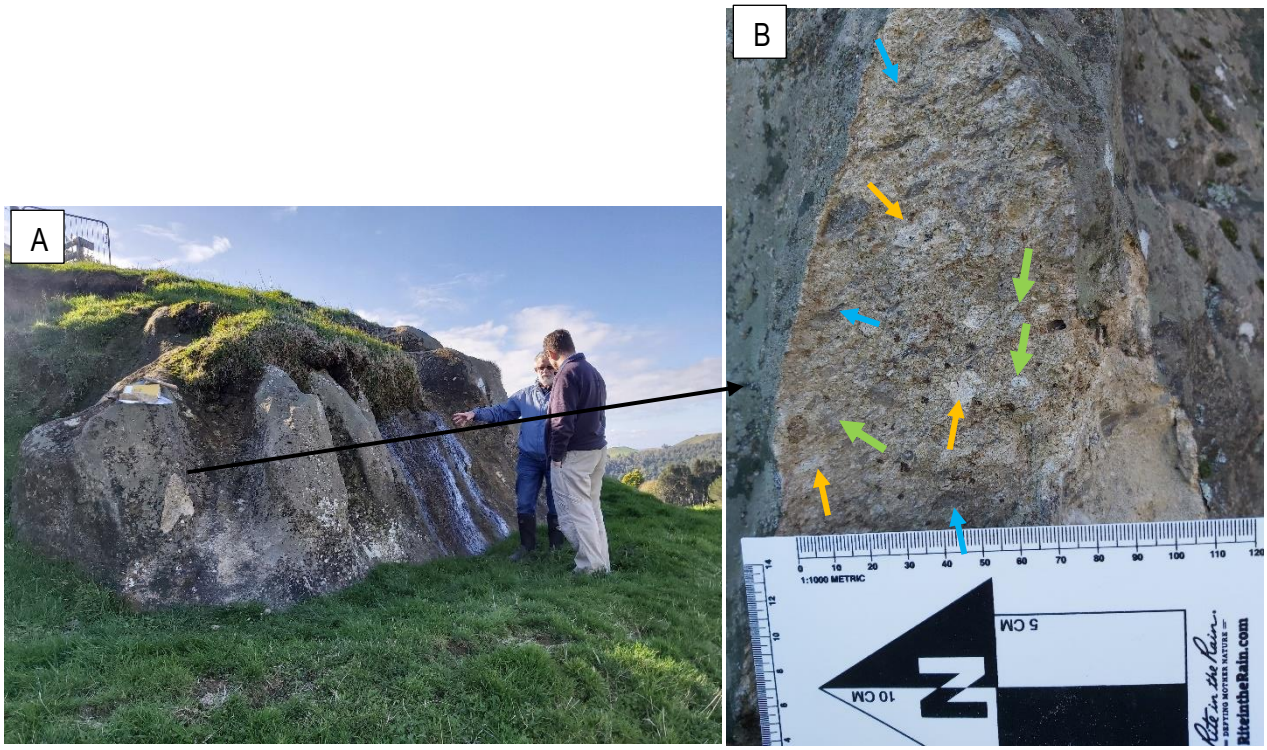

Figure 3.145 ***A:*** *Deposit studied at Locality 3, outcropped as a small bluff at an altitude of ~ 325 m.* ***B:*** *A close-up of a section in the outcrop showing a poorly sorted texture with large clasts of white pumice (yellow arrow), fiamme (blue arrow) and lithics (green arrow) set within a fine-grained matrix.*

The bluffs at L14 are massive with a dark brown to greyish black colour. The outcrop is ~13 m thick and the degree of welding increases with height, from a non-welded or soft near ground level to being partially welded to densely welded from 3 m above ground level to the highest point of the bluff. Pumice abundance also

increases upwards, from 5-7 % at 0.20 m above ground level to 25-30 % at 4-7.5 m. At 0.20 m to 1.50 m, black and white pumices are present, the latter height having more black than white. Average maximum pumice sizes range from 10.8 mm at 0.20 m, to 32 mm at 1.5 m, to 19 mm at 5.5 m. The whole outcrop is lithic-poor with an abundance of <1 % and an average maximum size range from 5.-20 mm. Lithics types include either or both andesites and greywacke.

3.3 Northern Waitao Road: Arateka Ignimbrite

Introduction

The Arateka Ignimbrite outcrops along a ridge (Figure 3.15) that separates the Waitao and Arateka streams upstream of their confluence – on the former Holmberg property mentioned in Hughes (1993), west of Waitao Road (Locality 11). At the foot of the bluffs, there are bush and pastures along the western side of the Arateka Stream valley. Towards the south of the valley (further upstream at Locality 10), there is an exposed outcrop of andesite, overlain by bedded sedimentary deposits (Figure 3.16).

Figure 3.6 Bluffs of the Arateka Ignimbrite, forming the ridge at Locality 11.

Lithology

At Locality 10, the exposed outcrop (Figure 3.16 A) is ~3 m thick and comprises two defined zones: a massive, grey or dark brown andesite (Figure 3.16 B) overlain by a bedded layer of pyroclastic material (Figure 3.16C). The andesite is a densely welded and crystal-rich deposit. The unit is ~1.2 m thick and very hard. The andesite is glassy with euhedral shaped crystals of very fine lapilli size. The overlying top unit is ~1.8 m thick and is interbedded with thin to medium beds of well-sorted, fine very fine pumice lapilli with some lithics, and very thin beds of fine to coarse ash. The pumice beds are 5 – 15 cm thick while the finer beds are 1 – 2 cm thick. At 2.4 - 3 m above the base of the outcrop, there is normal grading from very fine lapilli to coarse ash.

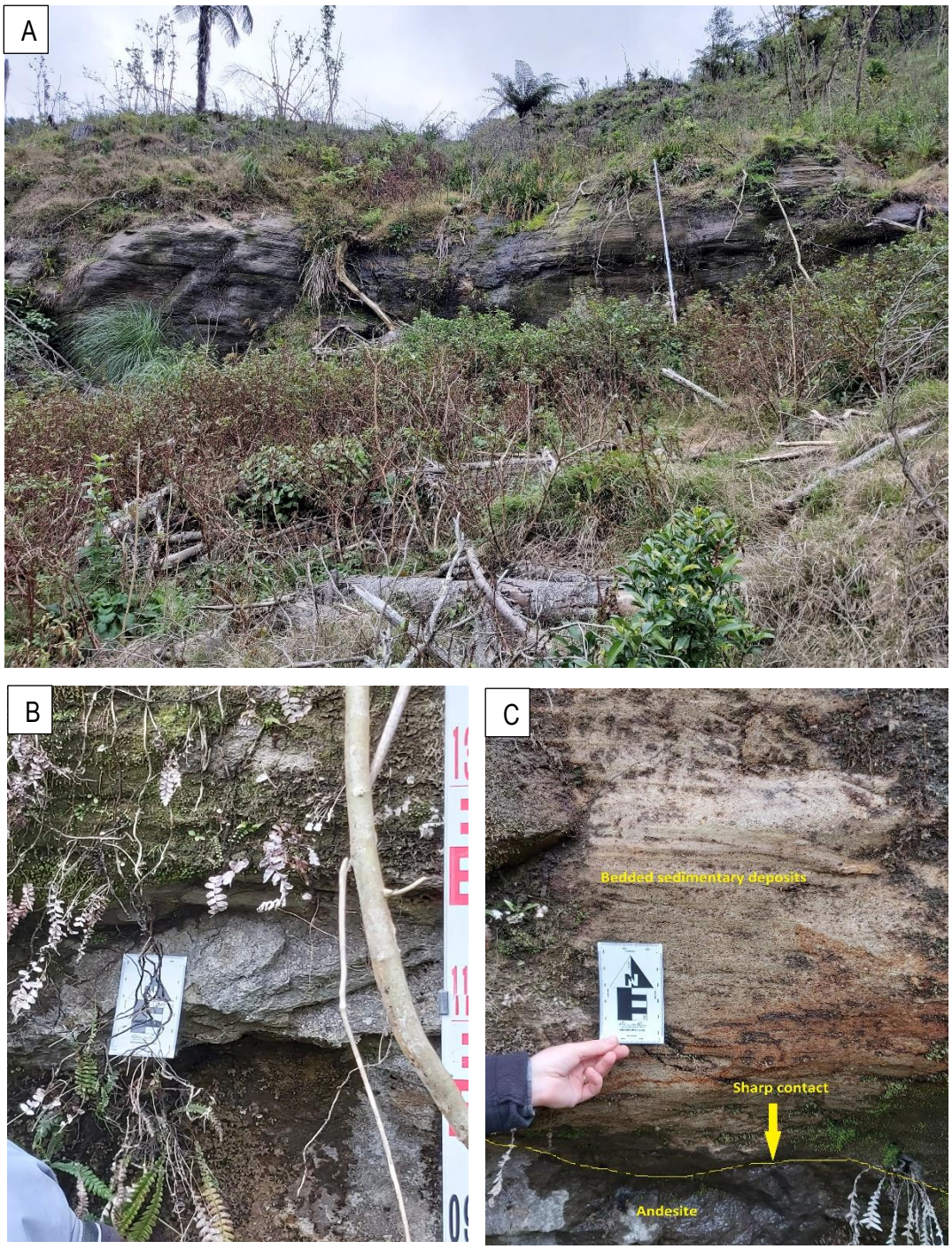

Figure 3.7 The studied outcrop at Locality 10. ***B:*** *Massive, densely welded andesite at the lower section of the outcrop at L10.* ***C:*** *Bedded pyroclastic material overlying the andesite in* ***B.***

The Arateka Ignimbrite occurs as bluffs along a ridge and was studied at Locality 11 (Fig. 3.17). The unit is massive with an orange to brown colour. The thickness of the studied outcrop is ~8 m and consists of fine- to medium-sized pumice clasts. Throughout the outcrop, there are both pink and black pumice clasts present. The abundance of pumice increases with height from 15% at 0.40 m, to 30% at 7 m. The average maximum pumice clast size range from 20.8 mm to 25.8 mm. Lithics abundance is constant at 2 % throughout the deposit. The average maximum lithic size ranges from 9 mm to 14.4 mm.

A stratigraphic log of the Northern Waitao Road is presented in Figure 3.18.

Figure 3.178 Weakly welded, bluff-forming outcrop of the Arateka Ignimbrite at Locality 11.

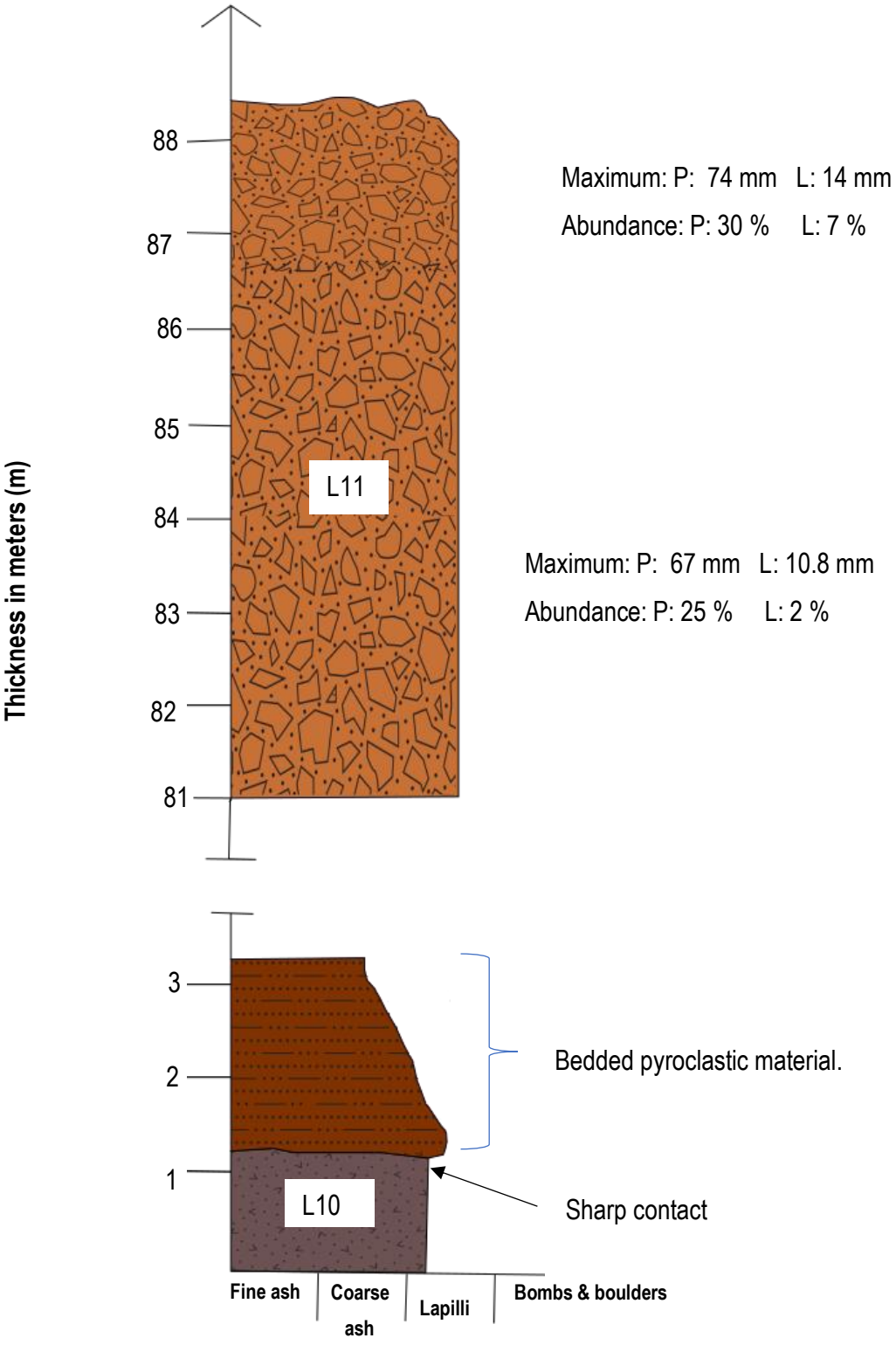

Figure 3.18 Stratigraphic log of L10 and L11, situated along the Northern Waitao Road.

3.4 Northern Reid Road: Otawera and Wharo ignimbrites

Introduction

The Otawera Ignimbrite is exposed at Locality 12 which is a farmland on the east side of the northern end of Reid Road, where it outcrops as bluffs (Figure 3.19) above a valley. The exposed deposit is approximately 20 m thick and shows an increase in the degree of welding from weakly welded – partially welded, with height. The Otawera Ignimbrite is overlain by the moderately welded Wharo Ignimbrite at a sharp contact and extends to the top of the ridge (Locality 13). At approximately 1.48 km southeast of L12 and L13, is the Papamoa Dome which stands at 224 m above sea level (LINZ, 2021). The Otawera Ignimbrite is also located at L15 but was not studied due to the poor exposure of the outcrop. A sample (sample number: #9) was collected from L15 was collected around five years ago but it was not analysed until this project was carried out.

Lithology

The exposed Otawera Ignimbrite is approximately 20 m and is comprised of three flow units which are beige to light brown in colour. The degree of welding increases with height, progressing from weakly welded at the bottom to partially welded at approximately 13 m below the top of the unit. From the exposed base of the unit to approximately 9 m above the base, large lithics were present: the maximum size being ~ 98 mm. From 9 to 11 m of the outcrop it is pumiceous, with a pumice abundance of 40-50 %, and relatively lithic-poor with a lithic abundance of 10-15 %. Above the 9 m level, at 24 cm below the sharp planar contact between the bottom and middle flow units, there is a reverse graded zone, grading from medium-lapilli to coarse lapilli. Above this contact, there is a 10 cm thick fine-grained layer (Figure 3.20 A and B). Overlying this thin layer is a 70 cm thick, lithic concentration zone(abundance of 25-30%) comprised mainly of andesites and rhyolite, also with a pumice abundance of 15-20 %. At 11.80 m, normal grading occurs, from medium lapilli to coarse ash. At 12 m, pumice and lithic abundances are 20% and 15%, respectively. At this height, the lithic size also decreases, having a maximum size of ~ 10 mm. From 12 – 13 m, the ignimbrite is reversely graded, from coarse ash to fine-medium lapilli. At a height of ~13.4 m, there was a layer (~30 cm thick) of rapid grading from fine to medium lapilli at the bottom of the layer to a sharp change to fine ash towards the top. From 14-16 m, the ignimbrite continues to be pumice-rich with a pumice abundance of 30 %. Lithics at this height were not observed.

Figure 3.99 Otawera Ignimbrite at Locality L12, overlain by the Wharo Ignimbrite which extends to the Pa Site, located at the top of the ridge (134 m is the highest point).

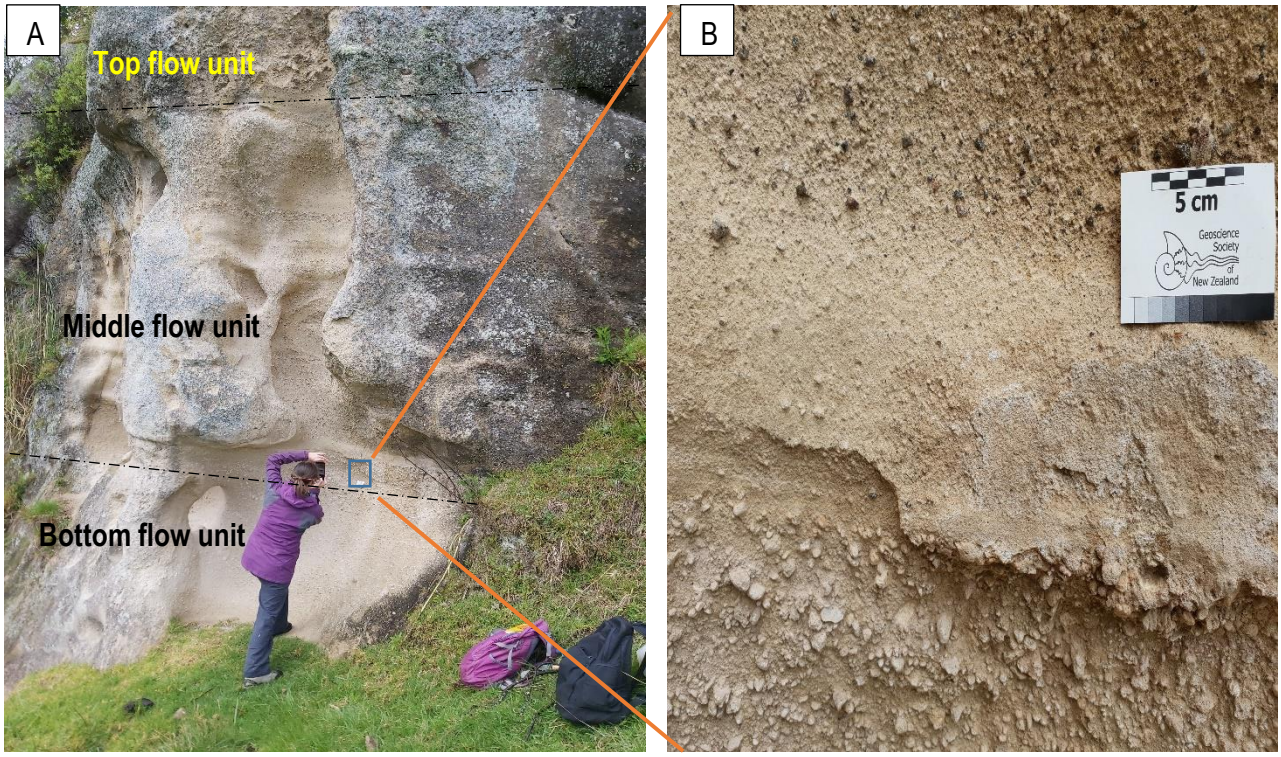

Figure 3.20 ***A:*** *The studied section of the bluff forming Otawera Ignimbrite. Three flow units could be identified within the outcrop.* ***B:*** *A close-up of a 10 cm thick, fine-grained layer, overlying the sharp planar contact between the bottom and middle flow units (Photo courtesy for image B: M. Prentice, 2020).*

The Wharo Ignimbrite in this area is a massive, greyish-brown and pumice-rich deposit (Figure 3.21 A). Lenticular or flattened pumice is present in the unit (Figure 3.21 B). The whole exposed outcrop is ~10 m thick and has crude, irregular jointing. Pumice abundance is at 35 %, and the average maximum pumice size is 91.2 mm. The average aspect ratio is 4.3. At 2 m, the size becomes coarser with average pumice sizes reaching 100 mm. Lithic abundance is at 25% with an average maximum size of 27 mm. Generally, lithics are < 25 mm in size. The lithics are typically andesite and greywacke.

A stratigraphic log displaying the stratigraphic relationship between the ignimbrites, pumice and lithics abundance and maximum sizes (where it was possible), is presented in Figure 3.22. For the missing maximum size or abundance estimations, the measurements could not be made for one of or a combination of the following reasons: 1) exposure of the pumice and/or lithic clasts was poor, 2) there was little to no pumice or lithic present and 3) the unit was too high to reach therefore estimations of abundance could be made only for the visible components (pumice or lithics).

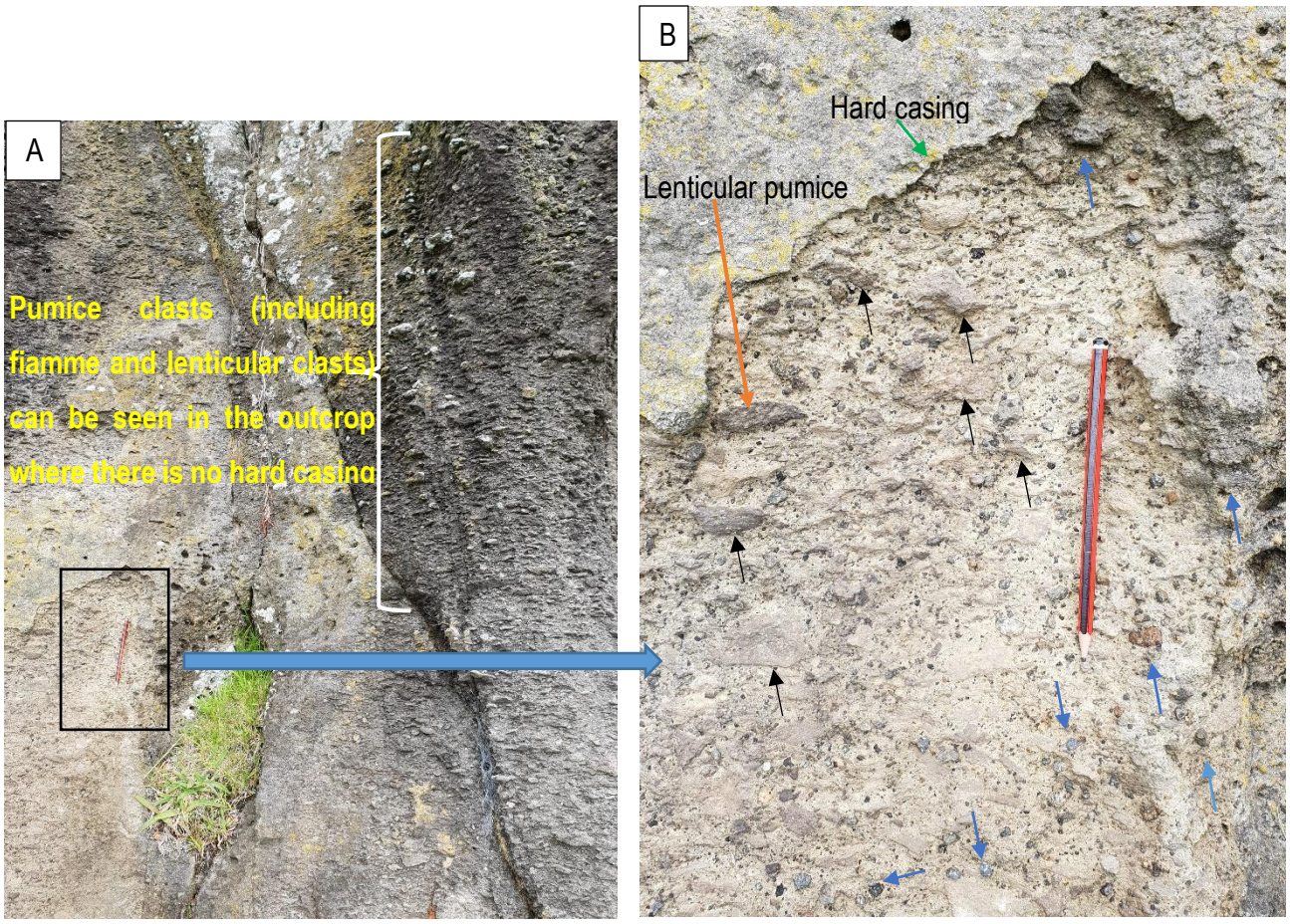

Figure 3.21 Studied section Wharo Ignimbrite at L13. ***B****: A close-up of a section of the Wharo Ignimbrite. A section of the outcrop at L13 showing pumice clasts (shown with black arrows) and lithics (shown with blue arrows) set in a fine-grained matrix.*

NORTHERN REID ROAD STRATEGRAPHIC LOG

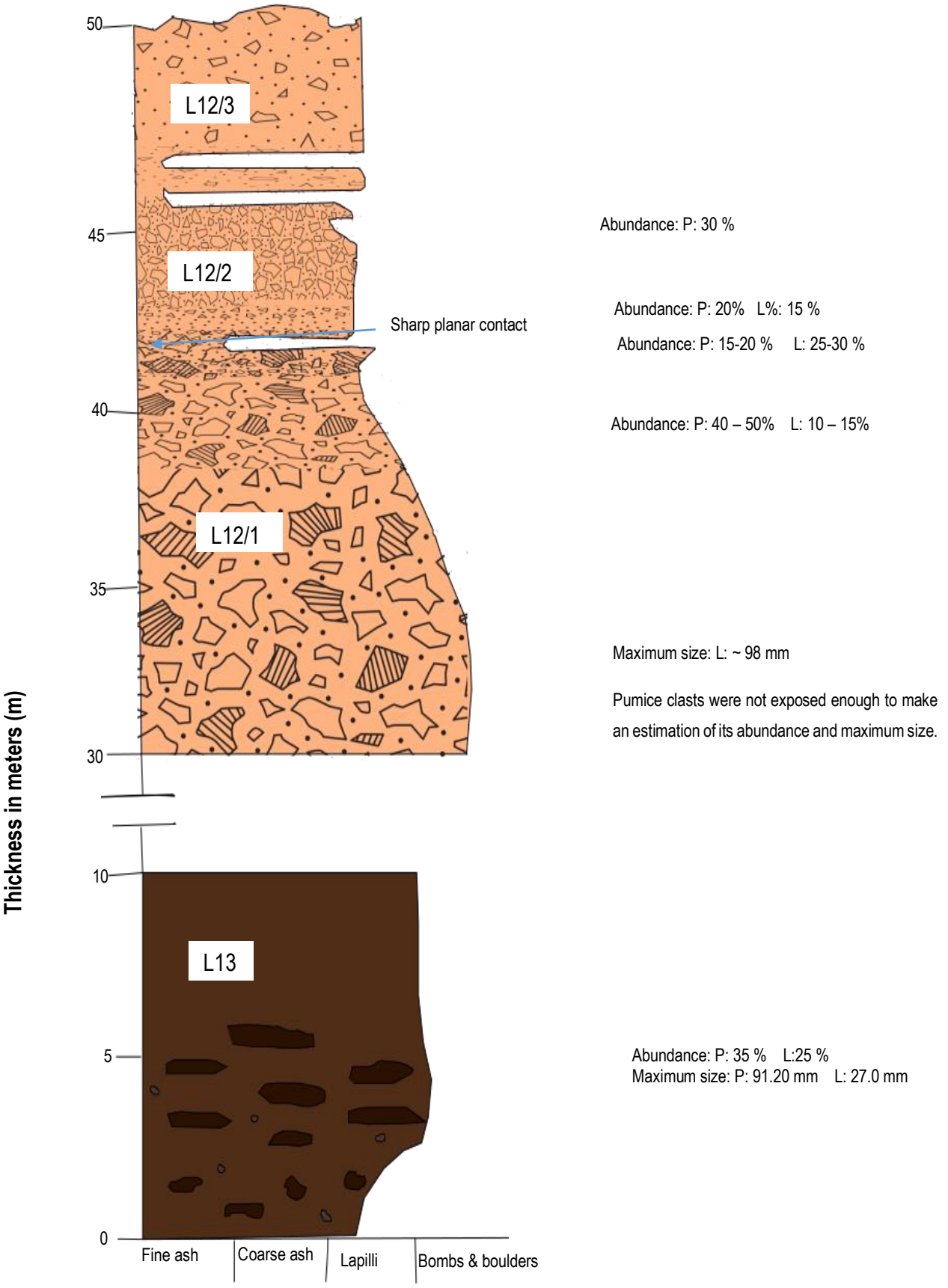

Figure 3.22 Stratigraphic log of the Northern Reid Road.

CHAPTER 4
PETROLOGY

4.1 Introduction

This chapter presents the petrographic and geochemical methods and results associated with understanding the petrology of the Papamoa Formation. The stratigraphy determined in the field (Chapter 3) formed the basis for collecting samples for further analysis for the petrology. Petrography or microscopic observations were made to determine the texture and composition of the different ignimbrites of the Papamoa Formation. Electron microprobe analysis (EMPA) was conducted on eleven (11) samples from the study area to determine major element compositions on glass shards in ignimbrites [Welcome Bay Ignimbrite, Wharo Ignimbrite, Arateka Ignimbrite, Otawera Ignimbrite and an Unknown Ignimbrite] and glass and crystals in black and white pumice from the Welcome Bay Ignimbrite collected from Locality 2. The trace elements of the same glass shards above were measured by laser ablation inductively coupled mass spectrometry (LA-ICPMS). X-ray fluorescence (XRF) spectroscopy was used to identify and measure the major elements compositions of bulk black and white pumice.

4.2. Petrography of the Papamoa Formation ignimbrites

Introduction

Optical microscopy is widely used in geological studies to classify and describe rocks in thin sections with the aid of a petrographic microscope. The petrography of all the five ignimbrites in the study area will be presented.

For this research project, a total of 37 thin sections were prepared and studied for all of the 14 localities (presented in Appendix 1) studied. Localities 4,5,6,7,8,9 or what is referred to in this research project as the "Addline Sequence" are situated east of the Rocky Cutting Road. Because the Addline Sequence provides the best exposure of the Welcome Bay and Wharo ignimbrites, a detailed petrographic description will focus

on this area. For the Arateka and Otawera ignimbrites, which are not found in the Addline Sequence but on the west and east of Rocky Cutting Road, respectively, petrographic descriptions of these two ignimbrites will also be presented.

4.2.1 Preparation of thin sections

Bulk ignimbrite samples collected from the study area were cut into blocks of 3 cm x 2 cm x 2 cm (length x width x height) using a diamond saw. In addition, both black and white pumice clasts and lithics from Locality 2 (i.e., from the Welcome Bay Ignimbrite) were also prepared. The blocks were then impregnated with Nuplex K36 resin and hardener using a ratio of 2:1, respectively, and left to cure at 60°C for 24-hours. Once the samples were set, they were polished using a glass plate and silicon carbide powder. Each polished sample block wase then mounted onto a petrographic slide, which was frosted to a range of -3 to -5 mm (the petrographic slides varied in thickness within this range), using Hillquist resin and hardener at the ratio of 2.3:1 by weight, respectively. The mounted blocks were left on a flat surface at room temperature to cure for more than 12 hours. Cured mounted blocks were further grinded down to ~0.03 mm– 0.05 mm using the Struers Discoplan. To complete the thin section preparation process, cover slips were placed over the cut samples, using Petropoxyl resin and hardener at the ratio of 5:10 (5 ml: 0.5 ml) by volume and left to set on a hot plate at 110°C.

4.2.2 Crystals/Phenocrysts

Plagioclase

Plagioclase is the most abundant mineral and occurs in all the units across the study area. Its abundance range in bulk ignimbrite is 20-30% and occurs as either an individual mineral (as in Figure 4.1A), as a member of a glomerocryst or as an inclusion in other minerals. Plagioclase occurs as phenocrysts in pumice clasts, as free crystals within the ignimbrite matrix and within lithics. The size range in the matrix is 0.60 – 1.8 mm with a maximum of 3.08 mm. Pumice clasts have a plagioclase size range of 0.64 – 1.66 mm, with a maximum of 2.05 mm. Some samples show that plagioclase crystals in the matrix are greater in size than those found in pumice clasts or lithics and vice versa. The morphologies of plagioclase are euhedral to subhedral and they are either internally twinned (simple and polysynthetic) or zoned. Some plagioclase crystals display embayments infilled with glass or groundmass, and inclusions of opaques.

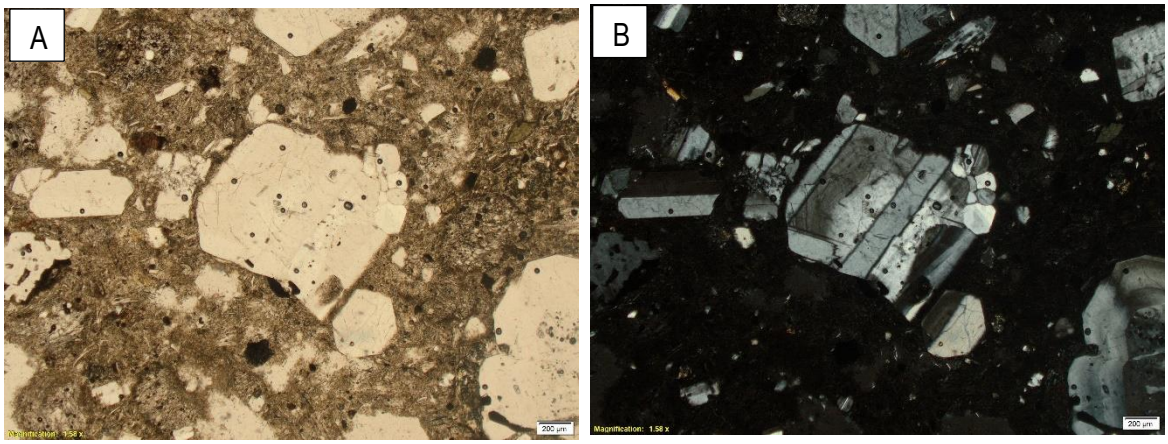

Figure 4.1 A plagioclase crystal (center) from sample L7/4 (Welcome Bay Ignimbrite) is shown in plane polarized light The plagioclase crystal is showing some minor fractures, with a melt inclusion and an opaque mineral inclusion in the bottom corner of the crystal. The plagioclase crystal is set in a mixture of fine-grained crystals and glass matrix. ***B:*** *This is the same plagioclase crystal in A but in cross polarized light. It shows polysynthetic twinning, and that the plagioclase crystal is a glomerocryst. Zoning can be seen in this crystal, and in the plagioclase in the bottom left-hand corner.*

Quartz

Quartz is a minor mineral and only occurs in some of the samples studied. The quartz crystals are euhedral to subhedral in shape and occur as either individual crystals or as part of a glomerocryst. Most of the quartz crystals observed display fractures or cracks on their surfaces. Other quartz crystals display either inclusions of glass, or embayments. Quartz is abundant and larger in some samples (L8, L9 and L12) less in quantity and smaller in size in other samples (L7.1, L11 and L13). It occurs mainly in the matrix of ignimbrites rather than in pumice. Where quartz is present, the abundance is ~ 1%. The size of quartz crystals ranges from 0.23 – 0.94 mm, with a maximum of 2.65 mm.

Hornblende

Hornblende is present in most of the samples and occurs as subhedral to euhedral shaped, whole or fragmented crystals. Some hornblendes occur as individual crystals (as exemplified in Figure 4.2 A) or as a glomerocryst, or in a few cases, as an inclusion in other minerals. Inclusions of opaques within hornblende are common, and plagioclase and glass inclusion are also present, and rare biotite inclusions. The size range for hornblende crystals

in the matrix is 0.25 – 1.08 mm, with a maximum of 3.18 mm, while as phenocrysts in pumice the size range is 0.32 – 1.12 mm, with a maximum of 1.55 mm. The abundance of hornblende is between 1 – 3%. One or two of observed hornblende crystals have simple twinning like that shown in Figure 4.2 B.

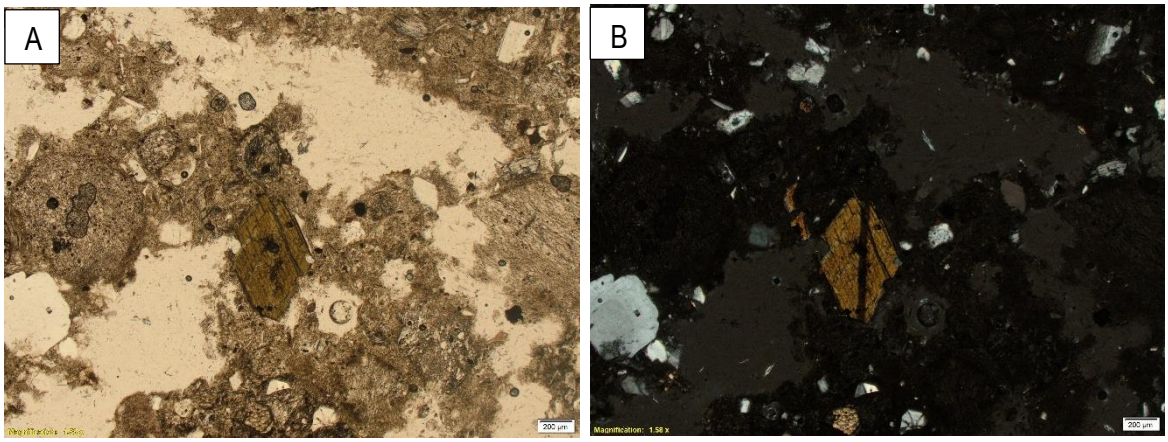

Figure 4.2 ***A****: A hornblende crystal (centre) in Sample L7/4 or the Welcome Bay Ignimbrite set in a matrix of fine-grained crystals and glass. Opaque inclusions can be seen at the bottom of the hornblende crystal.* ***B****: Same image and magnification as in A but in cross polar lighting.*

Pyroxenes

Pyroxenes that were observed include both clinopyroxene (Figure 4.3 A) and orthopyroxene (Figure 4.3 C). In some samples, one was more abundant than the other and vice versa (L2 and L7.3). In other samples (L2WP, L3) no pyroxene was found. The overall abundance of pyroxenes ranges from 2 – 3%. Pyroxenes are euhedral to subhedral in shape and occur as either whole or fragmented crystals. The pyroxenes in the studied samples were either individual crystals or parts of glomerocryst. Like hornblendes, the inclusion of opaques is common. Pyroxene sizes range from 0.37 – 0.97 mm, with a maximum of 1.38 mm.

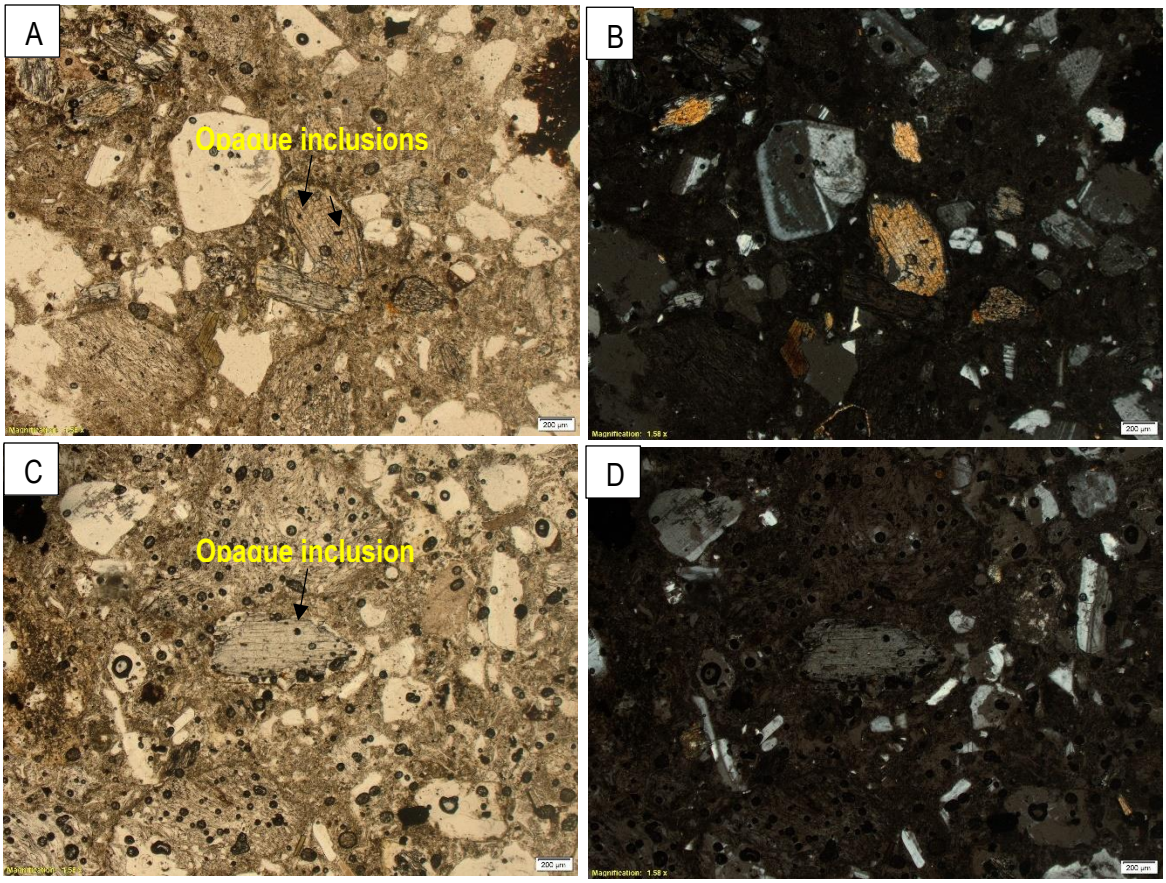

Figure 4.3 ***A:*** *A clinopyroxene crystal (center) from a sample of the Welcome Bay Ignimbrite matrix collected at L7/4. There are three anhedral opaque inclusions in the clinopyroxene, and it is a glomerocryst with an orthopyroxene crystal (bottom left). The clinopyroxene glomerocryst is embedded in a matrix of fine-grained crystals and glass.* ***B:*** *The same image as A but in cross polarized light.* ***C****: An orthopyroxene crystal (center) from sample of the Arateka Ignimbrite matrix collected from L11 in plane polarized light embedded in a matrix of fine-grained crystals and glass. The crystal has an opaque inclusion.* ***D:*** *Image* ***C*** *in cross polarized light.*

Biotite

Biotite occurs in a few of the analysed samples (L3, L9 and L12) as individual crystals (exemplified in Figure 4.4 A), part of glomerocryst clusters or as fragmented altered red flakes (Figure 4.4 B). The abundance of biotite is ≤ 1%, occurring in relatively high abundance in the Otawera Ignimbrite in the northern Reid Road study area. Biotite crystals are subhedral to anhedral in shape. The size range of biotite is between 0.17–0.30 mm, with a maximum crystal of 0.45 mm.

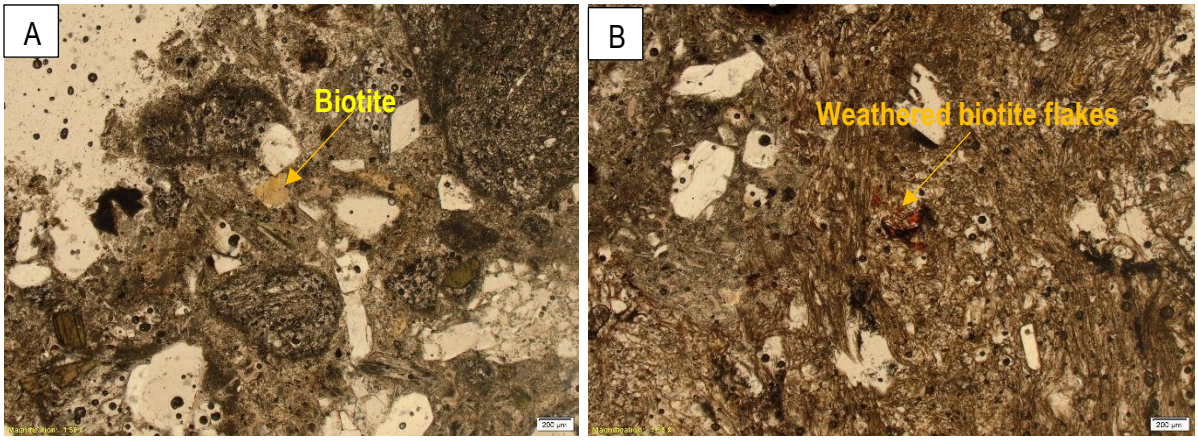

Figure 4.4 ***A:*** *A biotite crystal in a matrix sample the Welcome Bay Ignimbrite collected at L9, observed in plane polarized light. The biotite crystal is set in a matrix of fine-grained crystals and glass.* ***B:*** *Altered or weathered biotite flakes in sample L9 in plane polarized light. The flakes are set in a groundmass of glass, i.e., a brown pumice clast.*

Opaques/Titanomagnetite

Opaques are present in most the analysed samples as individual crystals (as in Figure 4.5), parts of glomerocryst clusters or as inclusions. In the white pumice sample opaques are rare. Opaques are subhedral – anhedral in shape and have an abundance range of 3 – 5%. Sizes of opaques range between 0.10 – 0.40 mm with a maximum of 0.68 mm in the matrix and a range of 0.22 – 0.33 mm and a maximum of 0.38 mm in pumice.

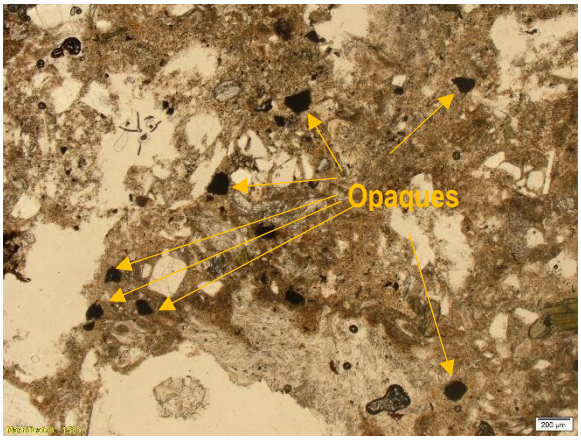

Figure 4.5 Opaques in a sample collected of the Wharo Ignimbrite matrix collected from L3, viewed in plane polarized light. The opaque minerals are set in a matrix of fine-grained crystals and glass.

4.2.3 Pumice

There are two types of pumice observed in some of the ignimbrite samples of both thin sections and present in the outcrops: white and black pumice. The occurrence of both these pumice types is illustrated in Figure 4.6. Both pumice types were collected from L2, with some other white pumice collected from L9. White pumice is predominant in the study area. Both pumice types comprise plagioclase, opaques, pyroxenes, and hornblende phenocryst. There are more hornblende phenocrysts than pyroxene in the white pumice. Except for opaques which have subhedral-anhedral shapes, all of the crystals are euhedral-subhedral in shape. The presence of lithics in both pumice types is lacking. Both pumice types have bimodal sized vesicles. In the white pumices collected from L9, there are more spherical-shaped and smaller-sized vesicles than those from L2. In addition, the crystals (plagioclase, hornblende and opaques) and altered biotite flakes in the white pumice from L9 are larger than the same minerals found in the white pumice from L2. Vesicles in the white pumice are larger than those found in the black pumice. The bulk texture of the white pumice is a mixture of spongy and fibrous while in the black pumice, bulk textures is a mixture of woody and spongy.

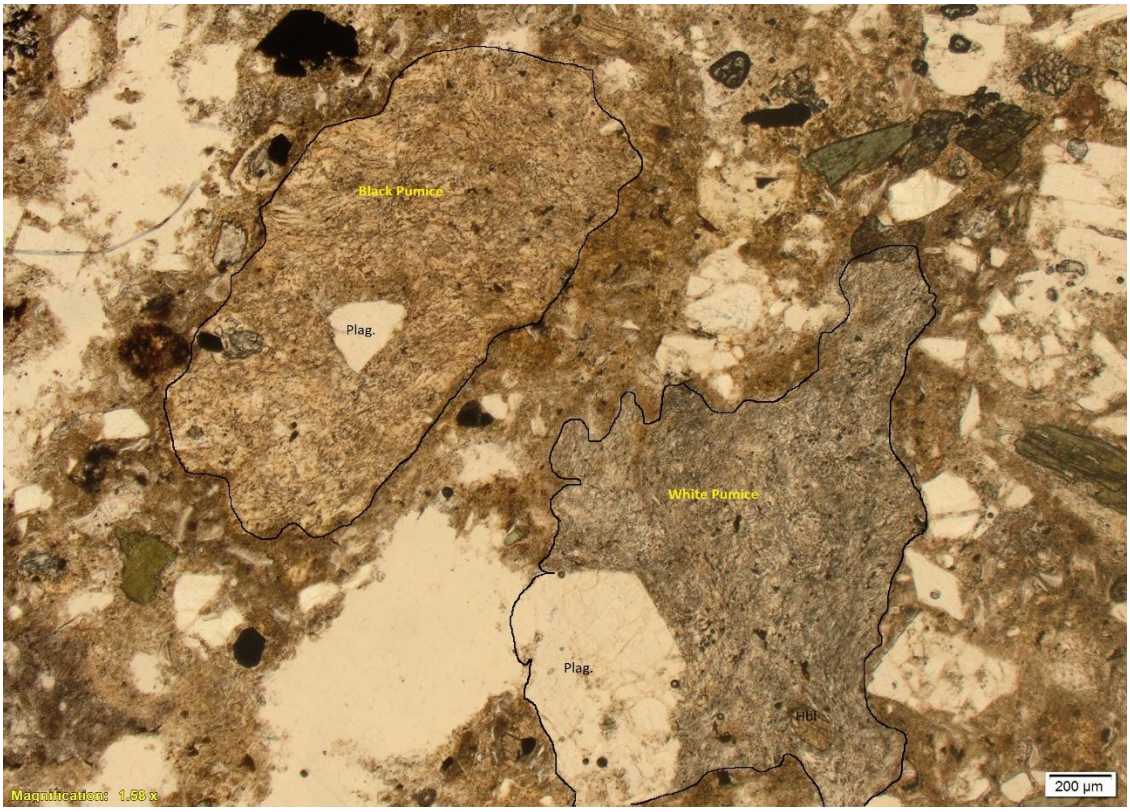

Figure 4.6 White and black pumice in a sample of the Wharo Ignimbrite at Locality 3, seen under plane polarized light.

4.2.4 Lithics

Lithics found within the ignimbrites in the study area include pyroclastic rocks, andesite (Figure 4.7 B) and rhyolite (Figure 4.7 A) and are up to 40 mm in size. The pyroclastic lithics comprise plagioclase, quartz, pyroxenes and opaques embedded in a fine-grained matrix. Andesitic lithics are comprised of mainly plagioclase and pyroxene phenocrysts set in a fine-grained groundmass of feldspar laths. The rhyolitic lithics are mainly comprised of plagioclase and quartz phenocrysts, embedded in a fine-grained groundmass of feldspar laths. Some rhyolitic lithics are aphyric and are solely composed of a felted textured groundmass.

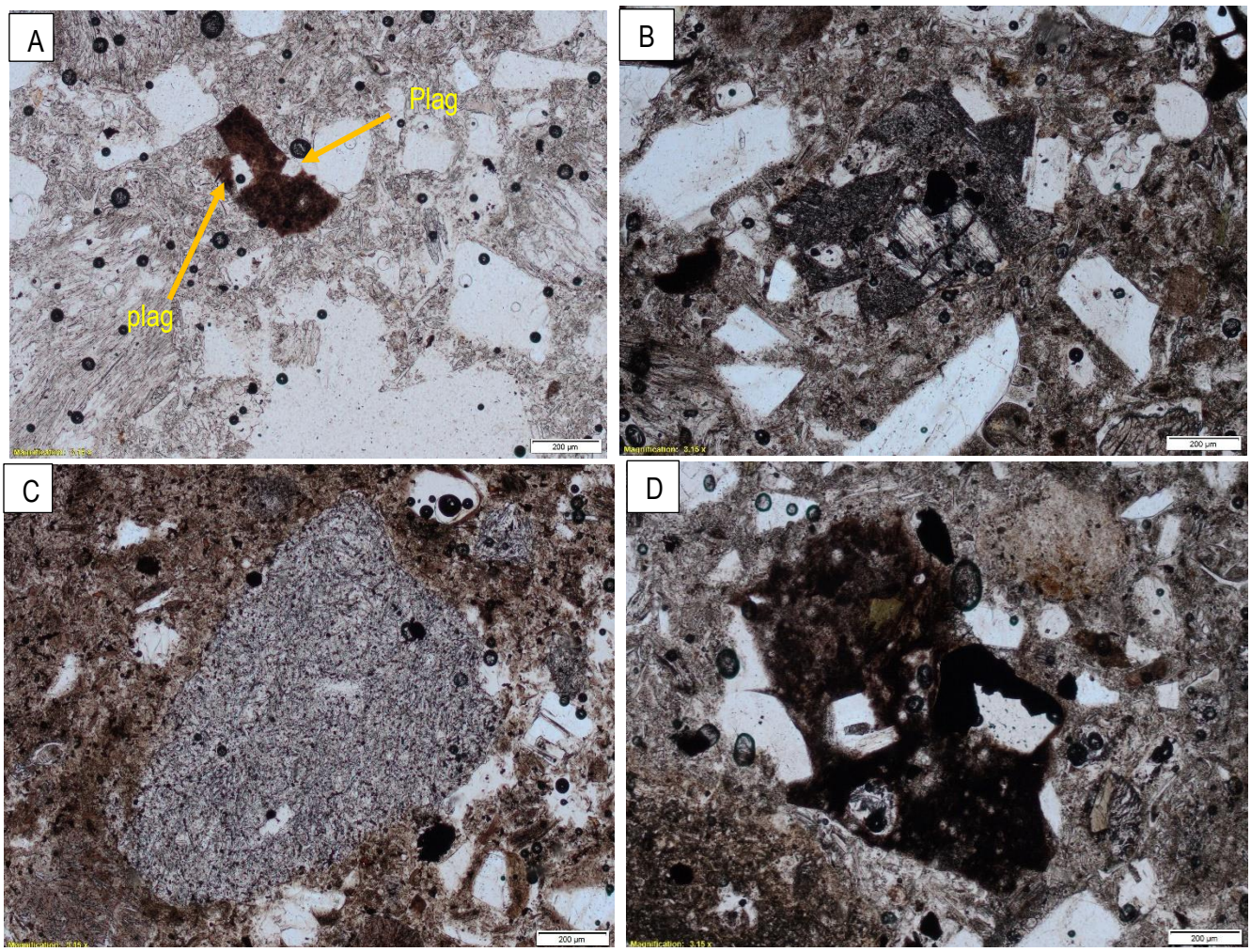

Figure 4.7 ***A****: An altered or devitrified rhyolite lithic (center).* ***B****: An andesitic lithic (center). Both A and B were present in the Arateka Ignimbrite at L11.* ***C:*** *An aphyric rhyolitic lithic (center) present in the Wharo Ignimbrite collected from L5.* ***D:*** *A devitrified or altered rhyolitic lithic found in L11.*

4.2.5 Summary of the petrography of the identified ignimbrites

Wharo Ignimbrite (L1, L3, L5, L13, L14)

The Wharo Ignimbrite occurs at Localities 1, 5, 13 and 14. This ignimbrite comprises of euhedral- to subhedral-shaped plagioclase, quartz, hornblende and/or opaque crystals. From the collected sample at L1, the phenocrysts of the ignimbrite were observed to be mantled by the surrounding matrix, creating a eutaxitic texture (Figure 4.8 A). For the other samples, the texture is vitrophyric or pyrophytic or a mixture of both. Throughout the Wharo Ignimbrite across the different localities, fiamme and the two types of pumice (black and white) clasts are present (L3, L5 and L14). At Localities 1 and 13, only fiamme and black pumice are present. The pumice clasts are highly vesicular, have bimodal vesicle sizes, and vesicle morphologies range from more elongated vesicles creating a woody texture, to more spherical vesicles forming spongy texture. Phenocrysts (mainly plagioclase) in the pumice clasts are mantled by the vesicles. The commonly occurring lithic type in the Wharo Ignimbrite is rhyolite.

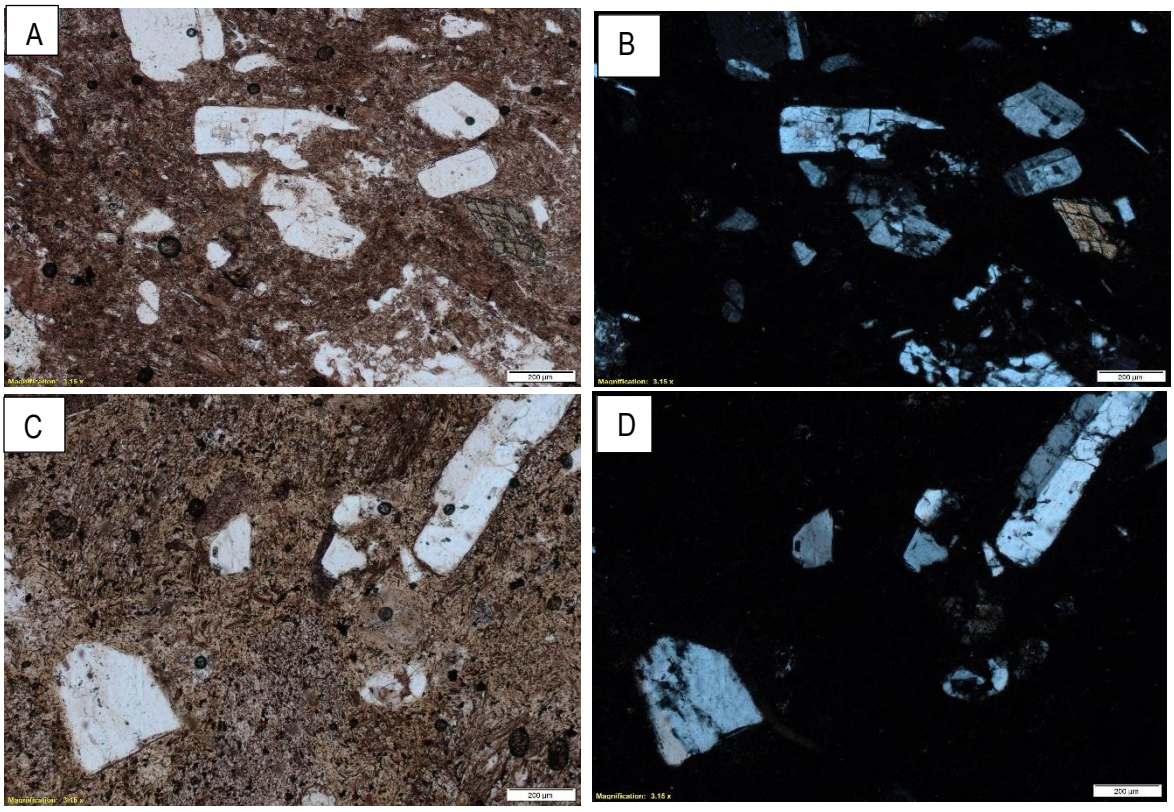

*Figure 4.8 Photomicrographs examples of the Wharo Ignimbrite matrix. **A** and **B** are the same image of a sample from Locality 1 in plane and cross polarised light, respectively. The rock texture observed is eutaxitic. **C** and **D** are the same image of a sample from Locality 13 in plane and cross polarised light. The rock texture is more porphyritic.*

Welcome Bay Ignimbrite (L2, L4, L7/4, L8, L9)

The Welcome Bay Ignimbrite outcrops at Localities 2, 7/4, 8 and 9.. The mineralogy of the Welcome Bay Ignimbrite comprises of plagioclase, quartz, pyroxene (clinopyroxene and orthopyroxene) and opaques, the phenocrysts of which are embedded in a fine-grained matrix. Like the Wharo Ignimbrite, the overall rock texture of this ignimbrite is either vitrophyric or porphyritic a mixture of both (Figure 4.9 A).

resent in the Welcome Bay Ignimbrite are both the black and white pumice types. Unlike the Wharo Ignimbrite, however, there are little to no fiamme present. The pumice clasts are highly vesicular with bimodal vesicle sizes, the majority of which are spherical forming a spongy texture. There are little to no phenocrysts in the pumice, but when observed, the common ones are hornblende and plagioclase, and both these phenocrysts are mantled by the surrounding groundmass or vesicles. Lithics in the Welcome Bay Ignimbrite comprise of fragmented pyroclastics, andesites and rhyolites. The fine-grained matrix is comprised of spherulites and glass shards of various shapes (Figure 4.9 C).

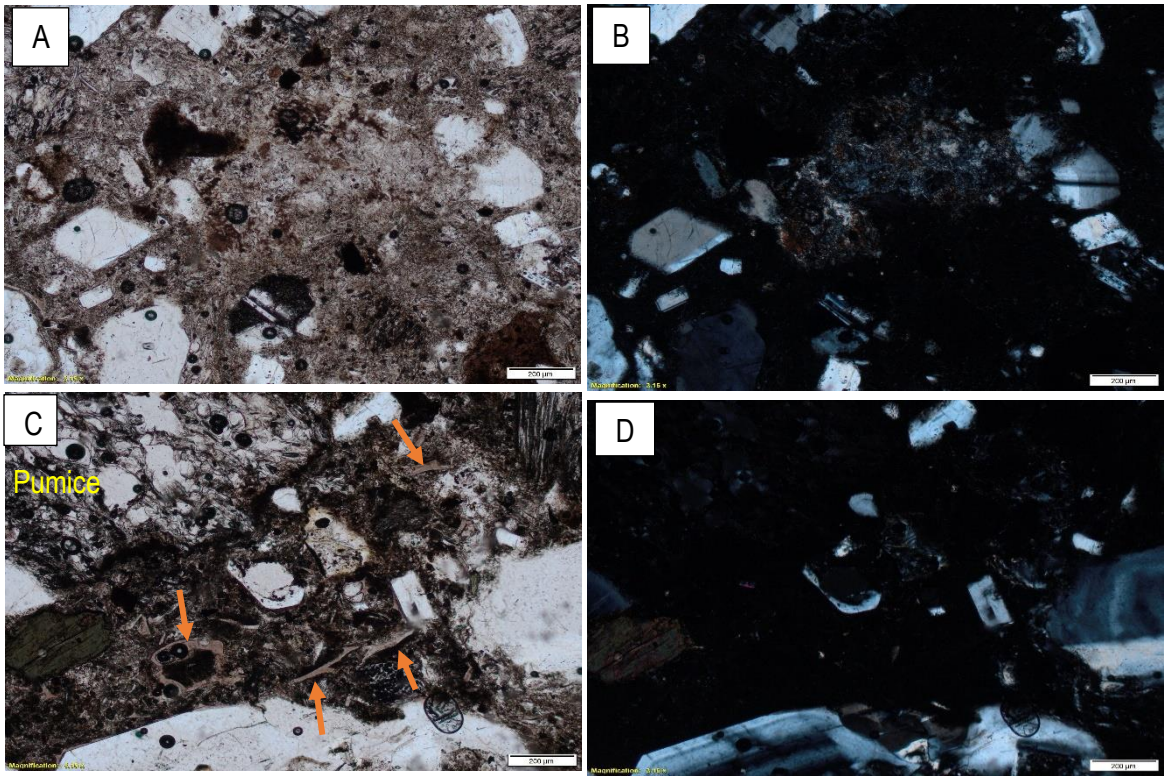

*Figure 4.9 Examples of the Welcome Bay Ignimbrite matrix**. A** and **B** are the same image of a sample of Unit D collected from Locality 7, in plane and cross polarised light, respectively. Glass shards are present in the matrix are minute. **C** and **D** are the same image of a sample from Locality 2 in plane and cross polarised light. Glass shards are shown with orange arrows. A pumice with a spongy texture is also outlined in yellow.*

Arateka Ignimbrite (L11)

Within the study area, the Arateka Ignimbrite only occurs at Locality 11. The Arateka Ignimbrite is composed of euhedral to subhedral shaped plagioclase, quartz, hornblende, pyroxene (both clinopyroxene and orthopyroxene), spherulites and opaque phenocrysts set in a fine-grained matrix of feldspar and glass shards (Figure 4.10). The overall texture of the Arateka Ignimbrite is porphyritic. Both black and white pumice types can be found in the Arateka Ignimbrite. The pumice clasts have a bimodal vesicle size, the majority of which are elongated, forming a woody texture. Rhyolitic and andesitic lithics are present in the Arateka Ignimbrite. The matrix has an abundance of glass shards, the majority of which are elongated.

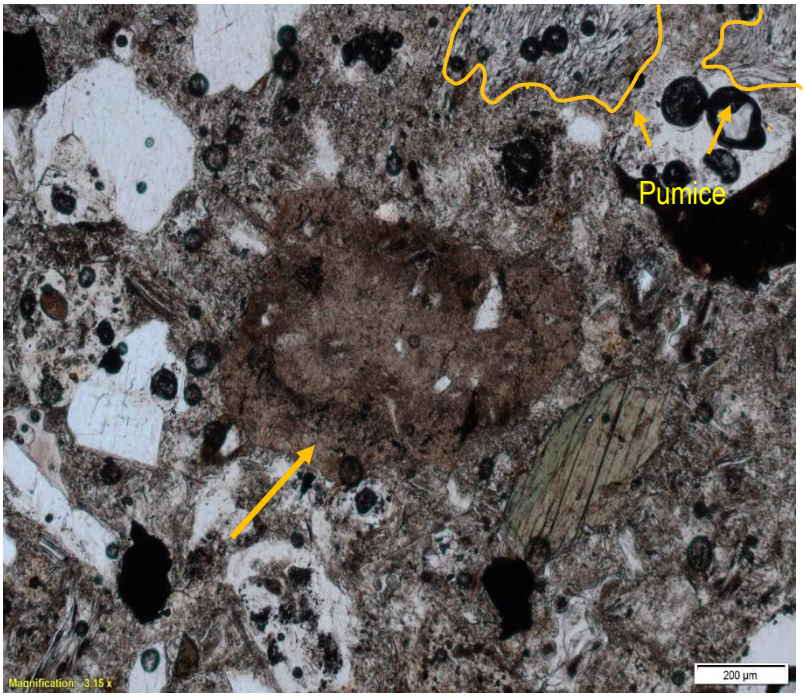

Figure 4.10 The Arateka Ignimbrite matrix. In the top right corner on the image, there are two are woody textured pumice clasts (outlined in yellow). In the centre is a rhyolite lithic (shown by the yellow arrow) surrounded by phenocrysts and matrix. The matrix is rich with glass shards.

Otawera Ignimbrite (L12, #9)

The Otawera Ignimbrite only outcrops at Locality 12. Making up the mineralogy of the Otawera Ignimbrite are euhedral to subhedral shaped plagioclase, quartz, hornblende and opaque phenocrysts, again, set in a fine-grained matrix. Unlike the other ignimbrites in the study area, the rock texture of this ignimbrite is either porphyritic, vitrophyric or a mixture of both. Lithics found in this ignimbrite are mainly rhyolitic, having plagioclase crystals embedded in a fine-grained groundmass of feldspar laths. There is only one pumice type (white) in the Otawera Ignimbrite. It is highly vesicular with bimodal sized vesicles, the majority of which are spherical. Phenocrysts in the pumice are mantled by the vesicles, forming a mixture of fibrous and spongy texture. The common occurring lithics are rhyolites and andesites. Also present in the matrix of this ignimbrite are spherulites and an abundance of glass shards of different shapes and sizes. There are more well-defined glass shards in the bottom (Figure 4.11, 12.1) to mid sections of the outcrop than the top section (Figure 4.11, 12.3). Compared to the glass shards found in the other ignimbrites in the study area, the shards present in this ignimbrite are larger in size.

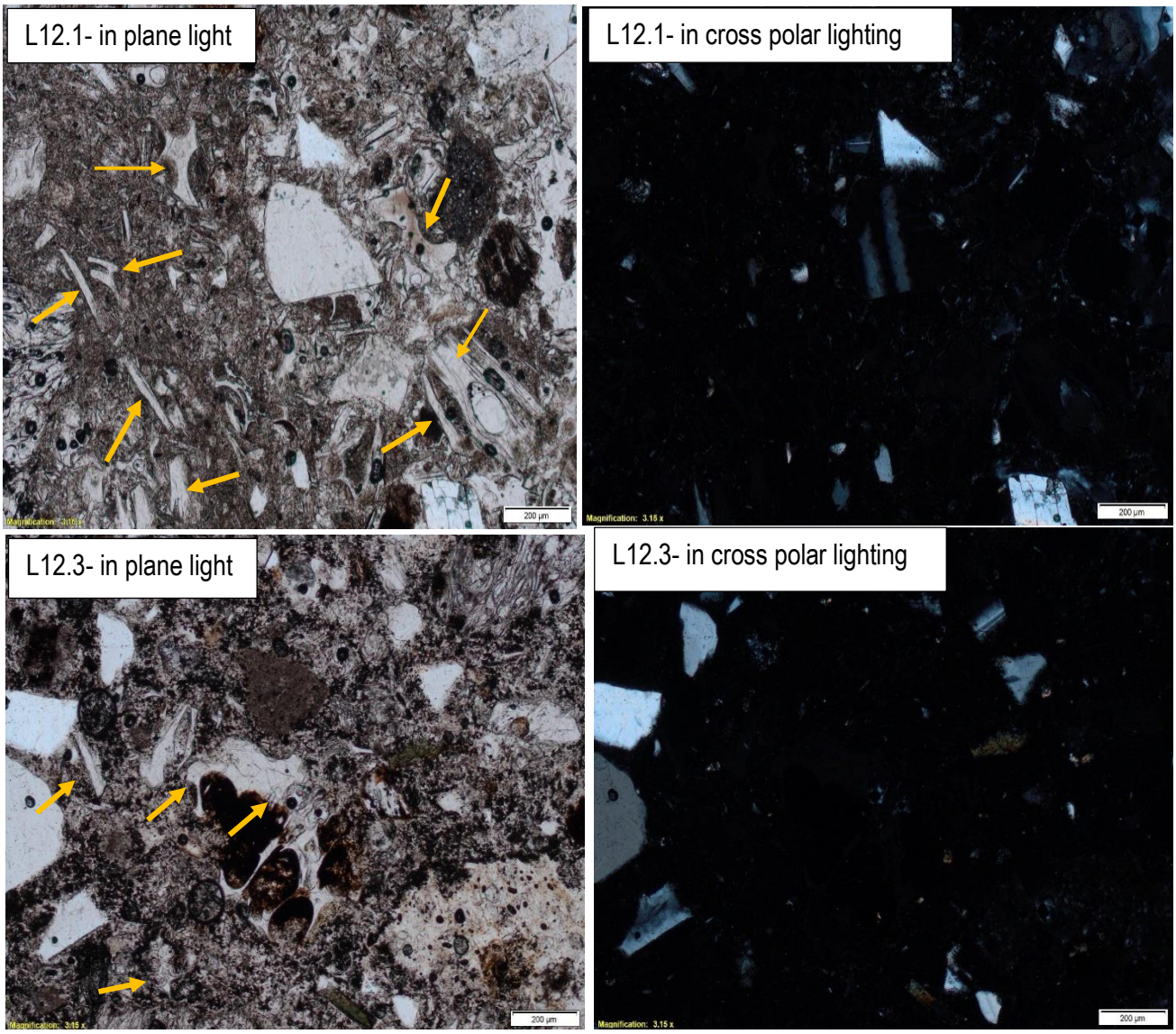

Figure 4.11 Samples of the Otawera Ignimbrite matrix. L12.1 is the bottom unit while L12.3 is the top unit of the Otawera Ignimbrite outcrop. Glass shards are shown with yellow arrows. It can be noticed that the glass shards in the sample from the bottom unit are greater in quantity and size than those found in the top unit.

Unit A- Unknown Ignimbrite (L7.1)

Unit A or the Unknown ignimbrite occurs at Locality 7. The Unknown Ignimbrite is composed of anhedral shaped opaque crystals and subhedral to euhedral shaped plagioclase and quartz crystals set in a fine-grained matrix. Unit A possess a vitrophyric rock texture. Unlike the Welcome Bay, Wharo and Arateka Ignimbrites, Unit A does not comprise of varying pumice types but is exclusively composed of fibrous textured grey pumice. Generally, Unit A is lithic poor.

From the petrographic observations made, the following similarities and differences are summarised. The mineralogy of the studied ignimbrites are similar, however, there is an absence of hornblende in the Welcome Bay Ignimbrite. The Wharo, Welcome Bay, Otawera and the Unknown ignimbrite Ignimbrites have textures of either vitrophyric or porphyritic or a combination of both, while the Arateka Ignimbrite generally possesses a porphyritic rock texture. Both black and white pumice types occur in the Wharo, Welcome Bay and Arateka ignimbrites, whereas the Otawera and the Unknown Ignimbrites had only one pumice type, white and grey respectively. Majority of the pumice have a spongy texture. The Otawera and Ignimbrite was exclusively comprised of fibrous textured white and grey pumice clasts respectively. Overall, the common occurring lithics in all the ignimbrites in the study area were rhyolites. The Unknown Ignimbrite, however, was found to be lithic-poor.

4.3 Electron Microprobe Analysis (EMPA): Glass and Pumice Crystal Analysis

The determination of major element compositions of the glass in matrix shards and pumice, and crystals of ignimbrites from the Papamoa Formation from localities: 2, 4, 5, 7, 11, 12 and #9 in the study area, was achieved using the electron microprobe at the University of Wellington. Four glass shard mounts and two polished thin sections for crystals in the black and white pumice clasts were used for EMPA.

4.3.1 Mount preparation for EMPA

Mounts of glass shards were prepared for EMPA. Rock samples were crushed using a mortar and pestle, and later mixed with water and sieved through the 250 µm, 125 µm and 64 µm strainers. The residue in the 125 µm strainer was collected by washing it down with water and collected in a storage jar. The collected samples were then dried in the oven at 55˚C for three days. Glass shards were extracted from the dried samples using magnetic and vibrating table gravity separation methods. Due to the intermediate composition of the samples, magnetic and gravity methods were not sufficient to extract the glass shards therefore, further handpicking was made using a microscope. Once glass shards were extracted, four mounts, comprising of seven bubbles in each, were partially filled with glass shards, one bubble per sample. The mounts were then filled with Nuplex K36 resin and hardener using the ratio of 2:1, respectively, and left to set on a hotplate at

60˚C for 24 hours. Once set, the mounts were polished using 0.3 µm polishing alumina powdered solution (powder mixed with tap water) on the Buehler Metaserv grinder-polisher machine.

4.3.2 Electron Microprobe Analysis for crystal analysis: Sample preparation and analysis

EMPA for crystal chemistry was only conducted on the two (black and white) pumice types found in the study area. The crystals analysed were plagioclase, hornblende and pyroxene (orthopyroxene and clinopyroxene).

Two polished thin sections, one of the black and the other of the white pumice, were prepared. Standard thin sections were produced, however without cover slips. Instead, the thin sections were polished using the Buehler Metaserv grinder-polisher machine and 0.3 µm polishing alumina powdered solution to better expose the surfaces of the crystals of interest. To avoid the charging of non-conductive samples, the thin sections were coated with a thin layer of carbon.

The major element percentages measured by EMPA, were first normalized to 100%. Then the for each sample the normalized total alkalis ($Na_2O + K_2O$ wt%) were plotted against their respective silica (SiO_2 wt %) content, in a total alkali versus silica (TAS) diagram by (Lebas, Le Maitre, Streckeisen and Zanettin 1986). (Figure 4.12).

4.3.3 Electron Microprobe Analysis for glass analysis

In situ major element analyses were undertaken on individual glass shards using a JEOL JXA 8230 Superprobe (EMPA) at Victoria University of Wellington (VUW). A beam size of 10 µm at ~8 nA was used to analyse for major elements as oxides (SiO_2, TiO_2, Al_2O_3, FeO(t), MgO, CaO, MnO, Na_2O, K_2O and Cl). During analysis, back-scattered electron images of the shards were taken to allow the relocation of analysis spots for subsequent LA-ICP-MS analysis.

The matrix-matched standards VG-568 and ATHO-G were run twice every 15 unknowns. VG-568 was used as a bracketing standard to monitor for instrument drift and ATHO-G as a secondary standard to evaluate analytical precision and accuracy. Concentrations were determined using the ZAF correction method, analytical totals for unknown glass were 92-97 % with the deviations from 100% attributed to variable degrees of post-eruption hydration (Lowe, Pearce, Jorgensen, Kuehn, Tyron & Hayward, 2017). Accuracy of the analyses was within 5 % of the recommended values for VG-568, with the exception of MgO (11.12) and MnO (10.14). Analytical precision (2sd) is 0.87 for all the elements. Refer to Appendix 2 for all the raw EMPA data.

4.3.4 *Glass major element chemistry*

The silica and total alkali contents of the sampled rocks range from 70.94 – 77.82 wt% and 6.68 – 8.90 wt%, respectively. These results classify the glass shards as having a rhyolite composition, with the one shard on the border of dacite and rhyolite composition. There are three distinguishable clusters in Figure 4.12. Sample L5 forms a cluster of its own with the lowest SiO_2 content. Clustered together with the highest silica content are samples: L12.1, L12.2, L12.3, L4, #9 and L2WP. In between the two extremes is a cluster comprising of L2BP, L7.4 and L7.1. Sample L11 is scattered randomly throughout the three clusters.

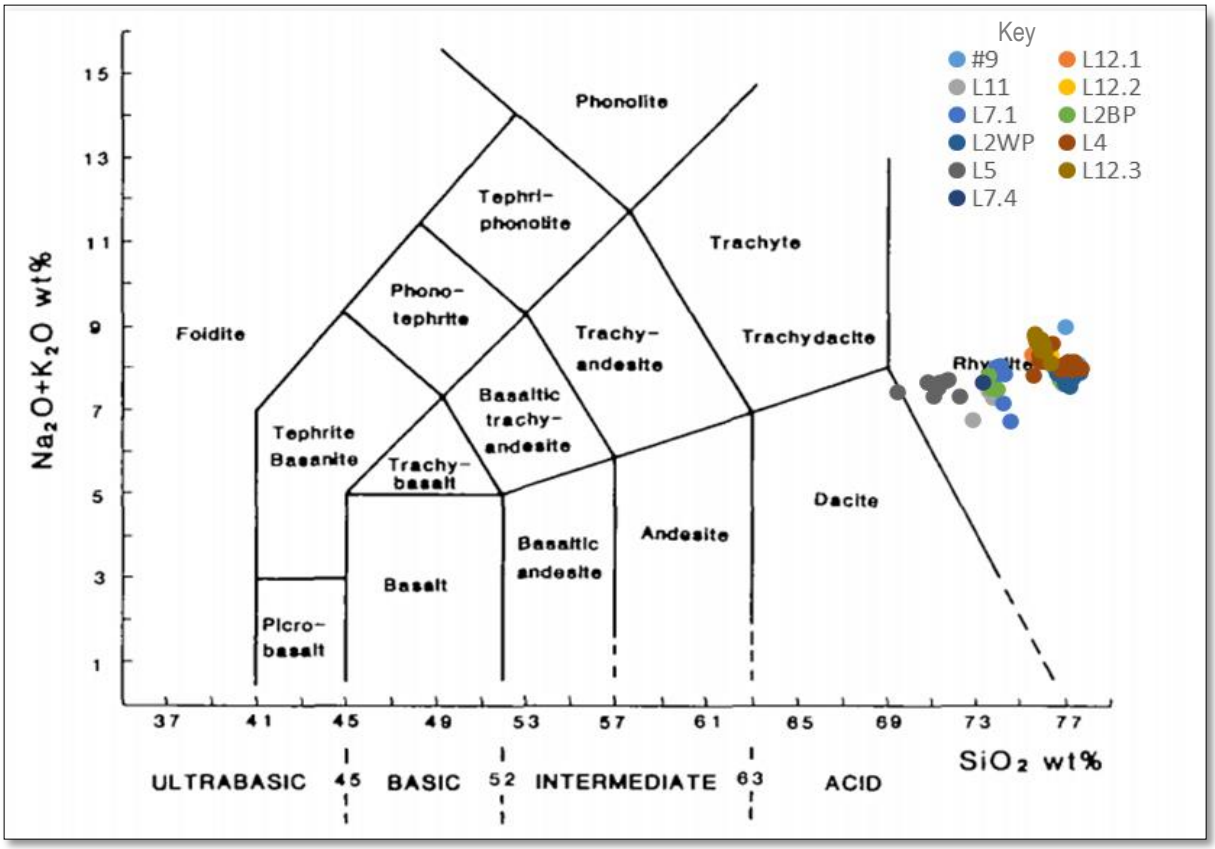

Figure 4.12 TAS diagram adopted from Lebas et al. (1986) showing the chemical composition of glass shards extracted from 11 samples from the study area.

To determine chemical variations within the magma, Harker Plots were produced (Figure 4.13), whereby values of each major element were plotted against silica content.

In Figure 4.8, the following major elements: CaO, Al_2O_3, FeO, TiO_2, MgO and MnO, show a negative trend, each decreasing as the silica content increases. The negative trend show that these major elements are

compatible and crystallised out of the melt in the process of fractional crystallisation. In terms of potassium, there is a slight positive trend consistent with potassium being an incompatible major element. Sodium did not show a distinctive trend.

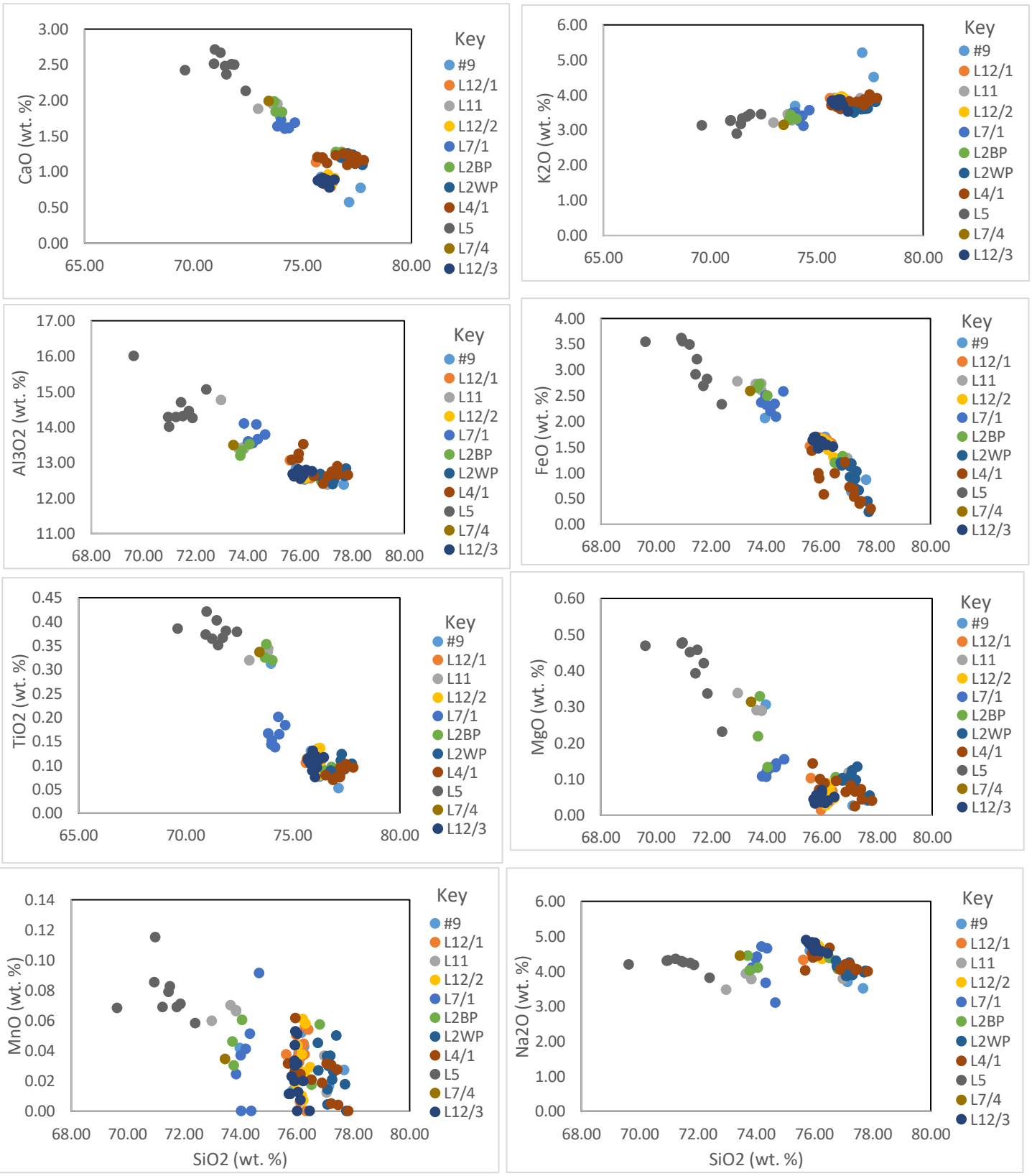

Figure 4.13 Harker variation plots for the major elements for the individual glass shards that were analysed using EMPA. Each sample is assigned a colour as shown in the key on the right side of the Harker plots.

4.3.5 Mineralogy of the black and white pumice

The minerals that are dominant in the black and white pumice clasts are: plagioclase, hornblende and pyroxene. It must be noted that in the white pumice, hornblende is dominant while pyroxene (especially clinopyroxene) is more dominant in the black pumice.

Two polished thin sections of these two pumice types, one per thin section, were prepared and analysed using the electron microprobe to determine the elemental composition of plagioclase in both the pumice clasts, pyroxene in the black pumice and hornblende in the white pumice. The results obtained have been plotted on a ternary diagram for plagioclase (Figure 4.14) and pyroxene (Figure 4.15).

In the ternary diagram for plagioclase, it was discovered that the elemental composition for plagioclase in both the black and white pumice ranged from andesine to labradorite.

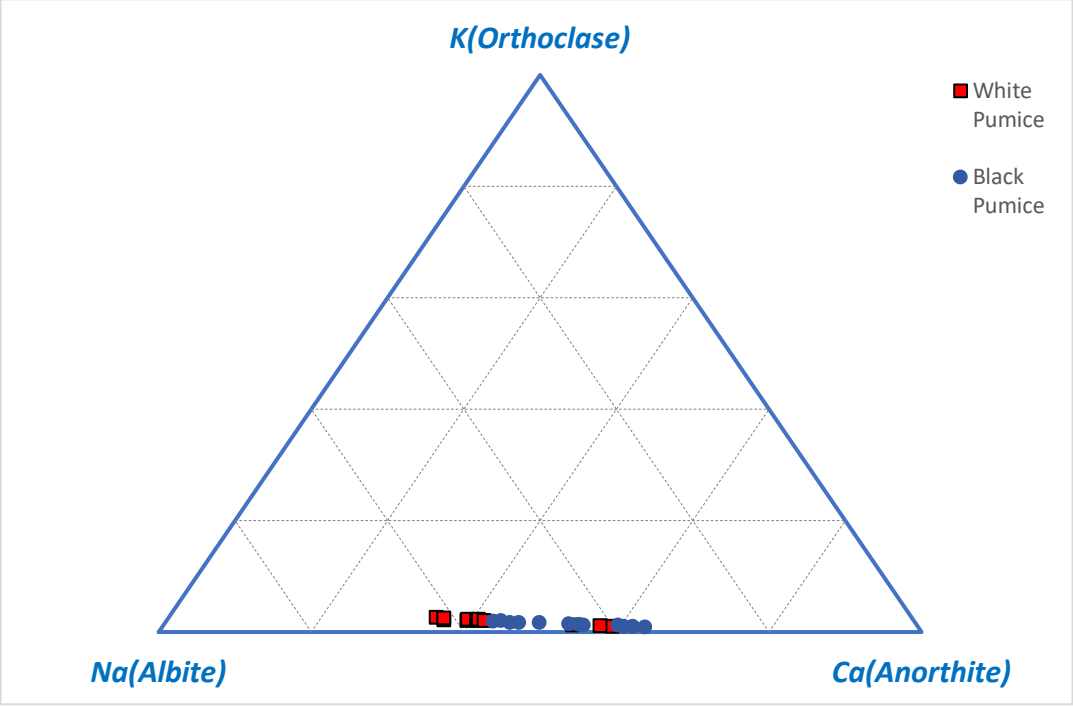

Figure 4.14 Ternary diagram for plagioclase in the white and black pumice.

In the ternary diagram for pyroxene (Figure 4.15), it shows that most of the pyroxene in the black pumice are orthopyroxenes.

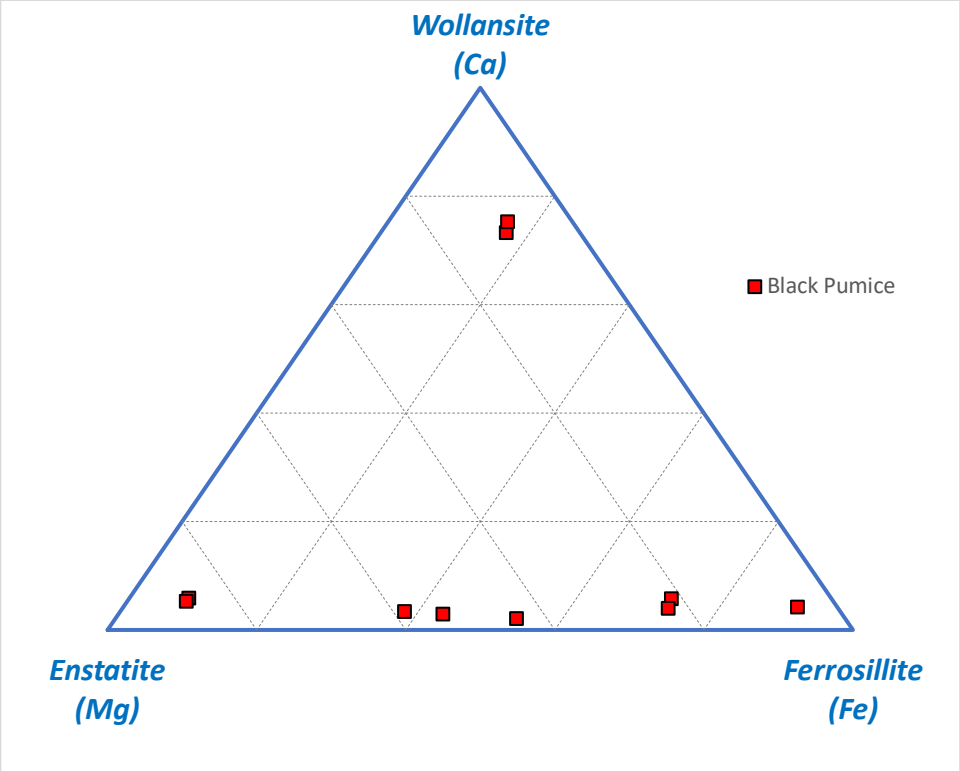

Figure 4.15Ternary diagram for pyroxene in the black pumice.

4.4 X-Ray Fluorescence (XRF) Spectroscopy Analysis: Sample Preparation and Analysis

4.4.1 XRF Sample Preparation

Major element proportions of white and black pumice, and also a grey pumice and a banded pumice, from the Welcome Bay Ignimbrite at localities 2 and 9 were measured using the Bruker S8 Tiger XRF machine at the University of Waikato.

Samples were dried in an over for four days at 105°C. The samples were then ground to powder using a tungsten-carbide ring mill. Each sample was ground for approximately 40 s – 1 min before being collected and stored in storage jars.

Fused discs were prepared by combining approximately 8 g of XRF Flux [Type: 12:22 (Granular), 35.3 % Lithium Tetraborate and 64.7 % Lithium Metaborate], 0.8 g of sample and approximately 0.1- 0.2 g of

ammonium iodide in a crucible. The mixture was then heated in the CLAISSE LE neo FLUXER fusion furnace at 1050˚C for 20 minutes. The molten mixture was then poured into a mold and fan-cooled for 6 minutes to form a disc.

To determine the loss on ignition (LOI) in the samples, the weight of a crucible was firstly recorded. Then, approximately 1-2 g of each sample was placed in separate crucibles and the total weight was recorded. The samples were then heated in the Nabertherm furnace at 1100˚C for an hour and left to cool. Once cooled, the weight of the heated sample and crucible was recorded again. The different in weight before and after heating is the LOI.

4.4.2 Major element geochemistry of whole pumice clasts

The compositions of the major elements are displayed in Table 1.

Table 1 Major element proportions of the black, white, banded and grey whole pumice analysed from XRF.

Sample Name	SiO2 (%)	Al2O3 (%)	TiO2 (%)	MnO (%)	Fe2O3 (%)	MgO (%)	CaO (%)	Na2O (%)	K2O (%)	P2O5 (%)	SO3 (%)	SrO (%)	BaO (%)	LOI (%)	Sum (%)
L2-GP	61.08	16.93	0.59	0.06	5.40	0.75	3.21	3.76	2.29	0.11	0.05	0.02	0.05	6.08	100.39
L2-BP1	63.31	16.01	0.64	0.08	5.45	0.88	3.41	3.74	2.34	0.14	0.03	0.02	0.06	4.18	100.29
L2-Banded Pumice	66.91	15.27	0.42	0.07	3.79	0.80	2.82	3.76	2.77	0.06	0.02	0.02	0.07	3.63	100.41
L2-WP1	66.68	14.79	0.38	0.06	3.66	0.84	2.78	3.92	3.11	0.06	0.05	0.02	0.08	3.80	100.24
L2-WP2	67.10	14.87	0.40	0.06	3.77	0.79	2.73	3.79	2.88	0.06	0.05	0.02	0.07	3.60	100.19
L2-WP3	61.29	17.02	0.61	0.07	5.83	1.09	2.78	3.36	2.41	0.08	0.18	0.02	0.06	5.64	100.43
L2-WP4	65.60	14.83	0.39	0.05	3.70	0.77	2.79	4.29	2.99	0.05	0.18	0.02	0.08	4.74	100.49
L2-BP2	62.69	15.84	0.62	0.07	5.37	0.83	3.19	3.72	2.39	0.13	0.03	0.02	0.05	6.51	101.48
L9-WP1	67.05	15.41	0.42	0.09	3.90	0.84	2.76	3.59	2.75	0.03	0.02	0.02	0.07	3.35	100.29
L9-WP2	67.45	15.44	0.41	0.06	3.85	0.79	2.75	3.61	2.77	0.03	0.02	0.02	0.07	3.31	100.58
L9-WP3	66.75	15.67	0.42	0.06	4.01	0.90	2.88	3.69	2.67	0.03	0.01	0.02	0.06	3.25	100.43
L9-WP4	64.75	16.46	0.49	0.07	4.65	0.98	2.87	3.42	2.47	0.04	0.03	0.02	0.07	4.25	100.57

*L2= Locality 2, L9= Locality 9 GP=grey pumice, WP= white pumice, BP = black pumice.

The silica and alkali contents of the different pumice types range from 60.84 – 67.06 % and 5.75 - 7.24 %, respectively. From the TAS diagram shown as Figure 4.16, the composition of the different pumice types that occur in the Welcome Bay Ignimbrite range from andesitic (black pumice) to dacitic (white pumice). The range in composition of the whole pumice types differ from that of the glass analysis presented in Figure 4.12 where glass shards from the same pumice types show a rhyolitic composition along with the rest of the other ten samples that were analysed from the study area. In both the EMPA (Figure 4.12) and XRF analysis (Figure 4.13) there are differences in SiO_2 and total alkali content in both pumice types.

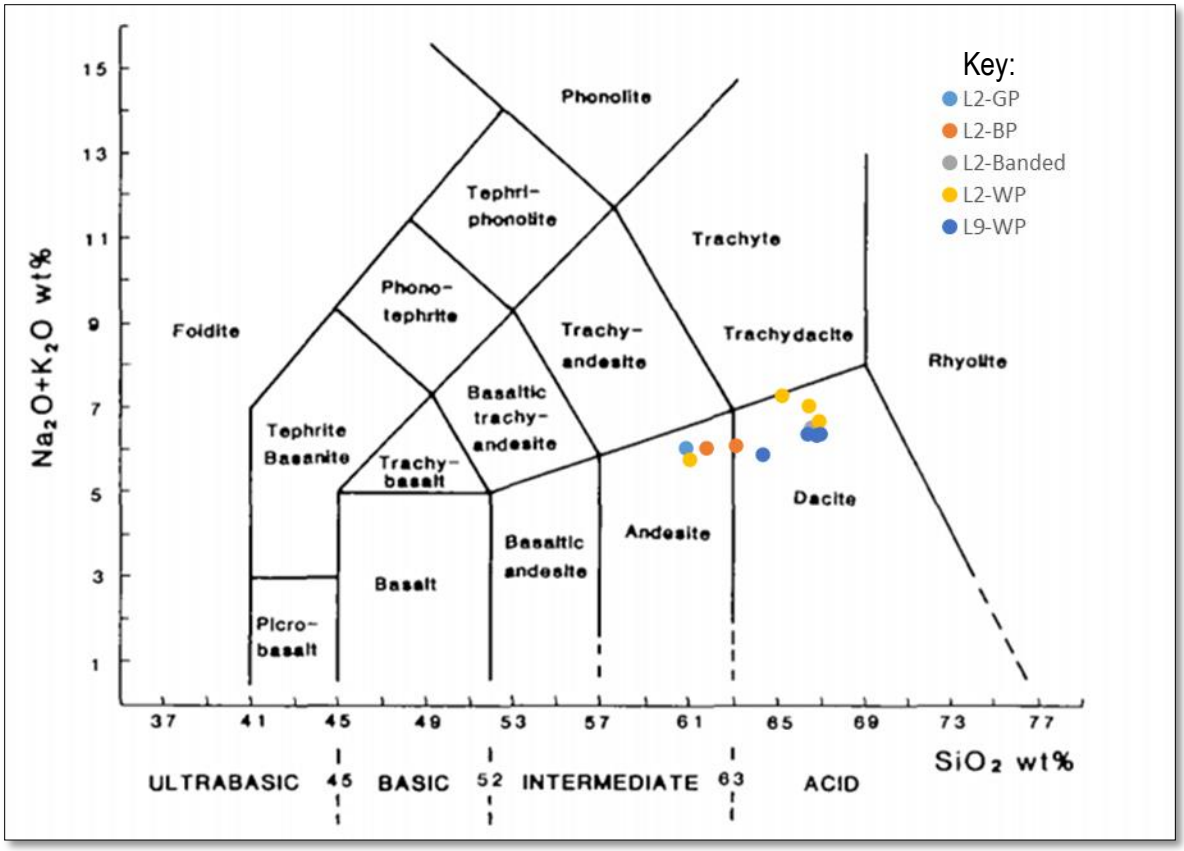

Figure 4.16 The chemical composition of the different pumice types found in L2 and L9, Ignimbrites on a total alkali versus silica (TAS) plot of Lebas et al. (1986). L2-GP = grey pumice from L2, L2-BP = black pumice from L2, L2-Banded = banded pumice from L2, L2-WP =white pumice found in L2 and L9-WP = white pumice found in L9.

Major Element Chemistry of Whole Pumice Clasts

The trends observed from the whole pumice XRF data (Figure 4.17) show that the chemistry of calcium, potassium, titanium, magnesium and manganese changed from being incompatible to compatible or these major elements evolved from remaining in the melt to crystallising out of the melt over some time. Iron and aluminum showed a negative trend or a compatible trend. Sodium showed a flat trend, i.e., as the silica content increased, the amount of sodium remained at a range 3.35 – 4.27 wt. %. The Harker plots below (Figure 4.17), show that the black and grey pumice all have high Fe_2O_3 whereas the white and banded pumice have low Fe_2O_3. The plots show that there is a rogue white pumice sample (L2-WP3) that seems to be plotting amongst the grey and black pumice clasts but more closely plotted with the latter.

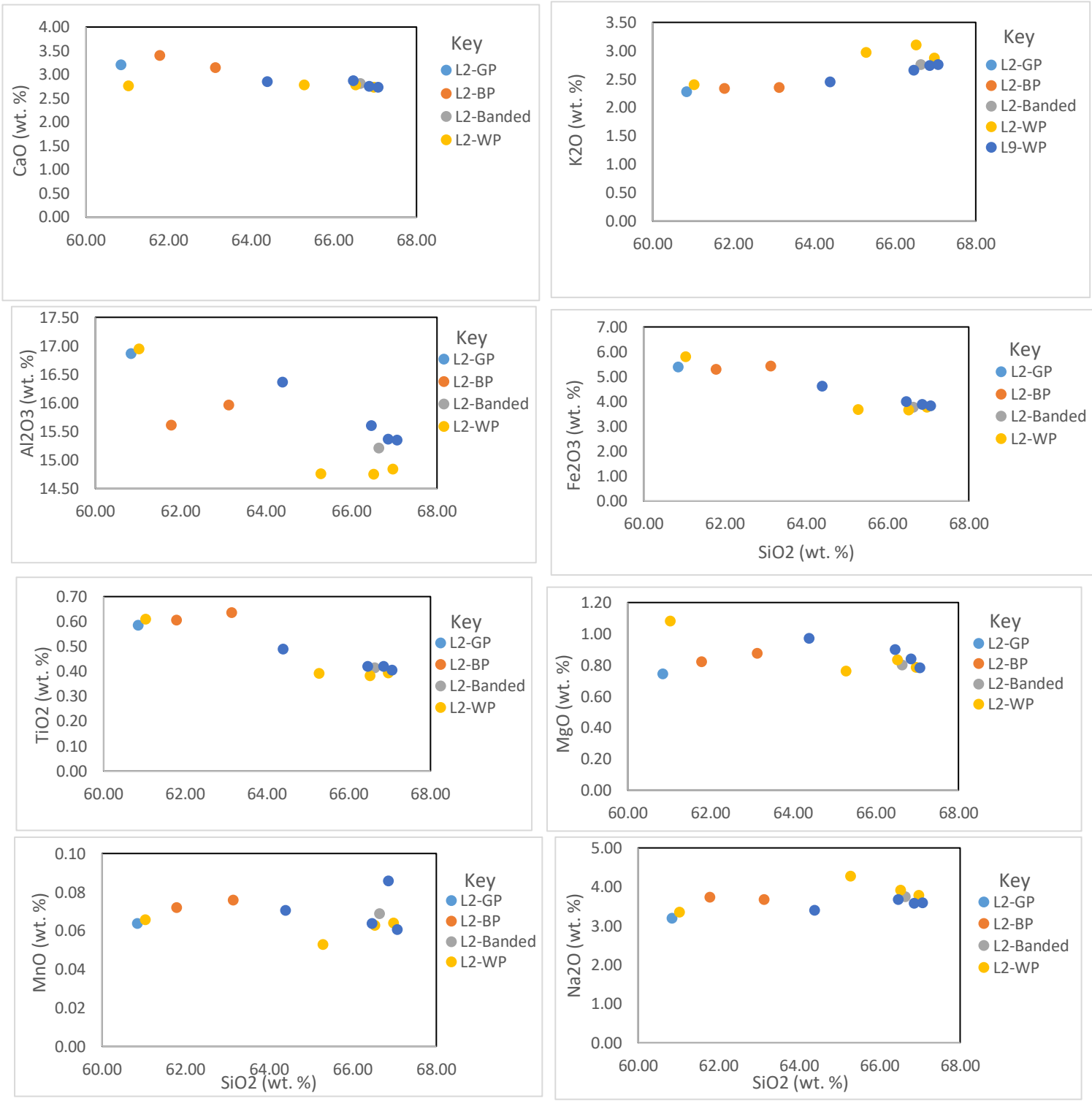

Figure 4.17 Harker plots of the major elements versus silica for the main types of whole pumice found in the Welcome Bay Ignimbrites are Localities 2 and 9 (L2 and L9), including one grey and one banded pumice. GP=grey pumice, BP=black pumice, WP= white pumice.

4.5 Laser Ablation Inductively Coupled Plasma Mass Spectrometry (LA-ICPMS) Analysis: Sample Preparation and Analysis

4.5.1 Sample preparation

Rare Earth element and trace element composition were determined using the LA-ICPMS at the University of Waikato. The same mounts that were used for the EMPA were again analysed using LA-ICPMS as the positions at which each scar/zap was made by the microprobe could easily be located and analysed for consistency in the results. Most of the microprobe positions were georeferenced before the samples could be analysed using the LA-ICPMS. Some probe scars/zaps, however, were challenging to relocate so new points were georeferenced on the same glass shard that was probed. For sample L7/4, there were no sufficient polished surfaces to georeferenced prior to conducting the LA-ICPMS analysis, hence, this sample was not analysed. Trace and rare Earth elements determined include: Zn, Ga, Rb, Sr, Y, Zr, Nb, Cs, Ba, La, Ce, Pr, Nd, Sm, Eu, Gd, Tb, Dy, Ho, Er, Tm, Yb, Lu, Hf, Ta, W, Pb, Th, and U. To ensure the accuracy and precision of the data, two standards were also analysed, along with the unknowns and internal standards, NIST612 as the primary standard and ATHO-G as the secondary standard. These two standards were analysed once before and after the analysis of each sample. The instrument specifications of the LA-ICPMS, standards analysis table and trace element raw data are presented in Appendix 3.

The concentrations of trace elements: barium (Ba), rubidium (Rb), thorium (Th), lanthanum (La), cerium (Ce), strontium (Sr), zirconium (Zr) and yttrium (Y) are in parts per million (ppm) and were plotted against SiO_2 (in wt. % and obtained from the EMPA data). The plotted Harker plots are presented in Figure 4.18. From Figure 4.51, rubidium shows a distinctive positive trend. Compatible trace elements include strontium (Sr) and zirconium (Zr). For barium, thorium, lanthanum, cerium and yttrium, there is no well-defined.

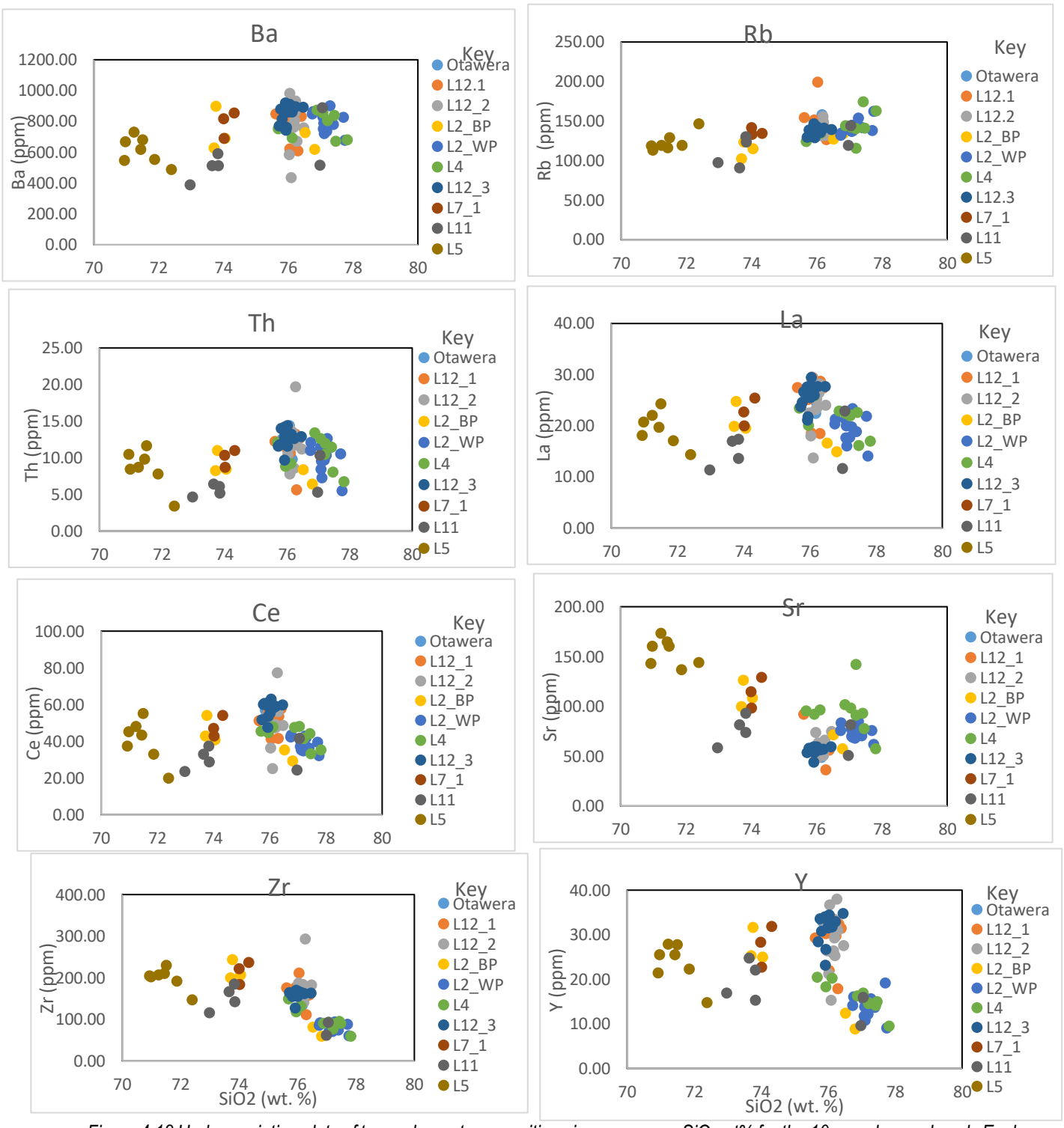

Figure 4.18 Harker variation plots of trace element compositions in ppm versus SiO_2 wt% for the 10 samples analysed. Each sample is assigned a specific colour as shown on the right of each Harker plot.

CHAPTER 5
DISCUSSION

5.1 Introduction

To determine the eruption history and volcanic processes involved in the geological formation of the study area, stratigraphic, petrographic and geochemical analysis of the Papamoa Formation was carried out. Section 6.2 compares the four ignimbrites of the Papamoa Formation in terms of their physical and geochemical characteristics. In section 6.3, the proposed volcanic origin of the units of the 'Addline Sequence' will be discussed. Section 6.4 focuses on the Wharo Ignimbrite and explains why it is the only densely welded ignimbrite in the study area. In section 6.5, the Otawera Ignimbrite is discussed, in particular the flow processes involved in the transportation and deposition of its three different flow units. Section 6.6 explains why there are pumice variations in three of the four ignimbrites of the Papamoa Formation and implications for the magmatic processes and conditions during the time of eruption. Section 6.7 covers the geological history of the study area; an evolution of the landscape of the eastern TgaVC. Finally, section 6.8 presents the limitations of this study and provides recommendations for future research work.

5.2 Comparison of the four significant ignimbrites

In studying the stratigraphy, petrography and geochemistry of the deposits in the study area, it was evident that there are more than two ignimbrites as previously proposed by Hughes (1993). Here, the Papamoa Formation includes five different ignimbrites: 1) Welcome Bay Ignimbrite (formerly Lower Papamoa Ignimbrite by Hughes, 1993) dated at 2.4Ma (Briggs et al., 2005) Wharo Ignimbrite (formerly Upper Papamoa Ignimbrite by Hughes, 1993) dated at 2.26 Ma (Prentice, unpublished data), 3) Arateka Ignimbrite (age yet to be determined), 4) Otawera Ignimbrite dated at 2.21 Ma (Pittari et al, 2021) and 5) an unnamed ignimbrite - Unit A of the Addline Sequence – that is stratigraphically older than the Welcome Bay Ignimbrite. Each of the five ignimbrites have unique geochemical compositions (Chapter 4) and indicate the products of five different

eruption events. Of the five ignimbrites, the darkest in colour and most densely welded is the Wharo Ignimbrite. The other four ignimbrites vary between non-welded to moderately welded. The Arateka, Wharo and Welcome Bay Ignimbrites are composed of both black and white pumice clast types. However, for the Wharo Ignimbrite, black pumice clasts are more abundant and, in some instances, they are the only pumice type present in studied sections. The Otawera Ignimbrite is unique in that it only contains white pumice and is made up of three flow units. A summary of the discussed similarities and differences amongst the Welcome Bay, Wharo, Arateka and Otawera ignimbrites is presented in Table 6.1. The unnamed Unit A ignimbrite was poorly exposed and found only at one locality, hence there is insufficient information to compare with the other four better-exposed ignimbrites.

Table 2 Summary of the similarities and differences of the ignimbrites in the Papamoa Formation.

Ignimbrite:	Welcome Bay Ignimbrite	Wharo Ignimbrite	Arateka Ignimbrite	Otawera Ignimbrite
Average Thickness (m)	9.3	8.6	8	20
Age	2.4 Ma (Briggs et al. 2005*)	2.3 Ma (M. Prentice, unpublished data)	To be determined	2.21 Ma (Pittari et al., 2021)
Colour of outcrop	Beige - brown	Dark brown - black	Beige-yellow brown	Beige
Textures	Vitrophyric	Eutaxitic	Vitrophyric	Vitrophyric
Welding	Non-weak	Moderate-dense	Weak	Non-moderate
Pumice composition	Black and white pumice present	Black and white pumice present but white pumice is dominant	Black and white pumice present	Exclusively white pumice present

*****The Lower Papamoa Ignimbrite referred to and dated by Briggs et al (2005) is here divided into the Welcome Bay Ignimbrite and Wharo Ignimbrite. The sample that was dated by Briggs et al (2005) is likely to have come from what is now called the Welcome Bay Ignimbrite.

5.3 Origin of the lower units of the Addline Sequence (Units A-D)

The Addline Sequence, as presented in Chapter 3 is comprised of the studied geological units at Localities 4, 5, 6, 7, 8 and 9. Locality 6 was not studied in detail as it comprised of the same as the ridge-forming geological unit at Locality 4. The Addline Sequence was studied from Locality 7 at the lowest point of the 940 Welcome Bay Road property, to Localities 8, 9, 5 and lastly to the highest point at Locality 4.

Discussed in this section will be the proposed origins of the geological Units A, B, C and D (Welcome Bay Ignimbrite) of the Addline Sequence studied at Localities 7, 8 and 9. The Wharo Ignimbrite – which forms the upper part of the Addline Sequence - will be discussed in section 6.4. Ignimbrites found in other parts of the study area are discussed in later sections.

5.3.1 Unit A – Unnamed Ignimbrite

Unit A is located at the bottom of the Addline sequence and is an unnamed ignimbrite. Ignimbrites are pumiceous deposits of pyroclastic density currents generated from large explosive volcanic eruptions (Francis & Oppenheimer, 2004). To determine the process origin of Unit A stratigraphic, petrographic and geochemical information was considered, albeit with the limited exposure. The true thickness of Unit A could not be measured as the bottom of the unit was not exposed. However, the hand specimen from the top of Unit A had a silty texture and comprised mainly of fresh to partially iron-stained grey pumice with tubular or elongated vesicles. From petrographic observations, generally, Unit A is lithic-poor and majority of the unit is poorly sorted and composed of pumice set in a glassy matrix, which is a typical texture of an ignimbrite.

Unit A was likely the earliest ignimbrite in the Papamoa succession produced by a Plinian eruption The geochemical data shows that the chemical composition of Unit A is unique from that of the other ignimbrites in the study area. Only the top part of the flow unit is exposed, so very little can be understood about the overall emplacement of this unit. To bring Unit A to its current condition, Unit A has been exposed by deep stream erosion and modified by groundwater from the overlying aquifer.

5.3.2 Unit B – Silicified or Reworked Unit A

Reworked pyroclastic deposits are secondary volcaniclastic deposits that were sourced from volcanoes and transported and deposited by sedimentary processes (Sohn & Sohn, 2019). From stratigraphic and petrographic observations of Unit B, the pumice and lithic clasts are embedded in a fine-grained matrix and the pumice clasts appear to be more rounded. These observations could support the idea that Unit B might have been derived from a pyroclastic deposit that was reworked (e.g. pumice rounding), buried and later hardened by silicification from groundwater; the spring emanating from this unit is evidence for an aquifer. The relationship between Unit A and Unit B is uncertain. Unit B could be the reworked upper part of Unit A, which is supported by the gradational contact. Alternatively, Unit B could be a reworked volcaniclastic deposit derived from elsewhere, which supports the introduction of lithics which are not found in Unit A.

5.3.3 Unit C – Airfall deposit

Pyroclastic fall deposits are the deposits from fall out from an explosive eruption column by the influence of gravity (Francis & Oppenheimer, 2004; Wright et al., 1980). Fall deposits are identified by their mantle bedding (i.e. maintaining a uniform thickness within restricted areas), well-sorted texture (due to winnowing with the aid of the wind) and at times internal stratification characteristics (Wilson, 1986; Wright et al, 1980). Because fall deposits from rhyolitic explosive eruptions are mainly comprised of pumice (50 – 90% abundance), a matrix is not present, hence making the deposits less consolidated.

Unit C of the Addline Sequence is an airfall deposit, possessing the typical well-sorted and lithic-poor texture, angular-shaped pumice clasts and absence of a matrix. In the Addline Sequence, Unit C is found to have an almost even thickness of ~1.2 m throughout the studied outcrop which again is characteristic of fall deposits.

It has been observed from studies of prehistoric deposits of explosive ignimbrite-forming eruptions that a characteristic sequence often occurs: an initial fall deposit, followed by the ignimbrite, and within close proximity of the vent, a lava dome (Wilson, 1986). This line of sequence reflects the downward tapping of a magma chamber that has decreasing volatile content from the highest at the top, to lowest at the bottom (Wilson, 1986). The higher the volatile content in a magma has, the more explosive the eruption (Francis & Oppenheimer, 2004), hence the characteristic sequence reflects the zonation of the most explosive eruptions (forming fall deposits and ignimbrites). Unit C or the fall deposit would have been produced by the same

Plinian eruption that produced the overlying Welcome Bay Ignimbrite. Evidence for this is the sharp planar contact between units C and D, and lack of evidence for a time break. The hardened base of Unit D is probably a later effect of cementation by groundwater. Unit C would have been the product of the initial phase of the eruption which would have been more energetic but would have not lasted longer than the second phase that produced the voluminous Welcome Bay Ignimbrite.

Future research work should include a comparison of the pumice clasts of Unit C and D which will assist in determining whether or not these two units are related or unique pyroclastic deposits.

5.3.4 Unit D - Welcome Bay Ignimbrite (WBI)

The Welcome Bay Ignimbrite is the most voluminous ignimbrite in the study area and makes up Unit D in the Addline Sequence but also occurs at Localities 2, 4, 6, 8 and 9. As mentioned in section 6.3.3, an ignimbrite often follows a fall deposit in the characteristic sequence of an ignimbrite-forming eruption. From this it is only plausible to think that the Welcome Bay Ignimbrite would have been produced during the second phase of the Plinian eruption that had also produced Unit C. Unlike the initial phase, this second phase of the eruption would have been sustained, producing the large volume of Welcome Bay Ignimbrite.

When an ignimbrite loses all its kinetic energy and eventually comes to a stop, the pyroclastic deposit flows down ridges and into valleys where they are deposited and accumulate to forming “flat-topped valley-pond deposits” (Ballance, 2009, p128). Being the most voluminous ignimbrite in the study area, the Welcome Bay Ignimbrite is also quite massive. In saying that, the Welcome Bay Ignimbrite can be identified as a thick valley -ponded deposit. The deposition of the Welcome Bay Ignimbrite would have been fueled by a sustained pyroclastic density current, transporting and depositing the ignimbrite to form the modern landscape. Because the Welcome Bay Ignimbrite is pumice-rich, it would have had a low flow bulk density enabling it to flow further (Pittari et al. 2006) down the northern flanks of a vent that would have been located in the southern parts of the study area. As the time lapsed, the Welcome Bay Ignimbrite would have accumulated, mantled the pre-existing topography and drained (under its own weight under the influence of gravity) into the valleys to form the valley-ponded deposits. For the ridges that are exposed as outcrop in the study area, they would have been exposed due to road cuttings or for the Welcome Bay Ignimbrite outcrops along the sides of valleys, their exposure could have been resultant of sedimentary processes such as erosion brought about by streams and or rivers.

5.4 Wharo Ignimbrite

The Wharo Ignimbrite, as mentioned earlier, is the only ignimbrite of the Papamoa Formation that is densely welded with a dark brown to black colour. The process of welding in pyroclastic deposits is mainly due to a combination of high emplacement temperature and the weight of the overlying part of the deposit, leading to the cohesion of the glassy fragments in the pyroclastic deposit to form a rock that is more dense and coherent (e.g. Francis & Oppenheimer, 2004; Sparks, Tait & Yanev, 1999). When a pyroclastic deposit is densely welded, the pumice clasts and shards in the deposit are flattened and form flame-like structures called fiamme, giving the rock a eutaxitic texture (e.g. Francis & Oppenheimer, 2004).

The controlling factors that determine the degree of welding is the chemical composition, the local temperature and the load pressure within the deposit (Wilson, 1986). The higher the alkali and/or volatile content in a deposit, the greater the degree of welding. Within an ignimbrite, there are variations due to the local temperature and pressure load at a particular point in the ignimbrite during the time of deposition. The base of an ignimbrite would be less welded than the mid-section due to the ground acting as a sink that absorbs the heat of the pyroclastic flow when it flows over the land surface. The temperature difference between the ground and the hot pyroclastic deposit gives rise to a lower degree of welding or non to weak welding. The mid-section of the ignimbrite, on the other hand, do not have a sink in which to transfer their heat therefor the heat remains within the ignimbrite, prolonging and restricting welding to occur, the mid-section being more welded than the basal layer (Wilson, 1986). The top section of an ignimbrite is exposed to the atmosphere which aids in the cooling of the ignimbrite as well as additional weather factors such as being exposed to the rain, hence welding is inhibited.

The Wharo ignimbrite outcrops in four localities of the study area: Localities 1,3,13 and 14. As discussed in Chapter 3, the outcrops display fiamme-rich sections which indicates welding. At all these localities, the Wharo Ignimbrite displays a vertical zonation in the degree of welding, ranging from a non-welded or weakly welded basal layer to a moderate to densely welded mid and upper sections of the outcrop.

With respect to the glass geochemistry of the Wharo Ignimbrite, a sample from Locality 5 was the only sample that contained sufficient glass shards to be analysed using EMPA and LA-ICPMS. As for the other localities, glass shards were already in their deformed state due to welding, hence the extraction of glass shards was impossible. Optical microscopy of the Wharo Ignimbrite showed the matrix to have a eutaxitic texture, again

another typical characteristic of welded ignimbrites. The results in Chapter 4 show that with respect to all of the analysed ignimbrites, the glass shards from the Wharo Ignimbrite (sample L5) have the lowest silica content, but a comparable alkali content causing the Wharo Ignimbrite to still fall into a rhyolite composition on a TAS diagram. The Wharo Ignimbrite also has the highest concentration of Ca, Al, Ti, Mg, Mn, and most significantly in Fe. The oxidation state of Fe in rocks, naturally occurs as both Fe^{2+} and Fe^{3+} and are normally analysed separately (Cox, Bell & Pankhurst, 1979). For this study, Fe was not analysed in the two different oxidation states but rather just as Fe (FeO), which includes both oxidisation states. The dark colouring of densely welded ignimbrites is possibly due to the different oxidation states of Fe (Koralay & Kadioglu, 2008; Wright, 1979).

5.5 Otawera Ignimbrite

Ignimbrite flow units comprise of three layers (e.g. Sparks et al. 1973; Wilson, 1986): 1) Layer 1 – the basal or ground layer, 2) Layer 2 - forming the bulk of the ignimbrite and 3) Layer 3 – which is typically a co-ignimbrite fall or pyroclastic surge deposit that overlies Layers 1 and 2 and covers a wider surface area. An example of an ideal single ignimbrite unit is presented in Figure 6. 1. The studied Otawera Ignimbrite showed clear boundaries of three flow units which would have occurred at three different timings or pulses during a Plinian eruption, forming a continuous compound ignimbrite. Figure 6.1 compares the Otawera Ignimbrite and Wilson's idealised ignimbrite flow unit (1986).

From the stratigraphic observations made of the Otawera Ignimbrite, there was evidence that Layer 1 (bottom flow unit) contained more and bigger sized lithics (up to 90 mm) and an abundance of 15 – 20 % of crystals. Due to these lithics and crystals having a high density, they would have been deposited first through the process of winnowing. The less dense, fine grained and lighter pumice would have been transported further by the large amounts of gas produced from the expansion of heated air that had escaped quickly from the front of the flow (Wilson, 1986). The main thick layer of each flow unit comprised a layer 2a with fine-grained pumice clasts, which is overlain by a lithic concentration zone around the mid-section of Layer 2. Above the lithic concentration zone, each flow unit is reversely graded upwards toward a pumice-rich upper layer. Grading in deposits is caused by the density contrast of individual fragments within the pyroclastic flow, i.e., the larger the clast sizes, the more effective the grading of the deposit (Wright, Smith & Self, 1980). In saying

that, the pumice-rich layer overlying the finer material would have floated to the top of the pyroclastic flow as it was being transported.

The three flow units would have been resultant of three different pulses of one Plinian eruption. The geochemical data supports this in that it shows that samples from the bottom, mid-section and top of the studied outcrop, all have the same chemical composition. The lower part of the Otawera Ignimbrite is more welded than the middle section, which is non-welded. Then in the upper part of the ignimbrite, the degree of welding slightly increases to weakly welded. This alternating degree of welding is typical of ignimbrites, perhaps an effect of multiple flow units. As mentioned earlier in section 6.4, the basal or ground layer of the ignimbrite would typically be less welded as this layer would have been the first to contact the colder land surface, hence cooling the basal layer quicker, making the materials in the deposit less coherent or non to weakly welded. It was observed in the field that there was an increase in welding toward the top of the outcrop. This could be resultant of the effect of a later flow unit coming in at a higher temperature than the lower flow unit. The biggest lithics in the whole outcrop were found at the ground layer indicating that the lithics were deposited by gravitational settling during transport of the pyroclastic flow. The size of lithics, pumice, crystals and the thickness of a deposit can assist in determining the distance from the vent, i.e., the greater the size of the components of an ignimbrite and its thickness, the closer to the source the deposit is (Spark, 1976; Wilson, 1986). In saying that, being approximately 20 m thick and having a bottom layer comprising large lithics (max size of 90 mm), the Otawera Ignimbrite is most likely to be close to its source. The energy of the eruption must have decreased over time as implied by the decrease in lithic size from the biggest lithic sizes at the bottom layer to the top of the studied outcrop.

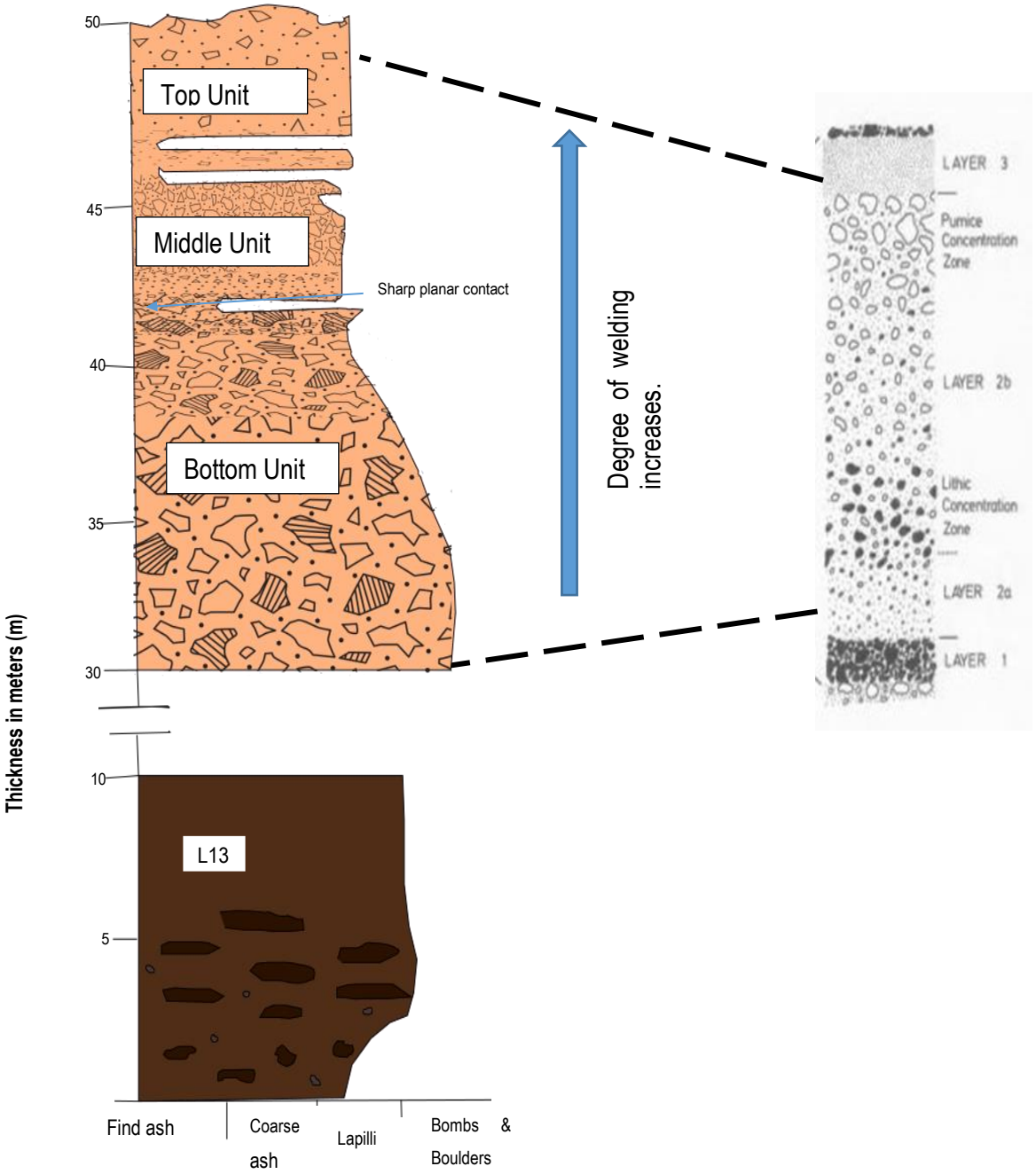

Figure 5.1 A comparison of the Otawera Ignimbrite against the Wilson's idealized single ignimbrite flow unit showing the layers and grading of the components of an ignimbrite (1986). White shapes denote pumice while lithics are represented by shaded (black) shapes, and dots are used to show fine ash matrix.

5.6 Pumice Variation

Ignimbrites are composed of three components: pumice (dominant), lithics, and crystals all set in a fine-grained matrix (Francis & Oppenheimer, 2004, Wilson, 1980; Wright et sl., 1980). Of the three components of an ignimbrite, pumice clasts are the most important as the geochemistry of the pumice provides valuable information with regards to the magma composition.

There are two pumice types that were observed in the study area: white and black pumice. Both pumice types are present in the Welcome Bay, Wharo and Arateka ignimbrites however the white pumice is less abundant or close to absent in some of the studied outcrops of the Wharo Ignimbrite. The white pumice is abundant in the Welcome Bay Ignimbrite, making up ~85% of the pumice population of the ignimbrite. The white pumice clasts found in the Welcome Bay Ignimbrite are also the biggest found in the study area compared to the Arateka and Wharo ignimbrites. All of the EMPA ignimbrite glass analyses of the Papamoa Formation are of a rhyolitic composition. However, the XRF results of the whole pumice clasts (presented in Chapter 4), found that the pumice composition ranged from andesitic –typically for black pumice to dacitic – typically for white pumice. There was the odd banded and grey pumice that were also analysed resulting in compositions between andesite-dacite. With the presence of grey and banded pumice found within the Welcome Bay Ignimbrite and the range of chemical compositions of the two types of pumice, it can be concluded that there was some degree of magma mixing that occurred prior to the eruptions of the Welcome Bay, Arateka and Wharo ignimbrites. The magma was evolving from an andesitic to dacitic composition or an andesitic magma could have mixed with a dacitic magma. For samples Welcome Bay Ignimbrite samples (collected from L7 and L8) that showed orange/pink coloured pumice clasts, the colouring could be resultant of the pumice clasts having undergone some form of chemical weathering.

From the petrography of the two pumice types, it was discovered that the main minerals present in the white pumice were plagioclase and hornblende whereas for the black pumice, the main minerals were plagioclase and pyroxene (both orthopyroxene and clinopyroxene but dominantly orthopyroxene). This information confirms that the black pumice is more mafic than the white pumice, hence may be a possible cause for the colour difference.

Both the abundance and size of white pumice population in the Welcome Bay, Arateka and Wharo ignimbrites decreases in each successive and younger ignimbrite. Although the numerical age of the Arateka Ignimbrite

is yet to be determined, it is inferred here that the Arateka Ignimbrite eruption occurred sometime between that of the Welcome Bay and Wharo ignimbrite eruptions. This order of eruption is suggested due to the Arateka being the only other ignimbrite, apart from the Welcome Bay (dominated by white pumice) and Wharo Ignimbrites (dominated by the black pumice), that comprises of both pumice types and its glass chemical composition (Figure 4.12) is positioned between the Wharo Ignimbrite (sample L5) and the Welcome Bay Ignimbrite (sample L4, L7.4, L2-WP). The Wharo Ignimbrite could have been sourced from the magma when it was evolving or mixing, from a more dacitic (Welcome Bay Ignimbrite) to an andesitic (Wharo Ignimbrite) composition. In addition, the stratigraphically, the location of the Arateka Ignimbrite is below the Wharo Ignimbrite or could have filled the palaeovalleys before being overlain by the Wharo Ignimbrite. The stratigraphic position of the Wharo Ignimbrite in the field could also be due to faulting. With regards to the size of pumice, lithics, crystals and/or grainsize, the greater the size, the closer the deposit is the vent from which it was sourced (Wilson, 1986). This would mean that the WBI would be the closest to its source or that the eruption that produced it was a powerful eruption. The same can be said for the Otawera Ignimbrite.

In terms of the Otawera Ignimbrite, the only pumice type present there is the white pumice. Whole rock geochemical analysis of the Otawera Ignimbrite shows that it is rhyolitic in composition, hence this eruption would have likely undergone minimal magma mixing.

5.7 Lithic clasts and their sources

Lithics found in the ignimbrites of the Papamoa Formation in the study area include: pyroclastics (mostly earlier ignimbrites), rhyolites, and andesites. The most common lithic in is rhyolitic in composition. In the Welcome Bay Ignimbrite, however, the majority of lithics are andesites. Prior to these ignimbrite-forming eruption events, the Tauranga Basin comprised scattered Minden Rhyolite domes surrounded by andesite of the Otawa Volcano. The Otawa Volcano was active between 2.54 Ma – 2.95 Ma while the Minden rhyolites were deposited between 1.95 Ma – 2.89 Ma (Briggs et al., 2005).

Andesitic lithics could be accidental lithics that were picked up by the pyroclastic flow of the Welcome Bay Ignimbrite as it travelled across exposed rock of the Otawa Volcano.

Rhyolite lithics are likely to have been derived from local Minden rhyolite domes exposed along the flow path.

5.8 Geological History of the study area

Ignimbrites are deposits of pyroclastic density currents produced by Plinian eruptions through fountain collapse (Francis & Oppenheimer, 2004). The collapsing of an eruption column occurs when the momentum of the gas thrust runs out and the eruption column becomes denser than the surrounding atmosphere then it collapses under the influence of gravity. In doing so, the fountaining pyroclastic material travels at high speed down the flanks of a volcano until the kinetic energy fuelling the collapsed eruption column is exhausted.

From field observations, it was noticed that the Papamoa Formation deposits dip to the north and is confined to the valleys and foothills of the Papamoa Range. The distribution of the Papamoa Formation would have been brought about by a Plinian style eruption column that would have collapsed and flowed down the northern flanks of the vent. In doing so, the ejected ignimbrites flowed down the paleo landscape to form the present-day ridges.

Prior to the eruptions that produced the Papamoa ignimbrites, the landscape of the TgaVC would have comprised of an early Tauranga Basin with the young volcanic landforms of Otawa Andesite stratovolcano (Briggs et al., 2005) surrounded by the early-formed the Minden Rhyolite domes which were scattered within the basin. From the radiometric ages of the studied Papamoa ignimbrites, it can be concluded that the eruption events that led to their deposition occurred around the same time, i.e., between 1.9 Ma – 2.4 Ma (Briggs et at., 2005; Pittari et al., 2021). Units A and B are the oldest-known units of the Papamoa Formation in the study area, although a radiometric age is yet to be determined. Unit A formed from pyroclastic flow from a rhyolite Plinian-style eruption and was then overlain by a reworked volcaniclastic deposit (Unit B). After an unknown period of repose, a second. Plinian eruption occurred around 2.4 Ma (Briggs et al., 2005) that produced the most voluminous deposit in the study area, the Welcome Bay Ignimbrite. The initial phase of the eruption was a Plinian fall deposit that produced Unit C of the Addline Sequence. Following the fall deposit, and probably due to the collapse of the same eruption column, the Welcome Bay Ignimbrite was deposited. Sparks (1980) point out that ignimbrites tend to flow into areas of negative relief to settle in valleys. The Welcome Bay Ignimbrite in the study area, would have flowed down the northern flanks of the vent, naturally dipping to the north, and infilling the low-lying areas. Subsequent erosion led to their development as ridges in the study area. Around 2.26 Ma (Prentice, unpublished data) another Plinian style eruption occurred, this time producing the Wharo Ignimbrite. The Wharo Ignimbrite, like the previous ignimbrites, flowed down and infilled the palaeovalleys in the study area. The Wharo ignimbrite would have had a higher

temperature than the other ignimbrites to cause its moderate to dense degree of welding. Another Plinian eruption occurred around 2.21 Ma (Pittari et al., 2021) producing the Otawera Ignimbrite. This ignimbrite, however, has only been found in the areas east of the Rocky Cutting Road. Upon being ejected from the vent, the Otawera Ignimbrite would have flowed towards the north, infilling the newly-formed palaeovalleys. From the stratigraphy of the Otawera Ignimbrite, it can be recognised that the eruption had lost energy over time, in that vertically up through the ignimbrite, the size of the lithics decreased and the pumice floated to the top of the pyroclastic flow. Since the Welcome Bay Ignimbrite was deposited first, entrained Otawa Andesite lithics from the exposed ground surface, such that there was little to no exposure of andesite for the Wharo and Otawera Ignimbrites to entrain when they were deposited. The following eruption is uncertain as there is currently no known age for the Arateka Ignimbrite. As mentioned earlier, from the stratigraphical position, petrography and geochemical properties of the Arateka Ignimbrite, the eruption that produced it would have occurred after the Plinian eruption that produced the Welcome Bay Ignimbrite. Further study of the Arateka Ignimbrite would assist greatly in making a better interpretation.

5.9 Conclusion

This research aimed at determining the volcanic history and processes of the Papamoa Formation using modern day techniques. From the findings obtained from the stratigraphic, petrographic and geochemical analysis, the following conclusions have been made:

Stratigraphic findings resulted in the development of a revised stratigraphy of the western Papamoa Region. Hughes (1993) had proposed that the Papamoa Ignimbrite was comprised of two ignimbrites: the Lower Papamoa Ignimbrite (now renamed to the Welcome Bay Ignimbrite) and the Upper Papamoa Ignimbrite (now renamed as the Wharo Ignimbrite). However, this study has found that there are five ignimbrites that make up the Papamoa Formation: Welcome Bay Ignimbrite, Wharo Ignimbrite, Arateka Ignimbrite, Otawera Ignimbrite and Unit A- an Unknown Ignimbrite. In addition, as opposed to the findings by Hughes (1993) that there were five (5) pumice populations, this study has identified only two pumice types: the black pumice and the white pumice.

Findings from the petrography of the Papamoa Formation showed that the ignimbrites shared a similar but not the same mineralogy (common occurring minerals such as plagioclase, hornblende, pyroxene and

opaques with minor minerals such as quartz and biotite). Although some minerals occurred in some samples, the same minerals were absent in other samples. This was exemplified by the two pumice clasts, the white having more plagioclase and hornblende while the black pumice comprised more of plagioclase and pyroxene. The vitrophyric and porphyritic rock textures was common in the five ignimbrites, however an eutaxitic texture was also evident in the Wharo Ignimbrite. The eutaxitic texture is characteristic of dense of higher degree of welding which the Wharo Ignimbrite is.

The Papamoa Formation has a rhyolitic chemical composition as proven by the results provided from the geochemical analysis of the glass shards extracted from each of the ignimbrites and the two pumice clasts. However, XRF data of whole pumice clasts showed that the black pumice was andesitic while the white pumice was dacitic. This would mean that the minerals in the pumice clasts would have played a part in pushing the two pumice types into the andesitic to dacitic chemical composition range. In addition, being more mafic would have been the reason behind the dark colour of the black pumice in comparison to the white pumice. The dacitic-andesitic chemical composition range of the two pumice types supports the idea that the Papamoa Formation was sourced from a magma that was evolving from a dacitic to andesitic chemical composition or that the magma had a mixed chemical composition. The five ignimbrites were distributed during five separate eruptions, each eruption event, the magma would have been mixing causing the unique chemical compositions of the ignimbrites of the Papamoa Formation.

5.9 Limitations and Recommendations for Future Research Work

For the most part of the study, detailed findings were provided for the Papamoa Formation found in the eastern parts of Rocky Cutting Road. More research should investigate the western side of Rocky Cutting Road. A key area to investigate would be at the Kaiate Falls, at a Department of Conservation reserve, where there is a thick ignimbrite overlying a bedded pyroclastic succession.

In terms of the data collected for XRF, sample sizes for the black pumice were very limited due to its availability out in the field. Although data obtained was good, better control could be obtained by sampling more sites at different stratigraphic levels.

In carrying out future investigations, additional ages for the undated ignimbrites in the study area should be determined so that a better understanding of the geochronology of the study area can be achieved.

Conducting this investigation will contribute to a better understanding of the overall geology of the TgaVC. It will provide us with a better picture of the eruptive events that would have led to the production, transportation and deposition of the geological deposits and eventually the evolution of landscape in the study area.

REFERENCES

Adams, C. J., Graham, I. J, Moore, P. R., Seward, D., & Skinner, D. N. B. (1994). Geochronological and geochemical evolution of late Cenozoic volcanism in the Coromandel Peninsula, New Zealand. *New Zealand Journal of Geology and Geophysics, 37*(1994), 359-379. https://doi.org/10.1080/00288306.1994.9514626

Ballance, P. (2009). New Zealand geology: an illustrated guide. Auckland, New Zealand: Geoscience Society of New Zealand.

Booden, M. A., Smith, I. E. M., Mauk, J. L., & Black, P. M. (2012). Geochemical and isotopic development of the Coromandel Volcanic Zone, northern New Zealand, since 18 Ma. *Journal of Volcanology and Geothermal Research*, *219-220* (2012), 15–32. https://doi:10.1016/j.jvolgeores.2012.01.005

Briggs, R. M., Hall, G. J., Hamsworth, G. R., Hollis, A. G., Houghton, B. F., Hughes, G. R., Morgen, M. D., & Whitbread-Edwards, A. R. (1996). Geology of the Tauranga Area. Sheet U14 1:50 000. Hamilton, New Zealand: University of Waikato.

Briggs, R. M., Houghton, B. F., McWilliams, M., & Wilson, C. J. N. (2005). 40Ar/39Ar ages of silicic volcanic rocks in the Tauranga-Kaimai area, New Zealand: Dating the transition between volcanism in the Coromandel Arc and the Taupo Volcanic Zone. *New Zealand Journal of Geology and Geophysics, 48*(3), 459-469. https://doi.org/10.1080/00288306.2005.9515126

Cox, K. G., Bell, J. D.,& (1979). THE INTERPRETATION OF IGNEOUS ROCKS. Chapman & Hall, UK. DOI: https//: 10.1007/978-94-017-3373-1

Francis, P., & Oppenheimer, C. (2004). Volcanoes. Oxford University Press, UK.

Gibe, M., Nicol, A., & Walsh, J. J. (2010). Evolution of faulting and volcanism in a back-arc basin and its implications for subduction processes. *TECTONICS, 29*(TC4020), 1-18. https://doi:10.1029/2009TC002634

Hamilton, A. R., Campbell, K. A., Rowland, J. V., Barker, S., & Guido, D. M. (2019). Fossilised geothermal surface features of the Whitianga Volcanic Centre (Miocene), Coromandel Volcanic Zone, New

Zealand: Controls and characteristics. *Journal of Volcanology and Geothermal Research 381* (2019), 209–226. https://doi.org/10.1016/j.jvolgeores.2019.06.009

Hayward, B. W., Black, P. M., Smith, I. E. M., Ballance, P. F, Itaya, T., Doi, M., Takagi, M., Bergman, S., Adams, C. J., Herzer, R. H., & David J. Robertson, D. J. (2001). K-Ar ages of early Miocene arc-type volcanoes in northern New Zealand, *New Zealand Journal of Geology and Geophysics, 44*(2), 285-311. https://DOI: 10.1080/00288306.2001.9514939

Hollis, A. G. (1995). Volcanic Geology of the Central Tauranga Basin, New Zealand [MSc Thesis]. Hamilton, New Zealand: University of Waikato.

Houghton, B. F., Wilson, C. J. N., McWilliams, M. O., Lanphere, M. A., Weaver, S. D., Briggs, R. M., & Pringle, M. S. (1995). Chronology and dynamics of a large silicic magmatic system: Central Taupo Volcanic Zone, New Zealand. *Geology, 23* (1), 13–16. https//: doi:10.1016/j.saa.2007.05.063

Hughes, G. R. (1993). Volcanic geology of the eastern Tauranga Basin and Papamoa Range [MSc Thesis]. Hamilton, New Zealand: University of Waikato.

Koralay, T., & Kadioglu, Y. K. (2008). Reasons of different colors in the ignimbrite lithology: Micro-XRF

Krear, D. (1994). A “least complex” dynamic model for late Cenozoic volcanism in the North Island, New Zealand, New Zealand Journal of Geology and Geophysics, 37(2), 223-236. https://DOI: 10.1080/00288306.1994.9514617

Le Bas, M. J., Le Maitre, R. W., Streekersen, A., & Zanettin, B. (1986). Chemical Classification of the Volcanic Rocks Based on the Total Alkali-Silica Diagram. Journal of Petrology, 27 (3), 745-750. London, UK.

Leonard, G. S., Begg, J. G., & Wilson, C. J. N. (2010). Geology of the Rotorua area. Institute of Geological and Nuclear Sciences 1:250 000 geological map 5. 1 sheet + 102 p. Lower Hutt, New Zealand: GNS Science.

Lowe, D. J., Pearce, N. J., Jorgensen, M. A., Kuehn, S. C., Tyron, C. A., & Hayward, C. L. (2017). Correlating tephras and cryptotephras using glass compositional analyses and numerical and statistical methods: Review and evaluation. Quaternary Science Reviews, 175, 1-44.

Moore, P. R. (2013). Obsidian sources of the Coromandel Volcanic Zone, Northern New Zealand. *Journal of the Royal Society of New Zealand, 152*(), 38-57. https://doi.org/10.1080/03036758.2011.576684

Mortimer, N. (2004). New Zealand's Geological Foundations. *Gondwana Research, 7*(1), 261-272.

Pittari, A., Cas, R. A. F., Edgar, Nichols, H. J.,Wolf, J. A., & Marti, J. (2006). The influence of palaeotopography on facies architecture and pyroclastic flow processes of a lithic-rich ignimbrite in a high gradient setting: The Abrigo Ignimbrite, Tenerife, Canary Islands. Journal of Volcanology and Geothermal Research, 152 (2006), 273-315. https://doi: 10.1016/j.jvolgeores.2005.10.007

Pittari, A., Prentice, M. L., McLeod, O. E., Zadeh, E. Y., Kamp, P. J. J., Danišík, M., & Vincent, K. A. (2021). Inception of the modern North Island (New Zealand) volcanic setting: spatio-temporal patterns of volcanism between 3.0 to 0.9 Ma. *New Zealand Journal of Geology and Geophysics*.

https//:DOI: 10.1080/00288306.2021.1915343

Prentice. M., personal communication, 3 May, 2021.

Shane, P. (2017). The Southern End of the Pacific Ring of Fire: Quaternary Volcanism in New Zealand. In J. Shulmeister (Ed.), Landscape and Quaternary Environmental Change in New Zealand, (pp. 35-66). Atlantis Press. https://doi.org/10.2991/978-94-6239-237-3

Son, C., & Son, Y. K. (2019). Distinguishing between primary and secondary volcaniclastic deposits. *Scientific Reports,* (2019)9: *12425.* DOI: https://doi.org/10.1038/s41598-019-48933-4

Sparks RSJ, Self S, and Walker GPL 1973. Products of ignimbrite eruptions. Geology, 1, 115-118.

Sparks, R. S. J, Tait, S. R., & Yanev, Y. (1999). Dense welding caused by volatile resorption. *Journal of the Geological Society*. 156 (1999):217-225. London, Great Britain.

Sparks, R. S. J. (1976). Grain size variations in ignimbrites and implications for the transport of pyroclastic flows. *Sedimentology*, 23 (1976), 147-188. University of Lancaster, United Kingdom.

Spinks, K. D., Acocellab, V., Cole, J. W., & Bassetta, K. N. (2005). Structural control of volcanism and caldera development in the transtensional Taupo Volcanic Zone, New Zealand. *Journal of Volcanology and Geothermal Research, 144* (2005), 7– 22. https:// doi:10.1016/j.jvolgeores.2004.11.014

Sprung, P., Schuth, S., Mu¨nker, C., & Hoke, L. (2007). Intraplate volcanism in New Zealand: the role of fossil plume material and variable lithospheric properties. *Contrib Mineral Petrol, 153*(2007), 669–687. https:// DOI 10.1007/s00410-006-0169-1

Stern, T. A., Stratford, W. R.., & Salmon, M. L. (2006). Subduction evolution and mantle dynamics at a continental margin: Central North Island, New Zealand. *Reviews of Geophysics, 44* (RG4002), 1-36. https:// doi.10.1029/2005RG000171

Sutherland, R. (1999). Basement geology and tectonic development of the greater New Zealand region: an interpretation from regional magnetic data. *Tectonophysics, 308* (1999) 341–362.

Wilson, C. J. N. (1986). Pyroclastic flows and ignimbrites. *Science progress*. 70 2 (278): p 171-207. Auckland, New Zealand.

Wilson, C. J. N., Houghton, B. F., McWilliams, M. O., Lanphere, M. A., Weaver, S. D., & Briggs, R. M. (1995). Volcanic and structural evolution of Taupo Volcanic Zone, New Zealand: a review. *Journal of Volcanology and Geothermal Research, 68* (1995), 1-28.

Wright, J. V. (1979). FORMATION, TRANSPORT AND DEPOSITION OF IGNIMBRITES AND WELDED TUFFS [PhD thesis]. London: Royal School of Mines, Imperial College.

Wright, J. V., Smith, A. L. & Self, S. (1980). A WORKING TERMINOLOGY OF PYROCLASTIC DEPOSITS. *Journal of Volcanology and Geothermal Research*. 8 (1980): 315 – 336. Elsevier Scientific Publishing Company, Amsterdam, Belgium.

APPENDICE

Appendix 1: Table of Sample and Localities

Sample number:	*W Numbers:*	*Location:*	*Locality number:*	*Easting (NZTM)*	*Northing (NZTM)*	*Elevation (m):*	*Analytical method applied on sample:*	*Sample type:*
L1		Welcome Bay Road, 893R Welcome Bay	***1***	1886608	5820326	42	TS	Ignimbrite
	W210001	Road						
L2		Rocky Cutting Road, near 354 Rocky Cutting	***2***	1886004	5817210	121	TS, EMPA, LA-ICPMS,	Ignimbrite, Black Pumice,
	W210002	Road					XRF	White Pumice, Lithics
L3	***W210003***	Arnie's Farm, 700 Waitao Road	***3***	1884997	5814227	325	TS	Ignimbrite
L4		Earthquake Paddock(EP),East of Rocky	***4***	1887378	5819275	112	TS, EMPA, LA-ICPMS	Ignimbrite
	W210004	Cutting Road(940 Welcome Bay Road)						
L5	***W210005***	Black Rock, Addline Property	***5***	1887590	5819156	105	TS, EMPA, LA-ICPMS	Ignimbrite
L6	***W210006***	Bluffs on right-hand side of track to EP	***6***	1887276	5819274	Sample not collected as same as L4		Ignimbrite
L7/1		East of Rocky Cutting Road(940 Wlcome Bay	***7***	1886761	5819156	35	TS, EMPA, LA-ICPMS	Fresh material, Ignimbrite??
	W210007	Road), by the valley, unit A						
L7/2		East of Rocky Cutting Road(940 Wlcome Bay	***7***	1886761	5819156	35.2	TS	Ignimbrite??
	W210008	Road), by the valley, unit B (silicified?)						
L7/3		East of Rocky Cutting Road(940 Wlcome Bay	***7***	1886761	5819156	35.8	TS	Fall deposit
	W210009	Road), by the valley, unit C (Fall deposit)						
L7/4		East of Rocky Cutting Road(940 Wlcome Bay	***7***	1886761	5819156	37	TS, EMPA, LA-ICPMS	Ignimbrite
	W210010	Road, by the valley), unit D (EP ignimbrite?)						
L8		Kidnapper's Valley Farm Track (Addline	***8***	1886822	5819373	60	TS	Ignimbrite
	W210011	Property)						

L9		Upper Kidnapper's Valley Farm Track	***9***	1886861	5819420	70	TS, XRF	Ignimbrite
	W210012	(Addline Property)						
L10	***W210013***	Holmberg Farm Valley	***10***	1884570	5816456	20	TS	Andesite
L11	***W210014***	Ridge, Holmberg Farm	***11***	1884279	5816602	100	TS, EMPA, LA-ICPMS	Ignimbrite
L12/1	***W210015***	McLeod's Farm, bottom unit, 79 Reid Road	***12***	1888279	5819439	41	TS, EMPA, LA-ICPMS	Ignimbrite
L12/2	***W210016***	McLeod's Farm, middle unit	***12***	1888279	5819439	50	TS, EMPA, LA-ICPMS	Ignimbrite
L12/3	***W210017***	McLeod's Farm, top unit	***12***	1888279	5819439	56	TS, EMPA, LA-ICPMS	Ignimbrite
L13	***W210018***	Gina's Farm, 123 Reid Road	***13***	1888273	5819394	100	TS	Ignimbrite
L14	***W210019***	Gavin's Farm, 890 Waitao Road	***14***	1884680	5813301	340	TS	Ignimbrite
#9	***W210020****		***15***	1886546	5815261		EMPA, LA-ICPMS	Ignimbrite

Appendix 2: Electron Microprobe Analysis (EMPA): Raw Data

Major element analysis of glass shards from 11 samples within the study area.

Sample:	VG568 (Primary Std)	ATHOG (2nd std)	#9	L2_BP	L2_WP	L4.1	L5	L7.1	L7.4	L11	L12.1	L12.2	L12.3
SiO2(Mass%)	76.46	75.46	73.03	72.14	73.08	72.99	66.98	69.11	68.02	71.24	73.11	73.60	72.62
Al2O3(Mass%)	12.06	12.18	12.18	12.53	11.92	12.22	13.70	12.82	12.49	12.69	12.16	12.22	12.12
TiO2(Mass%)	0.08	0.26	0.12	0.23	0.09	0.09	0.36	0.15	0.31	0.24	0.10	0.10	0.10
MnO(Mass%)	0.02	0.10	0.03	0.04	0.02	0.02	0.07	0.03	0.03	0.05	0.03	0.03	0.02
FeO(Mass%)	1.41	3.29	1.40	2.00	0.83	0.73	2.94	2.18	2.40	2.11	1.50	1.51	1.51
MgO(Mass%)	0.03	0.09	0.07	0.17	0.09	0.07	0.39	0.12	0.29	0.23	0.05	0.06	0.05
CaO(Mass%)	0.46	1.73	0.91	1.58	1.13	1.20	2.33	1.54	1.85	1.60	0.86	0.87	0.84
Na2O(Mass%)	4.02	3.91	4.13	4.05	3.83	4.02	3.96	3.87	4.12	3.65	4.41	4.38	4.52
K2O(Mass%)	4.98	2.75	3.86	3.32	3.51	3.61	3.07	3.17	2.92	3.36	3.68	3.68	3.61
Cl(Mass%)	0.08	0.04	0.17	0.15	0.15	0.12	0.12	0.15	0.17	0.17	0.17	0.18	0.18
Total(Mass%)	**99.61**	**99.82**	**95.90**	**96.22**	**94.65**	**95.06**	**93.93**	**93.14**	**92.61**	**95.32**	**96.07**	**96.63**	**95.57**

*Note: Figures provided are averages of the raw data. They were later normalized. It should also be noted that for sample L7.4, most of the data collected was discarded due to the poor quality of the data in comparison to the values of the standards used.

Raw Plagioclase data for the White Pumice type. Plag=plagioclase, Std=standard, pt=point.

Plag point	Plag Std	WP Plag1	WP Plag2	WP Plag3	WP Plag4	WP Plag5	WP Plag6	WP Plag7	WP Plag9	WP Plag11	WP Plag12	WP Plag13	WP Plag14	WP Plag15
SiO2(Mass%)	51.03	58.78	58.83	60.36	59.35	53.95	58.61	58.60	54.66	59.82	54.35	58.90	54.15	58.34
Al2O3(Mass%)	31.42	26.31	26.25	25.62	26.18	29.40	26.74	26.73	28.59	25.67	29.35	26.75	29.53	26.83
TiO2(Mass%)	0.02	0.01	0.00	0.01	0.00	0.03	0.00	0.00	0.02	0.00	0.00	0.00	0.01	0.00
MnO(Mass%)	0.01	0.00	0.01	0.01	0.00	0.00	0.00	0.00	0.00	0.00	0.00	0.02	0.02	0.00
FeO(Mass%)	0.38	0.09	0.15	0.18	0.18	0.36	0.15	0.15	0.13	0.17	0.25	0.16	0.17	0.21
MgO(Mass%)	0.14	0.01	0.02	0.01	0.01	0.02	0.00	0.00	0.02	0.01	0.00	0.01	0.01	0.01
CaO(Mass%)	14.06	7.91	7.91	7.06	7.56	11.81	8.36	8.10	10.73	7.18	11.65	7.95	11.71	8.46
Na2O(Mass%)	3.35	6.52	6.49	6.93	6.41	4.44	6.42	6.32	5.00	6.74	4.69	6.14	4.64	6.33
K2O(Mass%)	0.10	0.36	0.39	0.44	0.39	0.18	0.37	0.36	0.21	0.43	0.19	0.37	0.18	0.35
Total(Mass%)	**101.52**	**100.75**	**100.87**	**101.78**	**100.87**	**100.86**	**101.35**	**101.63**	**100.04**	**100.63**	**101.38**	**101.31**	**101.53**	**101.83**

Raw Plagioclase data for the Black Pumice type.

Plag point:	Plag Std	BP Plag1	BP Plag2	BP Plag3	BP Plag4	BP Plag8	BP Plag9	BP Plag10	BP Plag11	BP Plag12	BP Plag13	BP Plag14	BP Plag15
SiO2(Mass%)	50.96	53.10	57.27	53.68	55.51	58.22	53.55	55.28	54.81	56.65	52.33	55.04	57.37
Al2O3(Mass%)	31.32	29.60	26.49	30.44	26.46	26.35	29.38	28.22	28.73	27.37	30.01	28.66	27.16
TiO2(Mass%)	0.02	0.00	0.00	0.01	0.00	0.02	0.02	0.01	0.00	0.03	0.03	0.01	0.01
MnO(Mass%)	0.01	0.01	0.01	0.00	0.00	0.01	0.02	0.01	0.00	0.00	0.00	0.00	0.00
FeO(Mass%)	0.42	0.30	0.28	0.32	0.32	0.34	0.28	0.34	0.35	0.28	0.36	0.26	0.26
MgO(Mass%)	0.13	0.04	0.02	0.02	0.03	0.02	0.02	0.02	0.01	0.01	0.02	0.04	0.02
CaO(Mass%)	14.00	12.22	8.66	12.48	8.71	8.55	11.75	10.64	10.97	9.72	12.79	10.94	9.27
Na2O(Mass%)	3.31	4.30	5.91	4.18	5.65	6.08	4.27	5.05	4.93	5.40	4.00	4.81	5.74
K2O(Mass%)	0.11	0.17	0.35	0.18	0.29	0.33	0.22	0.25	0.23	0.28	0.16	0.22	0.29
Total(Mass%)	**101.15**	**100.42**	**99.97**	**102.12**	**97.69**	**100.36**	**100.47**	**101.02**	**101.18**	**100.64**	**100.66**	**100.81**	**101.11**

Raw Hornblende data for the White Pumice.

Plag point:	Hbl std	Hbl pt1	Hbl pt2	Hbl pt3	Hbl pt4	Hbl pt5	Hbl pt6	Hbl pt7	Hbl pt8	Hbl pt9	Hbl pt10	Hbl pt11	Hbl pt12	Hbl pt13	Hbl pt14	Hbl pt15
SiO2(Mass%)	39.17	45.52	45.49	44.95	46.02	45.47	46.31	45.46	44.49	45.88	45.38	45.98	45.52	46.01	45.32	45.96
Al2O3(Mass%)	9.64	7.53	7.46	7.83	7.25	7.43	6.95	7.54	8.22	7.38	7.50	7.15	7.56	7.24	7.59	7.35
TiO2(Mass%)	3.07	1.26	1.24	1.25	1.48	1.27	1.13	1.31	1.57	1.32	1.34	1.23	1.30	1.23	1.31	1.16
MnO(Mass%)	0.36	0.32	0.32	0.32	0.28	0.34	0.34	0.33	0.33	0.32	0.33	0.32	0.29	0.31	0.33	0.30
FeO(Mass%)	24.79	18.83	18.33	18.94	18.60	18.96	19.11	18.54	19.21	19.39	18.68	18.75	18.92	18.21	19.39	17.92
MgO(Mass%)	4.26	10.77	10.89	10.55	10.90	10.77	10.94	10.86	10.23	10.92	10.83	10.96	10.75	11.10	10.48	11.68
CaO(Mass%)	10.72	10.44	10.38	10.49	10.75	10.48	10.37	10.51	10.38	10.49	10.54	10.45	10.56	10.50	10.40	10.60
Na2O(Mass%)	1.91	1.29	1.36	1.33	1.27	1.21	1.19	1.32	1.38	1.27	1.29	1.25	1.29	1.24	1.41	1.23
K2O(Mass%)	1.41	0.39	0.46	0.49	0.40	0.39	0.38	0.44	0.46	0.39	0.51	0.41	0.43	0.38	0.45	0.39
Total(Mass%)	**96.02**	**96.82**	**96.56**	**96.85**	**98.02**	**97.44**	**97.64**	**97.26**	**97.77**	**98.15**	**97.43**	**97.38**	**97.53**	**97.00**	**97.37**	**97.53**

Raw Pyroxene data for the Black Pumice.

Sample:	Px Std	Px pt1	Px pt2	Px pt6	Px pt7	Px pt8	Px pt9	Px pt10	Px pt11	Px pt12	Px pt14
SiO2(Mass%)	53.47	50.17	49.70	51.00	50.51	50.52	51.15	47.77	49.79	49.29	50.00
Al2O3(Mass%)	0.75	1.42	0.72	1.11	0.63	0.76	1.10	0.78	0.41	0.44	0.56
TiO2(Mass%)	0.21	0.20	0.11	0.21	0.16	0.17	0.21	0.10	0.07	0.14	0.16
MnO(Mass%)	0.06	0.62	0.78	0.50	0.91	0.67	0.46	0.74	0.87	0.84	0.76
FeO(Mass%)	2.82	25.66	31.18	23.05	28.31	26.51	21.82	30.55	31.42	31.37	30.45
MgO(Mass%)	17.01	17.72	14.34	19.82	16.74	17.28	20.94	14.06	13.91	13.68	14.54
CaO(Mass%)	25.24	1.41	1.52	1.57	1.11	1.58	1.43	1.35	0.97	1.70	1.60
Na2O(Mass%)	0.20	0.02	0.00	0.03	0.01	0.03	0.04	0.05	0.02	0.02	0.00
K2O(Mass%)	0.00	0.00	0.01	0.01	0.00	0.00	0.00	0.05	0.01	0.01	0.01
Total(Mass%)	**100.74**	**98.04**	**99.136**	**98.072**	**98.945**	**98.178**	**97.93**	**96.372**	**98.494**	**98.419**	**98.77**

Appendix 3: LA-ICPMS Instrument Specifications, Raw Data and Geochemical Data

Instrument settings for LA-ICP-MS

ICP-MS		
Model		Elan 6100 DRCII ICP-MS (Perkin Elmer Sciex)
Gas flows	Plasma (Ar)	15 L.min
	Auxiliary (Ar)	1.2 L.min
	Carrier (He)	1.0 L.min
	Nebuliser	0.6 to 0.7 optimised range
Shield torch		Used for most analyses
Vacuum pressure		1 x 10^{-5} Torr
Software		Elan 3.4
LASER		
Model		RESOlution SE series excimer laser
Wavelength		193 nm
Repetition rate		5 Hz
Pre-ablation laser warm-up		Laser fired continuously
Spot size		15 µm
Incident pulse energy		c. 0.04 mJ
Energy density on sample (fluence)		5 J.cm^2
Software		Geostar v8.50
DATA ACQUISITION PARAMETERS		
Data acquisition protocol		Time resolved analyses
Scanning mode		Peak hopping, 1 point per peak
Detector mode		Pulse counting, dead time correction applied
Isotopes determined		^{27}Al, ^{29}Si, ^{43}Ca, ^{47}Ti, ^{55}Mn, ^{66}Zn, ^{71}Ga, ^{85}Rb, ^{88}Sr, ^{89}Y, ^{90}Zr, ^{93}Nb, ^{133}Cs, ^{138}Ba, ^{139}La, ^{140}Ce, ^{141}Pr, ^{142}Nd, ^{147}Sm, ^{153}Eu, ^{157}Gd, ^{159}Tb, ^{163}Dy, ^{165}Ho, ^{166}Er, ^{169}Tm, ^{172}Yb, ^{175}Lu, ^{178}Hf, ^{181}Ta, ^{182}W, ^{208}Pb, ^{232}Th, ^{238}U.
Dwell time per isotope		10 ms (Al, Si) and 50 ms (all other elements)
Quadrapole settling time		c. 2 ms
Data acquisition		85 s (40 s background, 45 s ablation)
Software		Elan 3.4
STANDARDISATION		
Calibration standards		NIST612
Sources for refrence material concentration data		GeoRem database
Internal standards		^{29}Si
Secondary standard		ATHO-G

Methodology	Paton et al., 2011
Software	Iolite 3
DRS	trace_element_IS

LA-ICPMS Raw Data

Sample:	Otawera	L12_1	L12_2	L2_BP	L2_WP	L4_1	L12_3	L7_1	L11	L5
Zn	62.83	56.15	63.08	58.21	32.49	49.40	56.31	39.76	129.79	86.70
Zn (2σ)	29.25	14.94	32.92	39.67	27.84	39.58	26.33	1.28	148.67	104.04
Ga	18.93	18.52	21.16	22.26	17.76	20.21	19.09	27.44	30.27	32.91
Ga (2σ)	7.40	7.13	10.33	5.28	4.68	7.50	10.54	4.53	20.27	53.87
Rb	143.28	144.38	139.98	120.44	142.41	141.62	137.98	137.65	117.58	121.56
Rb (2σ)	15.84	35.14	12.88	22.06	16.30	32.20	10.03	8.35	36.74	21.50
Sr	55.01	57.50	59.51	92.81	74.48	94.68	56.46	114.52	73.36	158.91
Sr (2σ)	6.69	23.23	14.81	50.01	12.94	40.13	7.61	21.66	28.95	31.77
Y	31.12	29.46	29.25	20.67	13.92	16.07	31.69	27.85	17.47	22.39
Y (2σ)	5.94	8.51	11.27	17.16	5.15	6.18	6.31	6.59	9.77	10.39
Zr	152.95	163.88	176.92	157.34	79.34	98.44	159.40	215.04	126.30	190.19
Zr (2σ)	24.99	41.45	67.20	147.76	19.32	50.53	19.19	39.63	84.42	62.21
Nb	8.39	8.41	8.74	6.57	5.06	5.41	8.86	7.01	4.65	7.94
Nb (2σ)	0.83	1.28	0.95	3.24	1.08	1.39	1.11	0.52	1.83	1.35
Cs	4.82	4.44	4.08	3.77	4.65	4.22	3.92	3.86	4.62	4.41
Cs (2σ)	1.12	2.37	0.94	0.72	2.13	1.29	0.84	0.99	2.66	4.00
Ba	826.90	805.66	796.67	712.79	793.85	773.89	859.90	796.25	568.62	608.63
Ba (2σ)	72.00	173.05	282.51	201.78	123.16	141.15	111.59	126.42	309.56	152.15
La	25.69	25.95	24.66	19.17	19.37	21.48	26.12	22.73	15.66	18.74
La (2σ)	3.91	6.69	8.13	6.75	5.00	5.61	4.60	3.85	8.01	7.03
Ce	54.62	53.15	51.17	40.36	38.86	42.86	57.73	47.68	31.34	38.70
Ce (2σ)	5.16	10.62	22.08	16.49	7.07	9.72	7.89	8.04	13.16	21.40
Pr	6.31	5.99	5.75	4.39	3.98	4.26	6.17	5.40	3.68	4.97
Pr (2σ)	0.34	0.92	2.21	2.14	0.92	1.26	1.08	1.29	1.69	2.16
Nd	26.46	22.25	22.39	18.81	12.48	15.42	23.87	23.93	13.95	18.33
Nd (2σ)	4.75	7.31	9.36	13.28	4.37	6.87	4.72	4.95	7.19	7.14
Sm	5.87	5.14	4.83	3.75	2.14	2.74	5.25	5.83	3.57	3.95
Sm (2σ)	2.37	2.70	3.10	2.80	1.99	1.57	2.28	1.55	2.56	2.04
Eu	0.70	0.68	0.69	0.83	0.37	0.52	0.67	0.80	0.59	0.92
Eu (2σ)	0.43	0.55	0.49	0.80	0.29	0.45	0.49	0.55	0.60	0.57
Gd	4.83	5.64	5.18	3.95	2.27	2.47	5.26	5.28	2.79	2.93

Gd (2σ)	1.05	2.73	2.19	2.62	1.40	1.26	1.97	2.58	2.87	2.85
Tb	0.71	0.83	0.78	0.59	0.30	0.40	0.85	0.81	0.36	0.71
Tb(2σ)	0.31	0.38	0.33	0.63	0.27	0.34	0.33	0.17	0.40	0.35
Dy	5.56	5.34	5.11	3.11	1.85	2.39	5.26	5.07	2.89	4.06
Dy(2σ)	0.99	1.19	1.69	3.21	1.73	1.33	1.85	2.09	2.52	1.16
Ho	0.96	1.04	1.00	0.90	0.47	0.57	1.00	1.10	0.59	0.78
Ho(2σ)	0.39	0.50	0.56	0.44	0.37	0.45	0.44	0.64	0.45	0.48
Er	3.07	3.18	3.09	2.01	1.46	1.73	3.14	3.13	1.81	2.58
Er(2σ)	0.67	1.57	1.19	1.74	1.32	1.24	1.24	1.27	1.21	*1.62*
Tm	0.51	0.40	0.44	0.34	0.24	0.23	0.46	0.50	0.23	*0.39*
Tm(2σ)	0.17	0.32	0.27	0.38	0.23	0.17	0.26	0.34	0.27	0.24
Yb	3.21	3.53	3.19	3.01	1.97	2.47	3.40	3.57	2.13	2.85
Yb(2σ)	1.90	1.44	1.45	2.07	1.57	1.62	1.76	0.99	0.98	1.80
Lu	0.48	0.50	0.50	0.53	0.34	0.35	0.51	0.43	0.35	0.39
Lu(2σ)	0.21	0.25	0.37	0.28	0.20	0.37	0.27	0.17	0.23	0.21
Hf	4.99	4.85	5.31	4.29	2.42	2.92	4.84	5.69	2.99	4.54
Hf(2σ)	1.09	1.46	1.47	3.26	1.03	1.62	1.06	1.12	2.07	2.81
Ta	0.74	0.60	0.64	0.40	0.44	0.50	0.68	0.42	0.35	0.61
Ta(2σ)	0.28	0.24	0.25	0.41	0.30	0.31	0.17	0.24	0.28	0.49
W	2.18	1.99	1.86	1.66	1.57	1.65	2.42	2.10	1.70	1.91
W(2σ)	0.42	0.51	0.58	0.69	0.21	1.17	3.89	0.30	1.17	1.56
Pb	33.36	29.45	29.69	22.12	29.28	30.74	29.89	40.90	24.42	37.67
Pb(2σ)	9.42	6.44	6.59	10.46	11.63	11.80	10.78	13.83	12.29	40.87
Th	12.42	11.78	12.21	8.48	9.99	10.47	12.76	10.08	6.30	8.06
Th(2σ)	3.15	3.97	5.16	2.92	3.97	4.18	2.36	1.71	3.79	5.39
U	3.40	3.11	2.79	2.25	2.56	2.57	3.00	1.58	2.12	2.07
U(2σ)	0.66	1.07	0.86	0.40	1.01	0.77	0.77	0.92	0.86	0.90